DYNAMICS OF CHROMOPHORIC DISSOLVED ORGANIC MATTER, CDOM, IN COASTAL TROPICAL WATERS

by
Patrick Reyes-Pesaresi

A dissertation submitted in partial fulfillment of the requirements for the degree of

DOCTOR OF PHILOSOPHY
in
MARINE SCIENCES
(Biological Oceanography)

UNIVERSITY OF PUERTO RICO
MAYAGÜEZ CAMPUS
2010

Approved by:

_____	_____
Fernando Gilbes Santaella Ph.D. Member, Graduate Committee	Date
_____	_____
Jorge E. Corredor Garcia Ph.D. Member, Graduate Committee	Date
_____	_____
Ernesto Otero Morales Ph.D. Member, Graduate Committee	Date
_____	_____
Julio M. Morell Rodríguez Ms. S. Member, Graduate Committee	Date
_____	_____
José M. López Díaz Ph.D. President, Graduate Committee	Date
_____	_____
Wilson Ramírez Martínez Ph.D. Representative of Graduate Studies	Date
_____	_____
Nilda E. Aponte Avellanet Ph.D. Chairperson of the Department	Date

ABSTRACT

Chromophoric Dissolved Organic Matter (CDOM a_{g355}) distribution in surface waters of Mayagüez Bay, Puerto Rico can be related to riverine allochtonous sources. Inshore CDOM a_{g355} had six times (0.55 m^{-1}), and offshore stations twice (0.22 m^{-1}), the values found at Caribbean Time Series (CaTS) station surface waters (0.100 m^{-1}). Spatial and temporal analysis of CDOM spectral slope values reveals no statistically significant difference ($p > 0.05$) between Mayagüez Bay and Caribbean surface waters (0.017 nm^{-1}). Correlation analysis between Chl-*a*, vs. CDOM suggests that phytoplankton is not a dominant CDOM a_{g355} source in Mayagüez Bay waters. Bottom sediment resuspension appears to be an important source of CDOM a_{g355} during the dry season. At this time of minimal river water discharges, half the average values of CDOM a_{g355} and non-significant temporal differences in TSS, CDOM a_{g355} spectral slopes were prevalent. Photodegradation does not appear to be an important process in explaining variability of CDOM a_{g355} nor the modification of the spectral slope of CDOM a_{g355}, locally.

Non-conservative behavior of CDOM a_{g375} was demonstrated in a mixing experiment consisting in step-wise dilution of marine waters end-members with Añasco River water end-member, including and excluding its typical suspended sediments loads. At low salinity dilution ($S < 8$), CDOM a_{g375} was lost from the dissolved fraction between 8.7 and 18.6 % in the absence of suspended particulate. In the presence of particles (at typical river water TSS concentrations), simple dilution produced a decrease in CDOM a_{g375} of between 13.9 and 9.7% suggesting loss by sorption; but at intermediate salinities, rising values suggested desorption. Spectral slope (S) shifts, above theoretical conservative dilution line values, suggested that CDOM a_{g375} was removed from the dissolved fraction. The values of S were not significantly different regardless

of level of dilution or whether suspended particles were absent or present in the mixture of river and marine water. At salinity values typical of Mayagüez Bay (33.20 - 35.91 psu), S values characteristic of the marine water end-member dominate. Far greater amounts of allochtonous CDOM than enters the Bay would be necessary to significantly change the resulting value of S in the mixed marine and river waters since the proportion of fresh river water is <7%. CDOM a_{g375} flocculation and adsorption onto clay-minerals can be important processes in the partition between dissolved and particulate phases.

Three characteristic Remote Sensing Reflectance (R_{rs}) spectral signatures were identified in Mayagüez Bay: inshore, offshore and in the vicinity of an underwater sewage outfall. A unique phytoplankton assemblage and unique combination of water constituents can cause the characteristic R_{rs} spectral signature near the underwater treated sewage outfall. Empirical algorithms were successful in reaching the validated uncertainty threshold, Absolute Percent Difference (APD < 35 %), for three of the four evaluated band ratios of acceptable APD. The best band ratios were $R_{rs}412/R_{rs}510$ and $R_{rs}510/R_{rs}555$ ($R^2 > 0.80$). The same band ratios were evaluated for Color Detrital Matter ($aCDM_{412}$) with better R^2 than obtained for CDOM for the first three band ratios ($R^2 > 0.80$), making these suitable for the $aCDM_{412}$ estimate. The empirical model may be enhanced through further validation.

RESUMEN

La distribución de Materia Orgánica Disuelta Coloreada (MODC a_{g355}) en la Bahía de Mayagüez se explica por la entrada de fuentes alóctonas en proporción al flujo de los ríos. Las estaciones costeras, tuvieron valores de MODC a_{g355} seis veces mayores (0.55 m^{-1}), y las oceánicas del doble (0.22 m^{-1}), de las encontradas en aguas superficiales del Mar Caribe circundante (0.100 m^{-1}). Las pendientes espectrales eran similares a las del Mar Caribe (0.017nm^{-1}) y análisis espaciales y temporales no demuestran diferencias significativas entre estaciones en la Bahía ($p > 0.05$). Diferencias temporales no-significativas en SST, pendientes similares y reducción de MODC a_{g355} en estaciones costeras, sugieren que este material podría originarse en la resuspensión de sedimentos de la bahía en época seca. Correlaciones entre Chl-*a* y MODC sugieren que el fitoplancton no es una fuente importante de MODC a_{g355}; y que la fotodegradación no parece ser un factor de importancia modificando las pendientes espectrales de MODC a_{g355}.

Se ha demostrado un comportamiento no-conservativo de MODC a_{g375} en un experimento de mezcla simple que consistía en diluciones seriadas entre aguas oceánicas y aguas del Río Añasco que incluían y excluían las concentraciones típicas de sedimentos suspendidos. A bajas salinidades ($S < 8$), se observó perdida de MODC a_{g375} de entre 8.7 y 18.6 % en ausencia de partículas. En presencia de partículas (concentraciones de SS típicas de aguas de río), las diluciones causaron una disminución de MODC a_{g375} de entre 13.9 y 9.7 % sugiriendo perdidas por adsorción; pero valores mayores de MODC a_{g375} a salinidades intermedias sugieren desorción. Desviación de los valores de S, de línea de dilución conservativa teórica, en las series de diluciones, sugieren que MODC a_{g375} fue eliminada de la fracción disuelta y que la

presencia de sedimentos suspendidos no alteró las pendientes espectrales. Los valores de S no fueron significativamente diferentes independientemente de la presencia o ausencia de partículas. A las salinidades encontradas en la Bahía de Mayagüez (33.20-35.91), los valores característicos de S para el miembro marino, son los dominantes. Cantidades mayores de MODC alóctona que las que entran a la bahía serian necesarias para cambiar significativamente los valores resultantes de S entre la mezcla de aguas marinas y aguas de río, dado que las proporción de agua de río es < 7 %. Procesos de floculación y adsorción de MODC a_{g375} a minerales arcillosos pueden ser importantes en el fraccionamiento entre las fases disuelta y particulada.

Tres huellas espectrales (costeras, oceánicas y de un emisario submarino de aguas residuales tratadas) fueron identificadas en la reflectancia teledetectada R_{td} en la Bahía de Mayagüez. Grupos fitoplanctónicos y constituyentes distintivos de estas aguas pueden causar la señal característica en el sitio del emisario). Los algoritmos empíricos alcanzaron al nivel umbral de incertidumbre de validación Porciento Absoluto de Diferencia (PAD < 35 %), apropiados para tres de las cuatro razones de banda evaluadas. Las mejores razones de bandas fueron R_{td} 412/R_{td}510 y R_{td}510/R_{td}555 (R^2 > 0.80). Razones de bandas similares fueron evaluadas para Materia Detrítica Coloreada ($aMDC_{412}$). Estas demostraron mejores algoritmos (R^2 > 0.80) que para MODC, haciendo esta propicias para estimados de MDC. Estos algoritmos mejoraran con validación subsiguiente.

ACKNOWLEDGEMENTS

I am grateful for Capt. Dennis Corales assistance in the field operations and to the crew from Magueyes Maritime Division Ricky Laracuente, Hugo Montalvo, Osvaldo Lopez (Chico), David López (el Peje) and David Ramos assigned to the R/V Sultana, and to Yvette Ludeña and Claudia Tapia who helped during the cruises. To Sea Grant for sponsoring with seed money grant PD-272 on the last cruise and all the staff of Sea Grant, for all the coffee and the patience they had dealing with me. And especially, to Dr. Fernando Gilbes who I am profoundly grateful to for sponsoring me and this study. To my friends Marcos Rosado, Ramón López, Vilmaliz Rodríguez, Suhey Ortíz, Marla Méndez-Silvagnoli and Belitza Brocco. I am also grateful to all the members of my committee to my advisor Dr. José M. López, Dr. Jorge E. Corredor. Mr. Julio Morell and Dr. Ernesto Otero.

And finally I am grateful and I dedicate this work to my wife Gloria M. Toro-Agrait and my daughter Patricia A. Reyes-González.

Fellowship and supported by the NOAA-CREST Grant # NA06OAR4810162.

TABLE OF CONTENTS

LIST OF FIGURES

LIST OF TABLES

INTRODUCTION

In the aquatic environments, four components are primarily responsible for light absorption, These are water, CDOM, phytoplankton and inanimate particulate matter known as tripton. Each one of them has characteristic absorption spectral signature, being CDOM and, tripton the most similar. CDOM has a maximum absorption in the UV-blue region and if present in large concentration they can reduce the water penetration of PAR (Photosynthetically available Radiation) thus affecting the primary productivity (D'Sa *et al*., 1999). The phytoplankton pigments are the component that absorbs light in the aquatic environment (in blue and red region of the visible light spectrum) and can be the most important factor in reflectance signal (Case I) that can be used in remote sensing to estimate the concentration, and hence, biomass of phytoplankton.

CDOM regulates the penetration of UV light into the ocean and mediates photochemical reactions, therefore playing an important role in many biogeochemical processes in the surface ocean including primary productivity and the air–sea exchange of radiatively important trace gases (Mopper *et al*., 1991; Arrigo and Brown, 1996; Zepp *et al*., 1998).

The colored fraction of this dissolved organic matter (CDOM) is a complex pool of autochthonous materials, derived from *in situ* photosynthetic activity and processed microbially, and of allochtonous materials that are rich in humic substances and largely derived from terrestrial environments (Blough and Del Vecchio, 2002). Offshore waters have been shown to have their own *in situ* sources and sinks of CDOM (Nelson *et al*., 1998; Nelson and Siegel, 2002; Siegel *et al*., 2002; Steinberg *et al*., 2004). CDOM is produced in the open oceanic environments due to heterotrophic bacterial processes in waters column (Nelson *et al*., 1998;

2004; Steinberg *et al*., 2004) and can be photodegraded by sun light in stratified surface waters (Chen and Bada, 1992; Nelson *et al*., 1998, 2004; Siegel *et al*., 2002, 2005; Del Vecchio and Blough, 2004; Vodacek *et al*., 1997).

CDOM has become a multi-disciplinary area of study recently; from geological studies in the sequestering of organic matter (Hedges and Keil, 1999) to biological studies and remote sensing water leaving radiance (Carder *et al*., 1991, 1999). CDOM in estuarine and coastal environments is originated from terrestrial sources (Land runoff or river discharge) (Blough and Del Vecchio, 2002). The study of Complex biogeochemical processes between organic substances, mineral surfaces and microbial interaction require balance coordinated approach across wide disciplinary fronts (Hedges and Keil, 1999).

LITERATURE REVIEW

Organic matter in the marine environment can be divided into two categories dissolved organic matter (DOM) and particulate organic matter (POM). The operational definition between dissolved and particulate is an everlasting issue. The method for particulate matter absorption coefficient determination used in remote sensing validation is established by collecting particulate matter on a GF/F filter (Kishino *et al*., 1985). The problem is that GF/F filters are known to permit the passage of colloids and some bacteria and viruses materials that are not truly dissolved (Del Castillo, 2005). Controversies regarding the filter media material and pore size, have been thoroughly discussed by Del Castillo (2005), as well as some other issues related CDOM measurement problems and spectral slope determination (Del Castillo, 2005; Blough and Del Vecchio, 2002). CDOM is another operational definition, where the optical properties of a filtered water sample are determined by spectrophotometric or fluorometric methods. The relationship between CDOM absorption and fluorescence, can be useful because absorption may be inferred from fluorescence measurements, which can be acquired more rapidly, and with greater sensitivity than absorption (Ferrari and Dowell, 1998). A problem is, that absorbance measurements do not permit a detailed characterization of CDOM optical properties because CDOM absorption spectra are essentially featureless (Del Castillo *et al*., 2001). CDOM fluorescence can be used to distinguish the origin of the material from its terrestrial or marine source sources (Coble, 1996).

This fraction was originally described as *Gelbstoff* (yellow substance in German) by Kalle (1966) and later as "*Gilvin*" (Kirk, 1976, 1994). The accepted term in the field of remote sensing is Chromophoric or Colored Dissolved Organic Matter and both can be used inter-changeably (Miller, 2000). This material has also been known as aquatic humic acids (Bricaud

et al., 1981; Duce and Duursma, 1977; Gjessing, 1976; Kalle, 1966; Kirk, 1976; 1994). This material is not defined; as a uniquely specific molecular structure (Gjessing, 1976). It is blend compose by humic and fulvic acids (Harvey and Boran, 1985; Carder *et al.,* 1989) that are chemically similar and only vary in molecular weights (Kirk, 1976). Weight of humic and fulvic acids can range from thousands to millions of Daltons (Harvey *et al*., 1983). Isolation of humic acids from water samples, have been thoroughly discussed in an excellent work by Thurman and Malcolm, (1981). What should be remembered is that CDOM and humic substance are not synonymous and the differences should be stated.

CDOM is the dissolved material that absorb visible and UV light in aquatic environments; where humic substances are the extractible material from a water sample (Blough and Del Vecchio, 2002). CDOM optical definition applies to all substance found in natural waters (fresh or marine) independent of its chemical structure; that in sufficient concentration that can contribute significantly to the attenuation of light in photosynthetic bands (Kirk, 1976; 1994).

CDOM sources have been related to the decomposition of structural components of plants tissue by microbial action forming a complex group of compounds, (Kirk, 1994). Humic acids are leached from soils by precipitation; and are later transported by runoff to the aquatic environment (Cauwet, 2002; Duce and Duursma, 1977; Guo *et al.,* 2007; Gjessing, 1976; Kirk, 1994; Stuermer and Harvey, 1974) during the rainy season (Guo *et al.,* 2007). Riverine CDOM is mainly composed of humic matter; with degraded characteristics of lignin and cellulose, with minor contributions of autochthonous riverine production (Cauwet, 2002).

Higher concentrations of humic substances are found near coastal zones due to the drainage of the terrestrial environments (Arringo and Brown, 1996; Blough and Del Vecchio,

2002; Cauwet, 2002; Carder *et al.,* 1989; Chen *et al.,* 2007; Guo *et al.,* 2007; Harvey and Boran, 1985; Kalle, 1966; Kirk, 1994; Moran *et al*., 1991). CDOM level distribution has been demonstrated to be highly variable temporally and spatially, with changes as a function of the CDOM concentration and absorption (Carder *et al*., 1989; Blough *et al*., 1993). In coastal areas bottom sediments re-suspension can liberate CDOM pumped from pore water (Del Castillo *et al.,* 2000; Del Castillo, 2005; Boss *et al.,* 2001).

CDOM absorbs light in the UV region and blue end of the spectrum (Carder *et al*., 1989; Kirk, 1976; 1999; Visser, 1984) which is the same region where Chl-*a* has a maximum absorption peak. Selective absorption causes that phytoplankton alter their pigment compositions in order to capture more light at other wavelengths and possibly increase their Chl-*a* concentration (Kirk, 1994). Higher concentrations of Chl-*a* were suggested as a physiological adaptation in the Mayagüez Bay to deal with light limitation (Gilbes *et al*., 1996).

Role of CDOM in controlling UV light penetration

Most of the UV radiation reaching the surface of the oceans interacts not only with living cells but also with nonliving matter (CDOM), especially in the costal environments (Kirk, 1994; Moran and Zepp, 1997). CDOM plays an important role as a natural UV screen in marine environments (Moran and Zepp, 2000), but this CDOM is susceptible to photochemical alteration. CDOM can protect organisms from UV damage and provides the primary barrier photon absorption that drives abiotic photochemistry in the oceans (Arrigo and Brown, 1997; Miller, 2000).

CDOM-Chl-*a* related problems and bio-optical issues

Remote sensing Reflectance (R_{rs}) can be related to Inherent Optical Properties (IOPs) such as the absorption coefficient a, and scattering coefficient, b (Garver and Siegel, 1997; Gordon *et al*. 1988; Kirk, 1993; Mobley, 1994. The uses of remote sensing techniques for the monitoring of CDOM dynamics in coastal and offshore processes is a growing field (Blough *et al*., 1993; Carder *et al*., 1989; Del Castillo; 2005; Del Castillo and Miller, 2007; D'Sa and Miller., 2003; Hu *et al*., 2003; 2004 a,b; Hoge *et al*., 1995; 2001; Johannessen *et al*., 2003; Menon *et al*., 2006; Miller and D'Sa, 2002; Müller-Karger *et al*., 1988; 1989; 1990; 1995; Seigel and Michaels, 1996). CDOM optical properties induce errors in both semi-analytical and empirical algorithms used in satellite imagery analysis (Carder, *et al*., 1991) causing the overestimation of Chl-*a* estimates. Bio-optical models used to estimate Chl-*a* often involves the separate estimation of CDOM as a correction (Carder *et al*., 1991; Lee *et al*., 1996).

Remote sensing techniques have been used over wide areas of the ocean to measure CDOM absorption (Hoge *et al*., 1995; Müller-Karger *et al*., 1988; 1989; Vodacek *et al*., 1995). These bring the possibility that CDOM can be used as a passive tracer for the indication of surface patterns for freshwater dispersion, and can be used to determine the concentration of DOC concentrations in surface waters (Ferrari and Dowell, 1998). CDOM absorption values are significant correlated with the Salinity in surface water (Ferrari and Dowell, 1998) and can be used to estimate Salinity concentrations (Binding and Bowers, 2003; Bower *et al.,* 2000; Bowers *et al.,* 2004). CDOM conservative behavior can be used to assess physical mixing and this can be further used as a tracer of other constituents (Pan *et al*., 2008), such as trace metal and pollutants during estuarine mixing (Hong *et al.,* 2005).

Phytoplankton CDOM related production

Plankton excretion and decomposition products are known to be important CDOM sources (Carlson, *et al*., 1983; Gjessing, 1976; Stuermer and Harvey, 1974; Biddanda and Benner 1997; Børsheim *et al*., 1999; Pettine *et al*., 1999; Stuermer and Harvey, 1974). Under laboratory conditions, a variety of phytoplankton species cultures are not responsible for CDOM fluorescence (Rochelle-Newall and Fisher, 2002). Results suggest that non-fluorescent organic matter derived from phytoplankton origin is transformed by bacterioplankton to CDOM (Rochelle-Newall and Fisher, 2002a,b). This finding further complicates the study of the transformation of the CDOM under natural conditions.

CDOM sinks in the marine environment

The two most important processes of removal of the CDOM is the photo-degradation (Del Castillo, 2005; Del Castillo *et al*., 1999; Vodacek *et al*., 1995,1997; Skoog, *et al*., 1996) and the bacterial degradation (Moran *et al*., 2000; Thurman, 1985), and CDOM adsorption to particles have also been suggested as possible sinks for CDOM (Thurman, 1985).

CDOM Photo-degradation

Natural sunlight significantly affects the properties of coastal DOM (Siegel and Michaels, 1996). Continental shelves are important sites for the photochemical process due to the high terrestrial and estuarine DOM inputs and light penetration in the water column (Miller and Moran, 1997). CDOM has been found susceptible to photo-degradation (Del Castillo *et al*., 1999; Skoog *et al*., 1996; Vodacek *et al*., 1997). It is estimated that direct photochemical mineralization of DOM to be 12-16 x 10^{16} g C to CO_2 annually (Moran and Zepp,2000).

Photochemical processes play a number of important roles in the biogeochemical cycling of dissolve organic matter (Miller and Moran, 1997). Water optical properties, biological

processes, and chemical elements distribution have been demonstrated to be affected either directly or indirectly by the DOM photoreactions (Siegel and Michaels, 1996). Photochemical reactions at the sea surface can have a much greater impact on oceanic biogeochemistry than just producing or consuming organic compounds. Photodegradation of DOM by sunlight has been demonstrated to increase secondary production of microbial communities due to the assimilation of low molecular weight carbon products (Moran and Zepp,2000). It has also been inorganic nitrogen has been identified as a by-product of the photo-degradation of the DOM (Bushaw *et al*., 1996; Moran and Zepp,2000; Morell and Corredor, 2001)

CDOM Photo-degradation has been documented from the waters originated from the Orinoco River in the Caribbean (Del Castillo *et al*., 1999). Photo-degradation by UV light of humic acids in Orinoco River water humic acids has been suggested as an important source of nitrogen in the eastern Caribbean (Morell and Corredor, 2001). Short intermittent exposure to sunlight can mediate losses of the DOM from costal environments on "short" time scales trough direct loss of volatile carbon photoproducts and to stimulation of biological degradation of the organic matter (Miller and Moran, 1997).

Bacterial CDOM degradation

The bio-reactivity of the DOM decreases along a continuum of size (from large to small) and diagenic state (from fresh to old) in both fresh and marine waters (Amon and Benner, 1996a). So the bulk of the high molecular weight DOM is more bioreactive and less diagenetically altered than the bulk of light molecular weight DOM; this known as size-reactivity continuum hypothesis (Amon and Benner, 1996a). This changed the concept that the lower the weight the more reactive the DOM with the result of an increasingly oxidized state of the lower molecular weight and greater solubility (Amon and Benner, 1996a). Interaction between DOM

and bacteria are a key role in aquatic carbon cycle, so that factors that regulating DOM production and consumption influence carbon fluxes (Amon and Benner, 1996a).

Estuarine mixing processes and CDOM flocculation and particle adsorption

Removal of humic and fulvic acids in estuarine systems has been previously reported (Ertel *et al*., 1986; Hair and Bassett, 1973; Seiburth and Jensen, 1968; Nissenbaum and Kaplan, 1972) and it is estimated that between 3-11% of the dissolved organic humic substances is removed from river water by flocculation in seawater (Sholkowitz, 1976). The interaction of humic compounds with clay-minerals suggests the lost of the material during estuarine mixing (Preston and Riley, 1982). Of particular concern is the adsorption/desorption reaction in the zone due to salinity/pH change and the fate of the particulate load in estuarine area (Duce and Duursma, 1977). Spectral changes have been observed affecting the nature and the composition of the organic matter during the estuarine mix (De Souza-Sierra *et al*., 1997).

The results of the estuarine interaction with clays, light and microbial processes are poorly understood. These this factors must be studied so that the fate of CDOM on coastal marine environment can be understood from a land sea interface relationship. Along with DOM, suspended particulate material also intercepts sunlight and can in turbid or very productive environment complicates theoretical calculation of light penetration and photoproduct formation (Moran and Zepp, 1997). This fact complicates the modeling of the dynamic of CDOM from terrestrial drainage and its transformation in the marine environment.

SITE DESCRIPTION

The study area is a semi-enclosed Bay of 100 km^2 located in the west coast of Puerto Rico between the towns of Mayagüez and Añasco (latitude 18° 09' and 18° 08' and longitude 67° 09' and 67° 15') (Figure 1). A multitude of studies have been done in the area relating physical oceanography (Alfonso, 1996; 2001; Capella and Grove, 2002), zooplankton ecology (Alfaro, 2002), phytoplankton ecology (Gilbes, 1992; Gilbes, *et al*., 1996; Parilla, 1996; Ludeña-Hinojosa, 2007; Tapia-Lario, 2007), geology (Grove, 1977; 1998; Morelock and Grove, 1977; Morelock *et al*., 1983; Rodríguez, 2004), bio-optical oceanography (Rosado-Torres, 2000; 2008;), and geo-optical properties (Cruise and Miller, 1994; Miller, *et al*., 1994; Otero *et al*., 1992; Rodríguez-Gúzman, 2008).

Historic land use setting

The Añasco River is the largest River of the west coast; and, its basin was traditionally used for intensive sugar cane cultivation in the past. The Yagüez River runs through the town of Mayagüez even when where its basin is the smallest of the three it is in a highly impacted state due to elevated population densities and developmental pressure. This makes the Yagüez River the most severely impacted river due to human actives of the three rivers in our study area. Previous land uses for the Guanajibo River basin were are similar in characteristic as that of the Añasco River, being mostly compromised in the sugar cane cultivation. Nowadays it seems that both rivers are having similar developmental land used trend since the sugar cane industry was discontinued and the land is devoted to urban development.

The Añasco-Mayagüez Bay is an ideal site to study natural processes and anthropogenic activities in a small geographic area (Otero *et al*., 1992) as industrial wastewater and sewage

waters are discarded directly to the Bay (Gilbes *et al*., 1996). Important industrial activities that impacted the Mayagüez Bay were the tuna canning factories between the early 60s to the early 2000s, discharging used industrial waste waters close to shore. Nowadays discharges have ceased and most companies have closed or greatly reduced operation since the start of this study (2004-2007). But the Puerto Rico Aqueduct and Sewage Authority (PRASA) has an outfall that dumps secondary water treatment plant effluents since 2002.

Precipitation in the study area

Precipitation is a periodic seasonal event, in Puerto Rico and the seasons can be divided between a dry and rainy season. The average precipitation for the Añasco-Mayagüez basin is between 200-250 cm/year (Morelock *et al*., 1983). The seasonal pattern of rainfall and river discharge in western Puerto Rico produce a marked rainy season go from April to October according to Morelock *et al*., (1983) and from August to November according to Gilbes *et al*., (1996). The dry goes from season can go from January to February (Morelock *et al*., 1983; Gilbes *et al*., 1996).

River discharge in the area

The Bay receives the discharge of three main rivers: the Añasco, Yagüez and Guanajibo Rivers. These three rivers have drainage basin areas that correspond to 479, 36 and 339 km^2 respectively (Grove, 1998; Morelock *et al*., 1983). Other minor inputs to the Bays are several small creeks like Caño Boquilla and Caño el Puente; south of the Añasco River; and Caño Corazones north of the Guanajibo River (Grove, 1977). River discharges during the rainy season have been identified as important environmental factor in the Bay (Alfaro, 2002; Gilbes, 1994; Gilbes *et al*., 1996; 2002; Grove, 1977, 1998; Rosado-Torres, 2000; Morelock *et al*., 1983).

The bio-optical properties in the Bay have a large spatial and temporal variability that can be related to discharge of the local rivers during the rainy season, is dominated by detritus, and inorganic particle absorption (Rosado-Torres, 2000). These particulate loads affect the biological and bio-optical characteristics of the Bay waters (Gilbes, 1992; Gilbes *et al*., 1996) and their influence can be recorded even at offshore stations (Rosado-Torres, 2000). In other studies tight relation between river discharge and Chl-*a* concentrations were not found in the Bay (Alfaro, 2002; Gilbes, 1992; Gilbes *et al*., 1996; Rosado-Torres, 2000).

Geological setting

The insular shelf is very narrow in the Bay between the Port of Mayagüez and the Añasco River (about three kilometers wide). A line of submerged coral reefs marks the edge of the shelf with the shelf break being about 10 to 15 meters depth. The shallowest depth measured on these barriers was six meters (Wilson Ramirez unpublished data). The shelf bathymetry is fairly irregular due to the structural and sedimentological history of the region. During lower sea level, the Añasco and Yagüez rivers discharged their sediments to the insular slope (about 80-90 meters below the present shelf break) and the shelf area was exposed to sub-aerial erosion (Wilson Ramirez unpublished data).

Circulation in the Mayagüez Bay

Circulation in the Mayagüez Bay is determined by the influence of the Caribbean-Atlantic offshore flows through the Mona Passage at the western boundary and by the local effects of barotropic tide, surface winds waves, waves and river discharges (Capella and Grove, 2002). Tide had the strongest component of circulation and variability in the Mayagüez Añasco Bay (Capella and Grove, 2002). Physical factors like semidiurnal tides and currents, have an important impact on the Bay (Alfonso, 1996). Diurnal (24-hours) and semi diurnal (12.4 hours)

tides were found to be approximately equal in magnitude in the Bay, but they can change between months (Capella and Grove, 2002).

Measured currents seeps at the Bay go from 2 to 38 cm/s with a surface currents flowing offshore, but the net flow is landward, towards the north and northeast (Capella and Grove, 2002). Strong currents are not generated due to the variability in wind direction and velocity and to the small tidal range and hence do not influence the transport of bottom sediments.

Table 1. Geographic positions, sampling depth and distance from the coast at the fixed stations in the Añasco-Mayagüez Bay from 2004-2007.

Station	Latitude	Longitude	Distance from the coast (km)
A1	18° 15' 997'' N	067° 12' 011''W	1.21
A2	18° 15' 998'' N	067° 15' 231" W	2.33
Y1	18° 12' 030'' N	067° 09' 792''W	0.38
Y2	18° 12' 023'' N	067° 12' 949''W	2.10
G1	18° 10' 255'' N	067° 11' 010''W	0.25
G2	18° 10' 049'' N	067° 14' 819''W	2.40

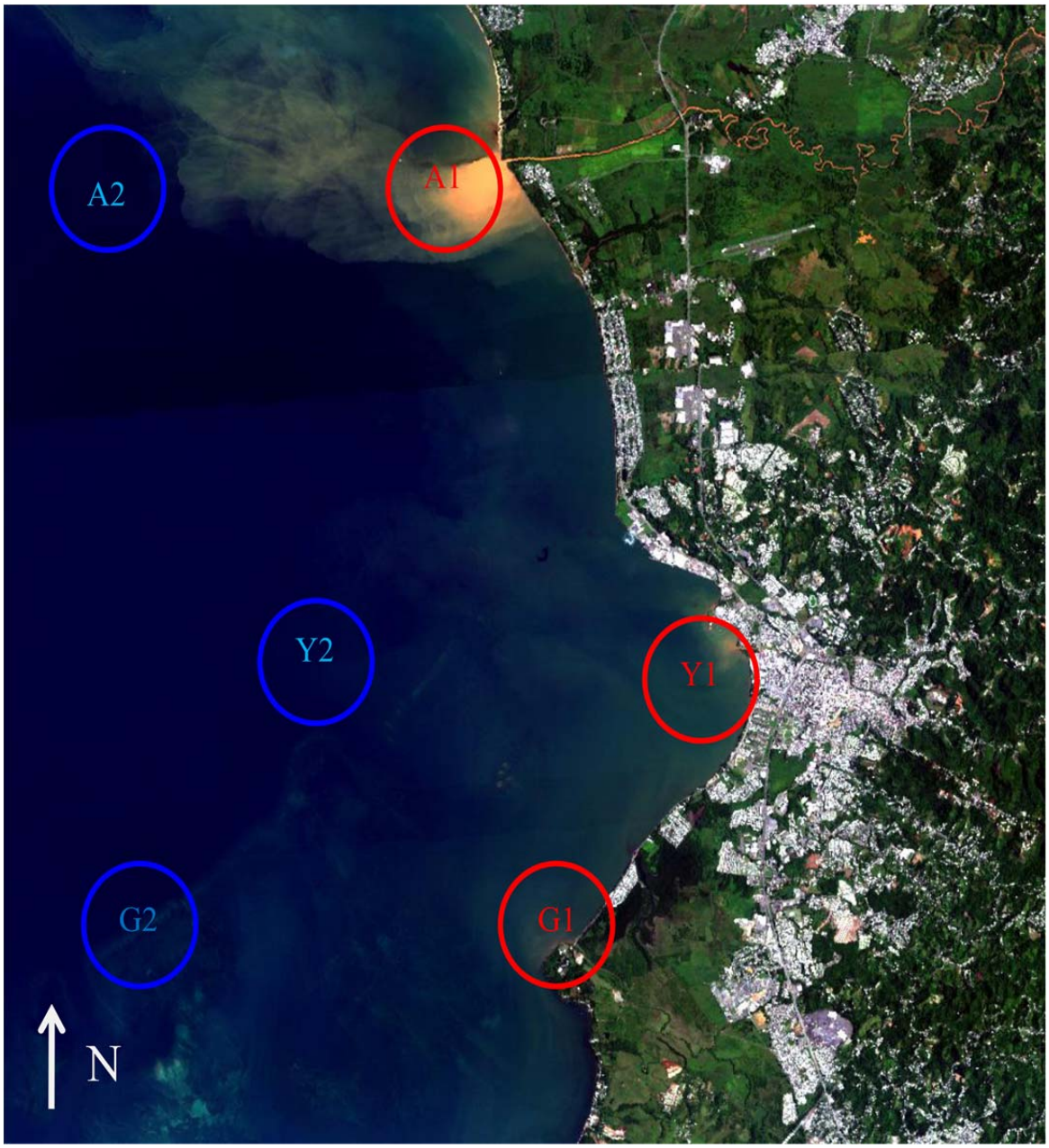

Figure 1. Mayagüez Bay Stations.

CHAPTER I
DISTRIBUTION AND SOURCES OF CDOM IN THE MAYAGÜEZ BAY

INTRODUCTION

Chromophoric Dissolved Organic Matter (CDOM) is one of the components that imprints natural water with its color and is one of the components (the other Color Detrital Material $aCDM_{412}$) that affect estimates of Chlorophyll-*a* (Chl-*a*) by remote sensing (since both absorb light at similar wavelengths) specially in coastal environments. The study of CDOM is important from the point of view of biogeochemistry the carbon cycle. Since CDOM has been estimated to be about 40-60% of the Dissolved Organic Matter (DOM) pool, one of the most important reservoirs of carbon in the biosphere (Hedges, 1992). The use of Remote Sensing Techniques to monitor this transport and biogeochemical alterations of terrestrial CDOM by rivers to the coastal zone and can help in the understanding of its role of CDOM on the primary productivity of coastal marine systems, in nutrient cycles, photochemical transport reactions and light penetration issues.

CDOM affects the quality and quantity of light (Kirk, 1994) at the lower end of the light spectrum, and is regarded as one of the most important component that control light penetration in the water column specially in the UV region (Del Castillo, 2005). CDOM optical properties make it both a reactant and controls the photochemical processes occurring in the water column, where its photoproducts are important in the biogeochemistry of Dissolved Organic Material (DOM) carbon sulfur and nitrogen cycles and included the production of a number of free radicals and hydrogen peroxides as photoproducts of CDOM (Mopper and Kieber, 2002).

Remote sensing techniques can be used to detect changes CDOM from space, airborne and *in situ* sensors. Combined with the signal of photosynthetic pigments and color detrital

material further complicating the retrieval of Chl-*a* pigment concentration estimates. When Semi-analytical algorithms are applied to determine Chl-*a* concentration these cause an overestimate of pigment concentration in coastal waters. The algorithms applied to determine Chl-*a* + degradation products concentration, have the problem of a noise signal due to the $aCDM_{412}$ and thus CDOM. This is a very active area of research where different approaches have been tested to solve this problem in the Mayagüez Bay (Rosado-Torres, 2008).

The Mayagüez Bay has a series of rivers and minor channels that drain to the Bay. It is an excellent environment in which to study the seasonal dynamics of CDOM in subtropical areas. Its small size; and great bio-optical and geo-optical variability has been related to local river discharges (Rosado-Torres, 2000, 2008; Rodríguez-Guzmán, 2008).

The Bay has the advantage that it can be relatively well sampled in one day of work; the disadvantage is that its small size causes problems with the spatial resolution of most OCS. Other sources of CDOM material related to anthropogenic inputs to the Mayagüez Bay come from municipal secondary water treatment plant, and industry residual waters from tuna canning factories. A number of previous works done in the area gave insights to different processes occurring in the Mayagüez Bay (Alfaro, 2002; Parilla, 1996; Gilbes, 1992; Gilbes, *et al*., 1996; Ludeña-Hinojosa, 2007; Rosado-Torres, 2000; 2008; Tapia-Larios, 2007; Rodríguez, 2004; Rodríguez-Guzmán, 2008).

Actually hydrological modeling (Giovanni-Prieto, 2007) and soil erosion (Rodríguez-Guzmán, 2008) models have been developed for local rivers. If all this could be integrated in the future effective models can be developed in the fate and transport for CDOM. Other studies address in the local river basins are related to nutrients transport (Corvera-Gomringer, 2005; Pérez-Alegría *et al.,* 2005; Sotomayor-Ramírez *et al.,* 2004; Villalta, 2004) bacterial inputs

(Sotomayor-Ramírez *et al.,* 2006 unpulished data) and TSS (Rodríguez-Guzmán, 2008; Villalta, 2004) to mention a few from a land-sea interface approach applied to tropical zones. The local rivers of the west coast of Puerto Rico make an excellent place to study different biogeochemical processes.

No study relating CDOM dynamics in coastal waters addressing the distribution of CDOM by local river and taking in account seasonal processes and biogeochemical alterations during estuarine mixing has been performed in Puerto Rico.

OBJECTIVES

1-Evaluate the importance of terrestrial/riverine CDOM inputs in explaining the spatial and temporal dynamics of CDOM in the Mayagüez Bay, regarding local rivers as the main source of this material.

2-To test the hypothesis that levels of terrestrial CDOM delivered by river discharge are diluted conservatively during estuarine mixing with Mayagüez Bay receiving waters. To this end perform laboratory mixing experiments between riverine and marine water end-members explore the influence of clay-mineral particles co-transported in riverine waters on CDOM behavior.

MATERIALS AND METHODS

Sampling cruises

To understand the relations between CDOM, and any other possible processes, eight fixed stations were sampled between, 2004-2007. Since sampling could not be done on an monthly basis it was decided to divide our samplings cruise by season related to river discharges. The seasons where defined as the months between December and June (dry season) and the rainy season as the months between July to November(Figure 2). Seasonality was taken in account as an important factor determining bio-optical (Rosado-Torres, 2000, 2008) geo-optical (Rodríguez-Guzmán, 2008) zooplankton ecological (Alfaro, 2002; Gilbes, 1995; Gilbes *et al*., 1996; Parilla, 1996) and geology (Grove, 1977, 1998, Morelock and Grove; 1976; Morelock *et al*., 1983; Rodríguez, 2004; Ramirez unpublished).

Field work

All the field work was done aboard the R/V Sultan and PezMar. Profiles were done at each of our eight stations to a maximum depth of 50 meters at the offshore stations, and between 3-10 meters for inshore stations (Figure 1 and Table 1) A bio-optical package that includes a SBE-19 CTD (Sea Bird Electronics Inc.) an AC-9 (WetLab Inc.) absorption and attenuation meter An Mpak3, data acquisition and power unit (WetLab Inc.) was used to collect the data from the different instruments in the bio-optical package. After transferring the data to a laptop computer another software program separated the different files generated for each individual instrument.

Data editing and processing

The raw data from the different bio-optical instruments were align by depth based on the time referenced to the CTD depth (WAP software developed by WetLab Inc) corrected them for

any instruments displacement intakes and time lag from the different sensor locations in the optical packaged. The data was separated between the up-cast and down cast; and was binned at 0.5 m for the up-cast. For the AC-9 absorption and attenuation meter profiler, three additional corrections were performed using the temperature and salinity data taken with the CTD and for scattering taken at the 715 nm channel of the same instrument (Pegau *et al*., 1997; 2003). Profiles were plotted for $aCDM_{412}$ (Color Detrital Material absorption coefficient).

CDOM sampling

CDOM samples were collected in I-Chem (Nalgen®) company amber glass bottle (125 ml) with Teflon lined caps previously cleaned in NaOH 2 N overnight, washed with HCl 20% volume/volume to neutralize the base, and then rinsed thoroughly with double distilled water. Excess water was removed from the bottle by rinsing with Fisher® Brand High Performance Liquid Chromatography (HPLC) grade methanol. Each bottle was sealed with aluminum foil that was tripled rinsed with HPLC methanol. Then these were ashed at 500^{o}C for at least 6 hour to eliminate any trace of organic matter in a muffle. GF/F filter were ashed simultaneously in an aluminum foil package, with the amber bottles. Teflon® bottle caps were soaked for two days in double distilled water that was changed daily, the caps were then soaked in HPLC grade methanol for two days and then were then oven dried overnight at 60^{o}C.

Samples were filtered through GF/F filters. These filters remove most plankton and particulate matter from the water (Kirk, 1976). But can permit that some materials not considered dissolve can be collected, in the samples like bacteria's, colloids and virus pass to the samples (Del Castillo *et al*., 2005). Another reason to favor GF/F filters is that it is accepted material for particle collection (detrital and alive) so that all components that absorb light in the water medium can be accounted measured, by optical measurements (Mitchell and Kieffer,

1984). Phytoplankton Chl-*a* absorption coefficient (Bricaud and Stramski, 1990) or detrital particles can be determining by extracting the sample from photosynthetic pigments with hot methanol (Kishino *et al*., 1985).

Water samples were taken with a pre-cleaned Van Dorne all Teflon® 4 liter bottles, after rinsing for approximately two minutes at the station. Samples where gravity filtered from the Van Dorne bottle by means of an all Teflon filtration unit (Schleicher + Schull, W. Germany) coupled to the bottle by Teflon® tubing connected to the bottle nipple. Ashed GF/F filters were manipulated by means of forceps and care was taken to not touch directly any part that could lead to contamination. Before taken taking the sample the filtration unit was purged of air and was left to drain for approximately 30 seconds, to release any possible contamination held within the filtration unit. The sampling bottles were rinsed three times with a small volume of samples before collecting. Samples are tolerant to degradation (Del Castillo *et al*., 1998) and were analyzed within two to four weeks later.

Laboratory work

CDOM optical density was determined with a Perkin-Elmer® Lambda 18 model UV/VIS dual beam spectrophotometer. The photometric precision of the instrument is ± 0.002 absorbance or an equivalent abortions coefficient of 0.046 m^{-1}. The scans were done using a 0.100 meter path length quartz cell. The cell were tripled rinsed with a minimum of three overflow rinses with Burdick and Jackson ultra pure water (certified solvent for HPLC) and then with the HPLC grade methanol to eliminate excess water. The cells were left at room temperature until completely dried and no trace of methanol was observed. Before scanning, the samples were left in a water bath at room temperature for at least one hour and then for an additional hour at room temperature.

This was done to avoid condensation on the quartz cells and to maintain the same temperature between the samples and the reference ultra pure water. Ultra pure water was used for the blank scan. Two scans were taken from each sample between 250-750 nm, at 1.0 nm interval. CDOM absorption can be expressed by and exponential decreasing function (Kirk, 1994; Del Castillo, 2004; Blough and Del Vecchio, 2002; Nelson and Siegel; 2002b) in the form

$$a_g(\lambda) = a_g(\lambda_r)\, e^{-Se(\lambda - \lambda r)} \qquad (1)$$

Or more generally

$$a_g(\lambda) = ae^{-Se\lambda} \qquad (1a)$$

Were λ is the reference wavelength, A is the amplitude and S_e (nm^{-1}) is the spectral slope parameter describing the steepness of the spectrum (Twardoski *et al*., 2004). Absorption is a proxy for the concentration, and the spectral slope (S) is used to account changes in CDOM composition including ratios of humic to fulvic acids (Carder *et al*., 1989; Blough and Green, 1995).

CDOM absorption coefficient (a_g) was calculated from the measured absorbance using the next equation

$$a_g(\lambda) = \frac{2.303\, A(\lambda)}{L} \qquad (2)$$

Where

a_g = CDOM absorption coefficient (m^{-1})
$A(\lambda)$ = absorption measured at a given wavelength
L = path length of the cell (0.100 m)

Samples were corrected for scattering of small particles and colloids by subtracting the absorption measurement at 700 nm (Bricaud, *et al*., 1981; Green and Blough, 1994).

$$a_g(\lambda)_{corr} = a_g(\lambda) - a_g(\lambda)_{700} \quad (3)$$

Where

$a_g(\lambda)_{corr}$ = absorption at a given wavelength (λ) corrected for scattering
$a_g(\lambda)$ = measured absorption at a given λ
$a_g(\lambda)_{700}$= measured absorption at 700 nm

CDOM spectral slopes (S parameter) were calculated as suggested by (Del Castillo, 2004) from the linear-least-square regression of the plot of $\ln a_g(\lambda)$ vs. wavelength, and were reported using the convention for an exponential decay fitting as a positive numbers.

A non-dimensional factor named "slope ratio" was calculated using several spectral slopes in the UV and visible (Helms *et al*., 2008). This approach has the convenience of avoiding of using values near the detection limit of the instrument focusing in areas where absorption change during estuarine mixing and photochemical alteration. The greatest alterations is S between samples of different sources occurs in narrow band between 275-300 and 350-400 nm (Helms *et al*., 2008). Even though the recommended band for the S-ratios determination was not used a similar region between 250-300 nm and 300-350 nm was evaluated as other regions. It was concluded the best results were obtained at the lowest possible wavelengths as suggested (Helms *et al*., 2008).

Chl-*a* measurements

Water samples were collected in duplicates in 500 ml plastic dark Nalgen® bottles from an inboard pump connected to a plastic hose that was lowered to the desired depth. The samples were immediately introduced in an ice chest full of ice during and were distributed so that they could be fully surrounded by ice to lower their temperature as fast as possible.

Samples were filtered through Whatman GF/F upon arrival to the laboratory. During the filtration procedure care was taken to avoid the exposition to ambient light by covering the filtration unit with aluminum foil. The filter containing the sample was immediately transferred to in plastic 15 ml centrifugation tubes and wrapped aluminum foil and stored at –20^{o}C overnight. The next day the tubes were filed with 10.00 ml of HPLC grade methanol; and left overnight in the refrigerator at -4^{o}C until the next day..

Chl-*a* concentration were measured by the fluorometric methods without acidification (Phinney and Yentsch, 1985; Welschmeyer, 1994) using a Turner TD-700 Bench Model Fluorometer (±.0001) equipped with a Non-Acidification optical Kit.

Chl-*a* concentrations were determined by

$$Chl\text{-}a\ (\mu g/l) = F_0 v / V_f \qquad (4)$$

F_0 = fluorescence measurement
v = volume of methanol used for extraction
V_f = volume of sea water filtered

A previous calibration curve was performed using a *Anacystis nidulans* Chl-*a* standard (Sigma Aldrich Cat. # C5753); a five point dilution. Chl-*a* concentration was expressed in µg/l based on average samples duplicate.

Gravimetric measurements of Total Suspended Sediments (TSS)

Water samples for TSS were collected as previously described for the Chl-*a* samples. Duplicated samples were collected in 3.78 liter plastic containers for offshore stations and 1.89 liter containers for inshore stations. The water samples were filtered through 47mm Millipore® HA 0.45 µm nitrocellulose filter. These filters were previously oven-dried over-night at 60^{o}C and pre-weighed ± 0.0001g, and stored individually in a desiccator over silica gel prior to being used.

Two sub-samples were taken after vigorously shaking the container for five minutes. Filtered volume varied between station (inshore and offshore) and depended on the amount of material present in the sample. Filtration was stopped when the filter became clogged and heavily "colored" and was recorded to the nearest tenth of liter. Filters were rinsed three times, with a small volume of de-ionized water to eliminate salts and collect remaining particles on the filtration unit. Samples were later oven dried over-night at (60^{o}C). The next day the filters were left cool for an hour in a desiccator, and were re-weighted.

TSS was calculated by difference in weight

$$TSS\ weight\ (mg) = (filter + sediments\ weight) - filter\ weight \qquad (7)$$

TSS concentration was determined as

$$TSS\ (mg/l) = \frac{TSS\ weight\ (mg)}{Filtered\ volume\ (l)} \qquad (8)$$

River discharge Data

River discharge data was downloaded from the waterdata.usgs.gov. from (January 1, 2004-June 30, 2007) for the Añasco and Guanajibo Rivers data is not available for the Yagüez River (Figure 2). One of the concerns was to define the cruise as being representative for a dry or rainy season's month based on river discharges. A mean was calculated for the cruise day discharge and the three previous day. A mean was calculated using the weekly discharge, a bi-weeks discharge and a fourth a monthly river discharge. In some instances discharge records were not available for a given day or time period, the values had to be inspected manually and corrected for the lack of data. This was done to avoid any bias at the time to calculate the river discharge means.

After an initial evaluation it was decided that any month having a total river discharge (sum of the Añasco and Guanajibo River discharges) lower that 10 m^3/s was defined as a dry month, discharges higher than 10 m^3/s were grouped has rainy season month. After making this "arbitrary" category for a dry or rainy season cruise we performed an ANOVA analysis between the total river discharge means between seasons were significantly different.

Statistical analysis between different variables analysis

Student T–test were performed to determine if there were significant differences between the rainy and dry season and between inshore and offshore stations in the values of CDOM a_{g355}, $S_{300\text{-}350}$, a_{CDM412}, Chl-*a*, TSS, and salinity. In most cases replicates were collected from the same sampling bottle or from water pumped collected in large volumes making these pseudo-replicates. The statistical significance is reported ($p < 0.05$) as significant or non significant ($p > 0.05$). Regression analyses were conducted between dependent CDOM $a_{g355,}$ spectral slope (S), S-ratios (S_r), taken as dependent, using in turn as independent variables, were taken as dependent variables and salinity, TSS and Chl-*a*.

RESULTS

Monthly river discharge for the Añasco and Guanajibo Rivers showed the same a general seasonal pattern for both rivers (Figure 2). During the rainy season the Añasco River had slightly larger mean river discharges for most of the sampling dates. Only in one instance, the Guanajibo River had a larger discharge (almost double) than the Añasco River (July 19, 2005) probably due to heavy precipitation at that river basin. August 2005 was the month with the highest mean river discharge followed by October 2005. The months with the lowest discharges during the rainy season were August 2004 and October 2006. During the dry season the Guanajibo River had relatively lower mean river discharges than the Añasco River, both rivers demonstrated the lack of precipitation at their basin. February 2004 and March, 2005, where the months with the lowest discharges of the dry season. During high to extreme precipitation events, very high river discharges were recorded the same day, indicating that increases precipitation discharge relation was tightly coupled observed in very short time scales (hours) as observed at the river flow and met monitoring stations.

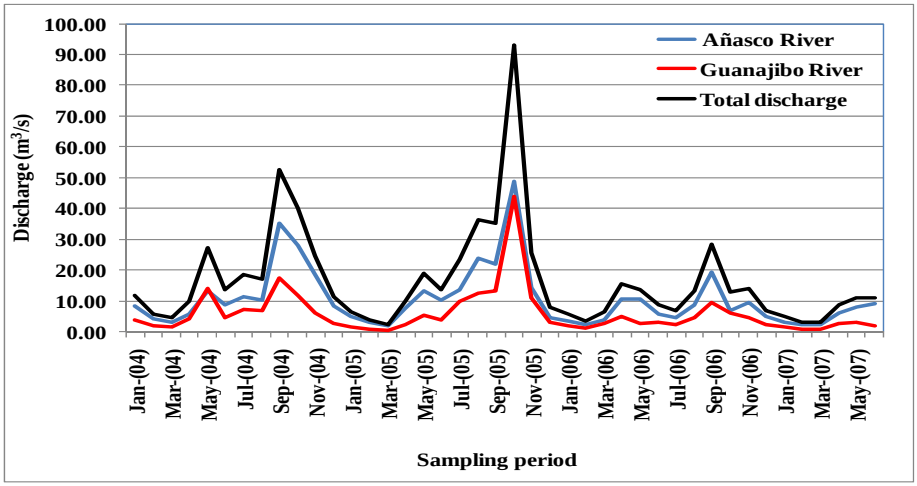

Figure 2. Daily river flow (m^3/s) for the Añasco and Guanajibo Rivers during the study period (USGS waterdata.usgs.gov.).

Seasonal river discharge

Previous studies suggested that seasonal river discharge was the principal factor controlling the optical properties in the Mayagüez Bay and in some instances river influence could be detected far (12 km) offshore (Cruise and Miller, 1994; Rosado-Torres, 2000). Sampling cruises were assigned to a dry or rainy season dates (Table 3) in order to evaluate the impact of seasonal river discharge on the fate and transport of terrestrially derived materials in the Mayagüez Bay. Dry season dates were considered to be those with mean discharges of < 10 m^3/s. where higher discharges dates were considered rainy season. ANOVA analysis (Table 2), confirmed statistically significant differences ($p < 0.05$) between the dry and rainy season regardless of period considered in calculated mean discharge (Table 2).

Table 2. ANOVA analysis evaluating four different mean river discharges to categorize the cruises as belonging to a dry or rainy season.

Time period of calculated mean discharge	p-value	significance
Same cruise day + three previous day	p = 0.0020	significant
weekly	p = 0.0003	significant
bi-weekly	p = 0.0255	significant
monthly	p = 0.0245	significant

Table 3. Cruises as defined by the total river discharge as classified to a dry or rainy season.

Dry season	Rainy season
January 12-14, 2004	August 19, 2004
February 12, 2004	July 19, 2005
March 10, 2005	August 17, 2005
December 6, 2005	September 20, 2005
March 8, 2006	October 19, 2005
April 21, 2006	September 26, 2006
May 1-2, 2007	October 26, 2006

T-test between inshore and offshore stations

We proceeded to evaluate the possibility of pooling spatial data if the means between inshore and offshore stations were not significantly different. It was decided to perform a Student T-test. The statistical analysis indicated that non-significant differences ($p < 0.05$) were observed between inshore and offshore for all the evaluated variables permitting the pooling of the data in one mean values for inshore stations and another for offshore stations per cruise.

But, the T-test demonstrated significant differences ($p > 0.05$) between inshore and offshore stations comparison and between A1-A2 and G1-G2 for the evaluated variables (Chl-*a*, CDOM a_{g355}, TSS and $aCDM_{412}$, and salinity). The analysis demonstrated significantly higher mean values for most of the variables inshore stations and lower means for offshore stations. The only exception was salinity with lower mean salinities recorded at inshore stations. The spectral slope is an interesting case since non significant differences spectral in slope mean values ($p > 0.05$) were observed spatially (inshore-inshore, Inshore-offshore and offshore-offshore) throughout the Bay. No significant differences ($p > 0.05$) were observed between dry and rainy season spectral slope values T-test analysis.

Table 4. Spatial Student T-test analysis between inshore and offshore stations.

T-test comparison between stations				P(T<=t) two-tail	(N=)*	(N=)**	Significance p < 0.05
Variables	**Student T-test comparison between**	**Mean***	**Mean****				
Salinity	**Inshore* and offshore****	**34.78**	**35.29**	**0.0003**	**31**	**37**	**S**
Salinity	A1inshore* and G1 inshore**	34.91	34.64	0.30	10	10	NS
Salinity	A2 offshore*and G2 offshore**	35.25	35.34	0.60	11	11	NS
Chl-*a*	**Inshore* and offshore****	**0.70 (ug/l)**	**0.28 (ug/l)**	**7.6 E-07**	**35**	**23**	**S**
Chl-*a*	A1inshore* and G1 inshore**	0.51 (ug/l)	0.75 (ug/l)	0.08	12	12	NS
Chl-*a*	A2 offshore*and G2 offshore**	0.32 (ug/l)	0.28 (ug/l)	0.69	11	12	NS
TSS	**Inshore* and offshore****	**7.93 (mg/l)**	**2.76 (mg/l)**	**8.0E-05**	**35**	**24**	**S**
TSS	A1inshore* and G1 inshore**	9.38 (mg/l)	8.95 (mg/l)	0.89	12	12	NS
TSS	A2 offshore*and G2 offshore**	2.43 (mg/l)	3.04 (mg/l)	0.54	12	12	NS
a_{g355}	**Inshore* and offshore****	**0.55 (m^{-1})**	**0.22 (m^{-1})**	**2.4E-07**	**35**	**23**	**S**
a_{g355}	A1inshore* and G1 inshore**	0.59 (m^{-1})	0.59 (m^{-1})	1.00	12	11	NS
a_{g355}	A2 offshore*and G2 offshore**	0.22 (m^{-1})	0.21 (m^{-1})	0.69	12	11	NS
$aCDM_{412}$	**Inshore* and offshore****	**0.73 (m^{-1})**	**0.13 (m^{-1})**	**9.6E-07**	**24**	**36**	**S**
$aCDM_{412}$	A1inshore* and G1 inshore**	0.49 (m^{-1})	0.93 (m^{-1})	0.06	8	10	NS
$aCDM_{412}$	A2 offshore*and G2 offshore**	0.18 (m^{-1})	0.045 (m^{-1})	0.089	9	11	NS
Spectral slope	Inshore* and offshore**	0.016 (nm^{-1})	0.017 (nm^{-1})	0.058	35	23	NS
Spectral slope	A1inshore* and G1 inshore**	0.017 (nm^{-1})	0.016 (nm^{-1})	0.14	12	11	NS
Spectral slope	A2 offshore*and G2 offshore**	0.017 (nm^{-1})	0.017 (nm^{-1})	0.44	12	11	NS

Table 5. Temporal T-test results between the different measured variables between dry and rainy season.

Student T-test comparison between seasons			P(T<=t) two-tail	Dry season (n)	Rainy season (n)	Significance p < 0.05
Variables	**Dry season mean**	**Rainy season mean**				
Salinity	**35.51**	**34.82**	**9.0E-08**	**23**	**45**	**S**
Chl-*a*	**0.41**	**0.62**	**0.025**	**23**	**35**	**S**
TSS	5.76	6.03	0.86	24	35	NS
$CDOMa_{355}$	**0.29**	**0.51**	**0.001**	**23**	**35**	**S**
$aCDM_{412}$	0.35	0.37	0.90	26	16	NS
Spectral slope	0.017	0.016	0.06	23	35	NS

Salinity in the Mayagüez Bay

Spatial salinity distribution analysis between inshore and offshore stations ($p > 0.05$) showed significantly lower mean salinities 34.79 (n = 31) at inshore stations and higher mean salinities at offshore stations 35.29 (n = 38) (Table 4). Temporal T-test analysis demonstrated seasonal salinities differences ($p > 0.05$) between the dry season 35.52 (n = 23) and rainy season 34.84 (n = 45) means(Table 5). Even though salinities are well within marine water values, the differences between the dry and rainy season means, was 0.68 PSU salinity, a minimal difference, but sufficient to be statistically significant in the T-test analysis.

Lower salinities due to river discharge can be noticed only at inshore stations during the rainy season; offshore stations lower salinities were observed only during high to extreme river discharges as small salinity reductions. The variability between inshore and offshore stations is minimal and measured salinities are always maintained at marine water values. This suggests that at our stations the riverine end-member are is highly diluted in marine waters.

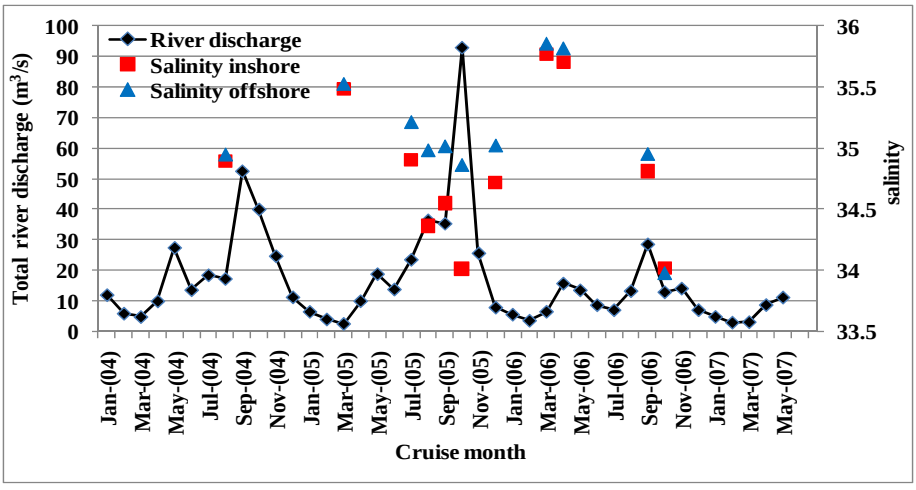

Figure 3. Monthly mean total river discharge (m^3/s) vs. Salinity for inshore and offshore stations.

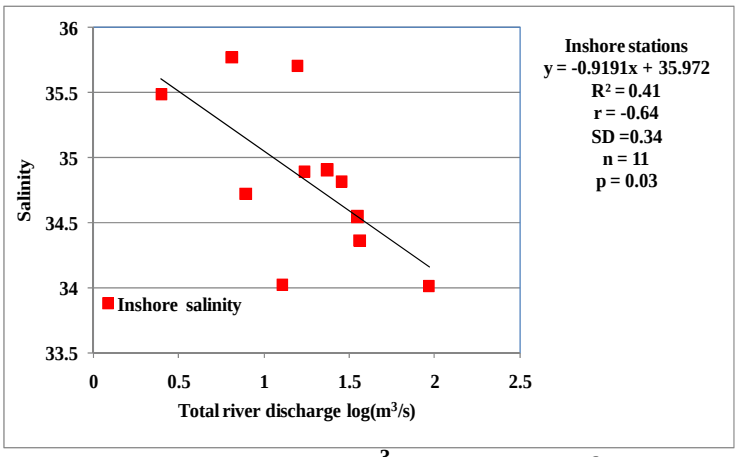

Figure 4. Total river discharge log(m^3/s) vs. Salinity for inshore stations.

Regression analysis between Salinity and other variables

Moderately significant correlations were found between salinity vs. inshore a_{g55}; and Salinity vs. inshore S-ratios ($p < 0.05$). Borderline significant correlation ($p = 0.07$) was found between Salinity vs. inshore Chl-*a* and Salinity vs. offshore Chl-*a* ($p = 0.07$); and Salinity vs. inshore spectral slope. (Table 6).

Table 6. Regression analysis between Salinity and the different measured variables between inshore an offshore stations.

	Regressed					
Station	X	Y	R^2	r	n	p
Inshore	**Salinity**	**CDOM a_{g355}**	**0.48**	**-0.69**	**11**	**0.02**
Offshore	Salinity	CDOM a_{g355}	0.06	-0.25	11	0.46
Inshore	Salinity	TSS	0.03	-0.18	11	0.59
Offshore	Salinity	TSS	0.0007	-0.002	11	0.94
Inshore	**Salinity**	**Chl-*a***	**0.32**	**-0.57**	**11**	**0.07**
Offshore	**Salinity**	**Chl-*a***	**0.35**	**-0.59**	**11**	**0.07**
Inshore	**Salinity**	**S. Slope**	**0.31**	**0.56**	**10**	**0.09**
Offshore	Salinity	S. Slope	0.14	0.37	10	0.29
Inshore	Salinity	$aCDM_{412}$	0.01	-0.10	10	0.78
Offshore	Salinity	$aCDM_{412}$	0.0005	-0.02	10	0.95
Inshore	**Salinity**	**S-ratios**	**0.42**	**0.65**	**10**	**0.04**
Offshore	Salinity	S-ratios	0.0002	0.02	10	0.97

CDOM (a_{g355}) absorption coefficient

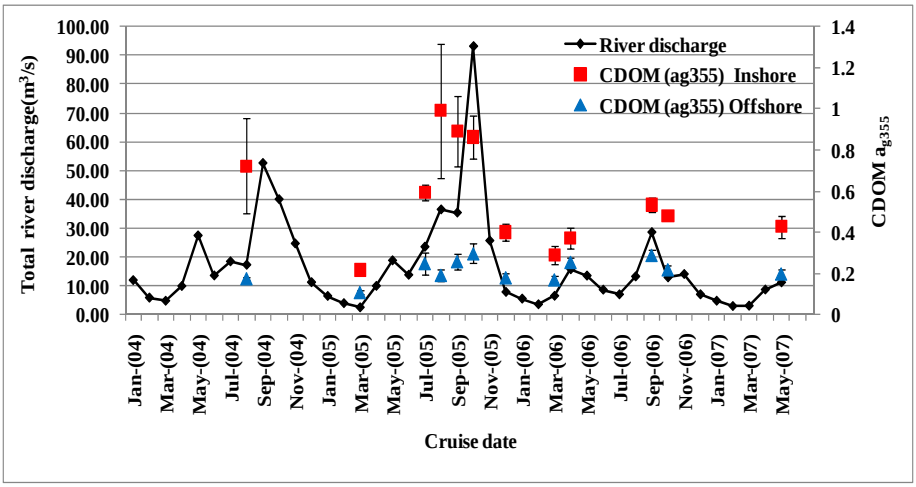

Figure 5. Monthly mean total river discharge (m^3/s) vs. CDOM a_{g355} for inshore and offshore stations.

Inspection of the monthly total river discharge vs. CDOM a_{g355} time series, suggests that a tight relationship might be established between river discharge and CDOM a_{g355} at inshore stations. The low CDOM a_{g355} values and lack of variability observed at offshore stations might suggest a minimal river influence at offshore stations.

CDOM a_{g355} T-test

Spatial CDOM a_{g355} distribution between inshore and offshore stations demonstrated significant differences ($p < 0.05$) between inshore 0.55 m^{-1}($n = 35$) and offshore stations 0.22 m^{-1} ($n = 23$) (Table 4). Non-significant differences ($p > 0.05$) were observed between inshore-inshore means, offshore-offshore means comparison; indicating that similar processes are acting at inshore stations (like river discharge mixing and resuspension) that maintain similar CDOM a_{g355} values Lowe values at offshore stations may be the results of mixing and photo-degradation process.

Temporal CDOM a_{g355} distribution between dry and rainy season indicates that significant differences ($p < 0.05$) exist between the means for the dry 0.29 m^{-1} ($n = 23$) and rainy season 0.51 m^{-1}($n = 35$) (Table 5).

Regression analysis between Salinity and other variables

Since salinity is the variable of choice to study mixing and dispersion processes occurring in the marine environment, it was used to regress against the other variables (Table 6). Salinity regressed against CDOM a_{g355} demonstrates a moderately significant inverse correlation ($R^2 = 0.48$; $p < 0.05$) in Mayagüez Bay. Also a moderately significant inverse correlation ($R^2 = 0.41$; $p < 0.05$) was established between river discharge and salinity (Figure 4). These relationships indicate that inshore stations are exposed to a significant low salinity high CDOM input, coastal rivers.

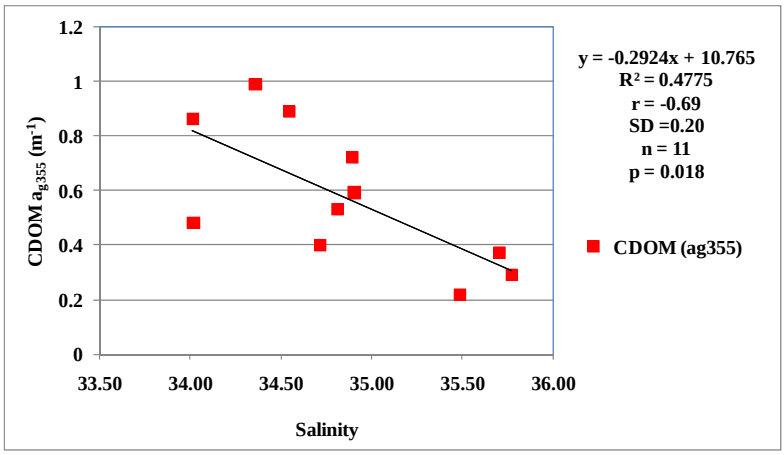

Figure 6. Correlation analysis between Salinity vs. CDOM a_{g355} for inshore stations.

Spectral slope related results

Total river discharge vs. spectral slope separated between inshore and offshore stations, present very similar spectral slope magnitudes for inshore and offshore stations. This marked

lack of variability suggests that the spectral slope the marine end-member overwhelms the terrestrial contribution to the spectral signature of Mayagüez Bay CDOM. Or said on other way the terrestrial riverine CDOM signature is greatly diluted in the receiving water medium

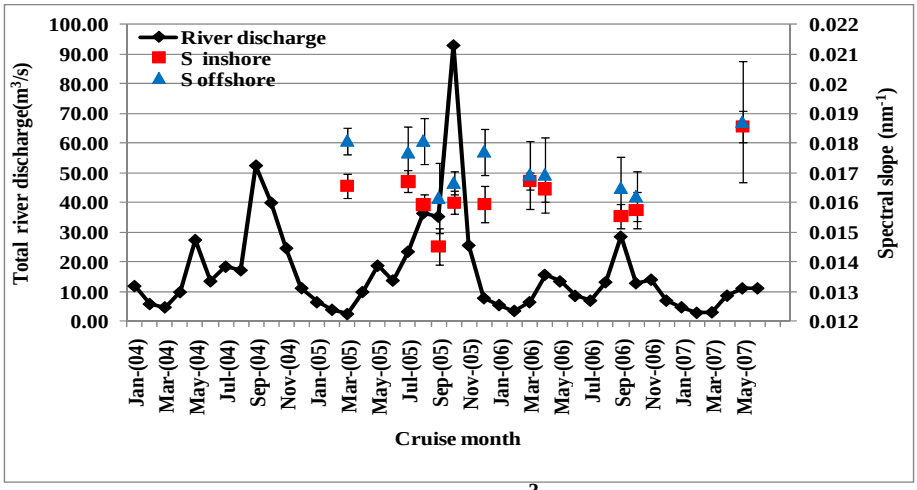

Figure 7. Monthly mean total river discharge (m^3/s) vs. spectral slope (300-350 nm) for inshore and offshore stations.

Spectral slope T-test analysis

Spatial TSS T-test analysis demonstrated non-significant ($p > 0.05$) differences between inshore spectral slope 0.016 nm^{-1} ($n = 35$) and offshore stations 0.017 nm^{-1} ($n = 23$) means (Table 4). Temporal TSS T-test analysis demonstrated non-significant ($p > 0.05$) differences between the dry season 0.017 nm^{-1} ($n = 23$) and rainy season 0.016 nm^{-1}; ($n = 35$) means (Table 5).

Spectral slope co-variation between different variables

Spectral slopes were not found to co-vary with any of the variables measured. In only one instance was co-variation found between salinity and spectral slope.

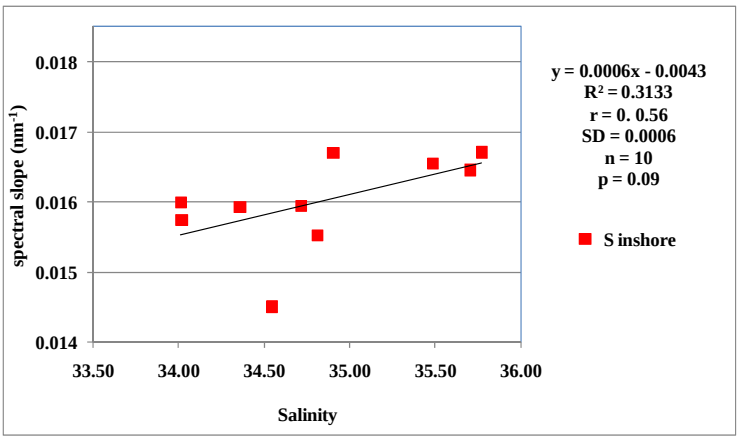

Figure 8. Correlation analysis between Salinity vs. Spectral slope (300-350 nm).

Spectral slope-ratio

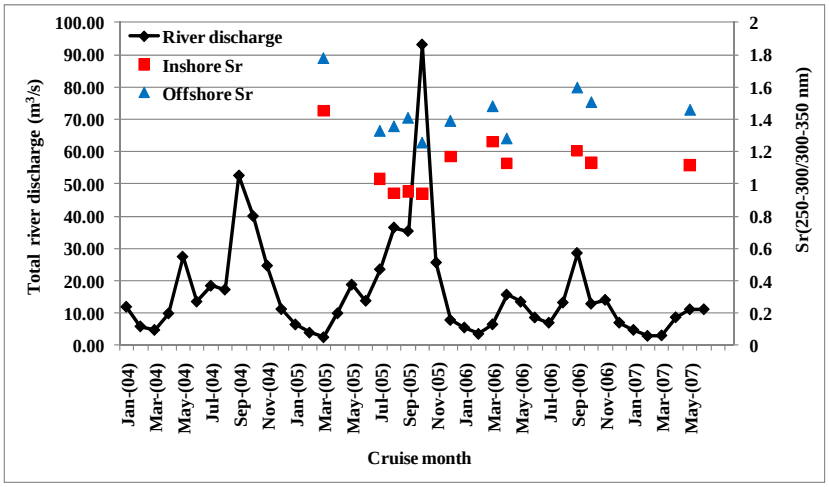

Figure 9. Monthly mean total river discharge (m^3/s) vs. S-ratios for inshore and offshore stations.

The comparison between (Figure 7 and Figure 9) monthly river discharge vs. spectral slope and monthly river discharge vs. S-ratios, suggests that a similar behavior is observed (Figure 9). These suggest that, S-ratios may be a more useful proxy of spectral differences than provide than spectral slopes. Error bars are not presented since these are ratios and are thus dimensionless.

The comparison amongst between the correlations between salinity and S (Figure 9) and Salinity vs. S-ratios (Figure 10) indicates a significantly higher determination coefficient R^2 = 0.42; ($p < 0.05$) of the latter. The use of the S-ratios suggests that it has the capability of resolving processes related to changes in the spectral slope that are impossible to observe by using only the spectral slope.

The lack of evidence of other processes acting on CDOM like microbial or photochemical degradation and desorption of some material cannot be dismissed. But river discharge seems to be an important factor controlling the distribution of CDOM. Offshore stations had poor determination coefficients ($R^2 < 0.40$) indicating that other processes like microbial or photodegradation might be important CDOM sinks that alter CDOM spectral slope. Resolving the contribution of these process on the spectral slope modification is difficult, and adding the dilution processes further complicates the evaluation. Another CDOM source, may be phytoplankton production.

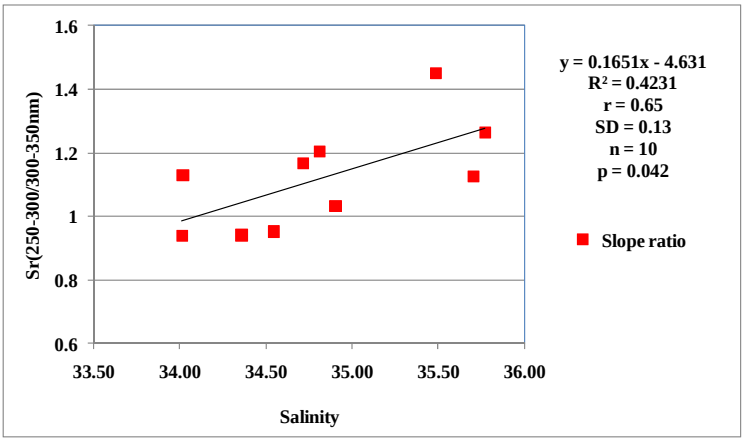

Figure 10. Correlation analysis between Salinity vs. spectral slope ratio.

Total Suspended Solids

Mean monthly total river discharge vs. TSS suggests that higher concentrations are found at inshore stations and lower at offshore stations (Table 11). Mean TSS concentrations at offshore stations are maintain in fairly constant values levels with a minimum of variability through the sampling period. Only in one event, higher mean concentrations were recorded which that corresponded to a high river discharge event. At inshore stations a greater variability in TSS concentration can be observed than in offshore stations (Figure: 11).

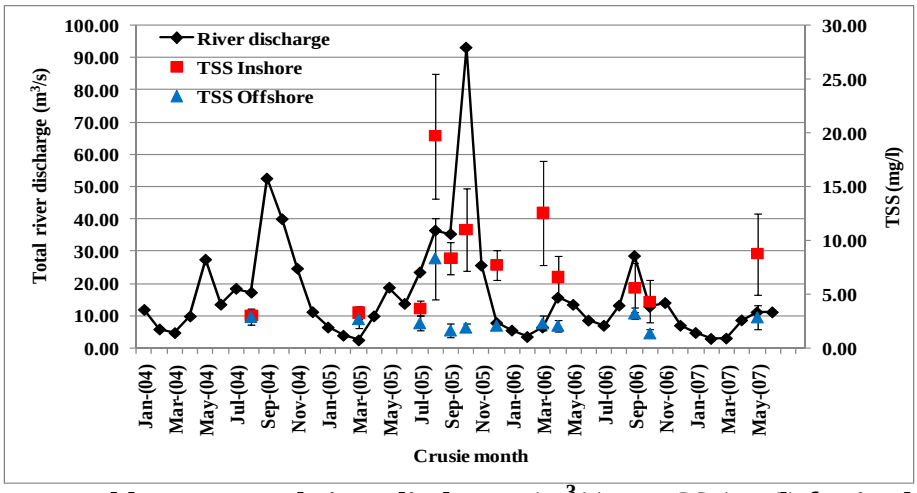

Figure 11. Monthly mean total river discharge (m^3/s) vs.TSS (mg/l) for in shore and offshore stations.

Spatial TSS T-test analysis demonstrated significant differences ($p < 0.05$) between inshore 7.93 mg/l ($n = 36$) and offshore 2.76 mg/l ($n = 23$) stations means (Table 4). No-significant differences were observed between inshore-inshore and offshore-offshore stations comparison (Table 5). TSS distribution observed at the A1-A2 and G1-G2 stations suggest that higher concentrations of TSS can be related to river discharge or to other inshore shore processes.

Temporal TSS T-test analysis, demonstrated non-significant ($p > 0.05$) differences between the dry season 5.76 mg/l ($n = 24$) and rainy season 6.03 mg/l ($n = 35$) means. Similar

TSS concentrations may arise from quite different coastal processes such as resuspension by wave action and river discharge events during opposite seasons.

Regression between TSS and other parameters

The only strong, positive correlation (Figure 13), was found in the inshore stations between TSS as independent variable, and $aCDM_{412}$, ($R^2 = 0.77$, $p < 0.05$). This co-variability inshore, appears to be sustained regardless of seasons likely the resultants of a combination of processes on the near shore waters. These may fueled by energy from river discharge wind, waves and tides on a wide range of time scales.

Table 7. Regression analyses between TSS and the different measured variables.

Station	Regressed X	Regressed Y	R^2	r	n	P
Inshore	TSS	CDOM a_{g355}	0.23	-0.48	11	0.14
Offshore	TSS	CDOM a_{g355}	0.039	-0.20	11	0.56
Inshore	TSS	Chl-*a*	0.0003	0.02	12	0.96
Offshore	TSS	Chl-*a*	0.03	-0.17	12	0.58
Inshore	TSS	S	0.006	-0.08	10	0.82
Offshore	TSS	S	0.29	0.54	10	0.11
Inshore	TSS	S Ratio	0.22	-0.47	11	0.14
Offshore	TSS	S Ratio	0.0024	-0.05	11	0.89
Inshore	**TSS**	**CDM**	**0.77**	**0.88**	**10**	**0.0008**
Offshore	TSS	CDM	0.012	-0.11	10	0.77

Since $aCDM_{412}$ is an index abundance of colored organic suspended particulate pool (+ CDOM pool), its covariance with TSS is consistent. This results suggests that a large share of the TSS is in effect particulate organic matter (POM), as it explains 77 % of the variability

Physical processes other than simple conservative mixing may need to be invoked to explain the lack of correlation between Salinity and TSS (Figure 12). The lack of correlation of TSS with other variables suggest a complexity of unresolved factors (beyond river discharge and thus salinity) that cannot be entirely related to river discharges and thus salinity can influence the distribution of TSS in the Bay (Table 7).

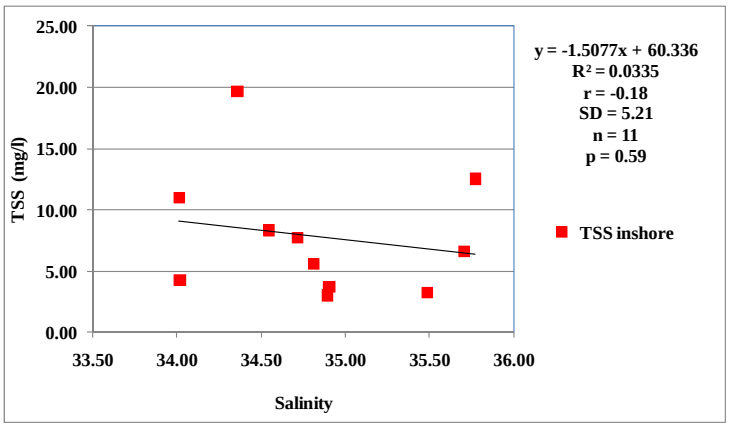

Figure 12. Correlation analysis between Salinity vs. TSS (mg/l).

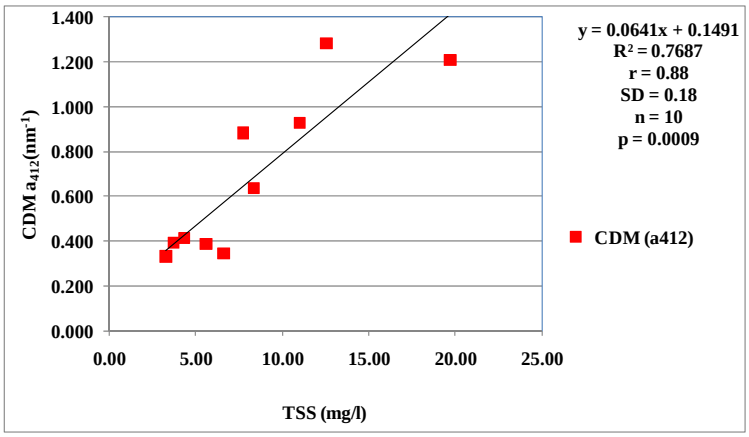

Figure 13. Correlation analysis between TSS (mg/l) vs. aCDM$_{412}$.

Color Detrital Material aCDM$_{412}$.

Mean monthly total river discharge vs. a CDM$_{412}$ suggests that higher concentrations of aCDM$_{412}$ are found inshore and lower are found offshore (Figure 14). Higher concentrations observed during high river discharge would be expected to be related to salinity.

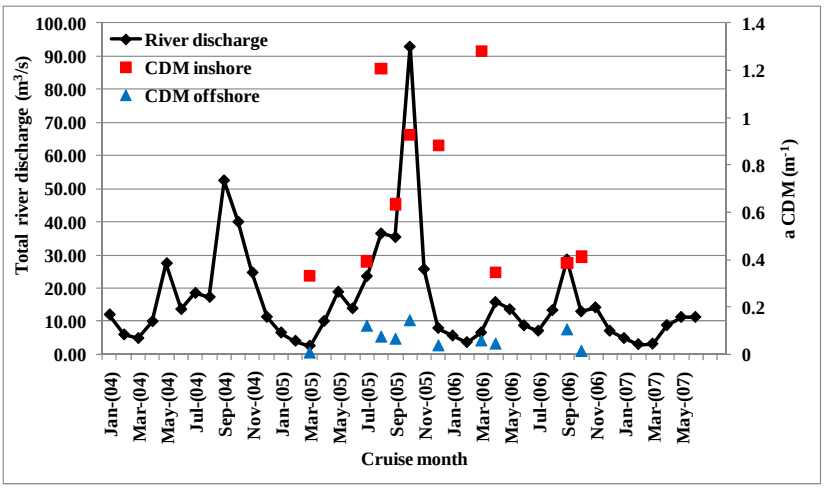

Figure 14. Monthly mean total river discharge (m^3/s) vs. $aCDM_{412}$ for inshore and offshore stations.

Spatial $aCDM_{412}$ T-test analysis demonstrated significant differences in means ($p < 0.05$) between inshore 0.73 m^{-1} ($n = 24$) and offshore 0.13 m^{-1}($n = 36$) stations (Table 4). Temporal $aCDM_{412}$ T-test analysis between seasons demonstrated non-significant differences ($p < 0.05$) between the dry 0.35 m^{-1} ($n = 21$) and rainy of 0.37; ($n = 43$) season means (Table 5).

$aCDM_{412}$ relation with other variables

Regression analysis performed between $aCDM_{412}$ used as the independent variable did not demonstrated any significant correlation with the other measured variables (Table 8). As previously discussed only $aCDM_{412}$ demonstrated a tight correlation with TSS used as the independent variable.

Table 8. Regression analysis between CDM and the different measured parameters.

Station	Regression		R^2	r	n	p
	X	Y				
Inshore	$aCDM_{412}$	S slope	0.002	-0.05	10	0.90
Offshore	$aCDM_{412}$	S slope	0.019	-0.14	10	0.70
Inshore	$aCDM_{412}$	S Ratio	0.082	0.29	10	0.42
Offshore	$aCDM_{412}$	S Ratio	0.280	0.53	10	0.12

Chl-*a* distribution relation in the Bay.

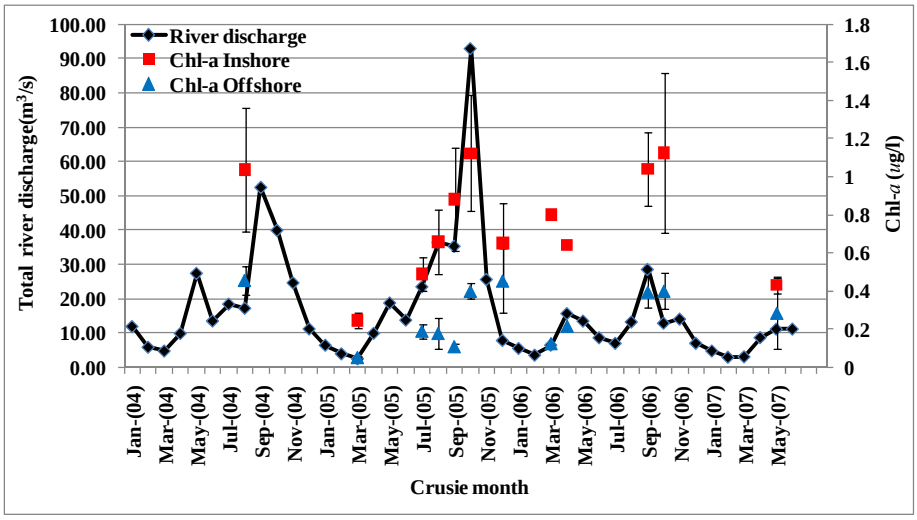

Figure 15. Monthly mean total river discharge (m^3/s) vs. Chl-*a* (µg/l) for inshore and offshore stations.

Mean monthly total river discharge vs. Chl-*a* suggests that higher concentrations are found at inshore stations and lower at offshore (Figure 15). Mean TSS concentrations, at offshore stations, are maintained in fairly constant values with a minimum of variability through the sampling period. Inshore stations demonstrated a greater Chl-*a* variability that may be related to river discharge.

Chl-*a* T-test analysis

Spatial Chl-*a* T-test analysis demonstrated significant differences ($p < 0.05$) between the inshore station of 0.70 µg/l (n = 37) and offshore mean 0.28 µg/l (n = 23) stations means (Table 4). Temporal Chl-*a* T-test analysis demonstrated significant differences ($p< 0.05$) between the dry 0.41 µg/l (n = 23) and rainy season 0.62 µg/l (n = 35) means (Table 5). .

Table 9. Regression analyses between Chl-*a* vs. the different measured variables.

	Regression					
Station	X	Y	**R^2**	**r**	**n**	**p**
Inshore	Chl-*a*	CDOM a_{g355}	0.058	0.24	11	0.45
Offshore	Chl-*a*	CDOM a_{g355}	0.054	0.23	11	0.47
Inshore	Chl-*a*	$aCDM_{412}$	0.025	-0.16	10	0.66
Offshore	Chl-*a*	$aCDM_{412}$	0.051	-0.23	10	0.53
Inshore	**Chl-*a***	**S. slope**	**0.335**	**-0.58**	**11**	**0.06**
Offshore	Chl-*a*	S. slope	0.046	-0.21	11	0.53
Inshore	Chl-*a*	S. ratio	0.170	-0.41	11	0.21
Offshore	Chl-*a*	S. ratio	0.067	-0.26	11	0.44

Chl-*a* regression analysis demonstrated a lack of co-variation between Chl-*a* and other dependent variables $R^2 = 0.34$ ($p > 0.06$) only Chl-*a* vs. inshore spectral slope demonstrated a borderline significance (Table 9).

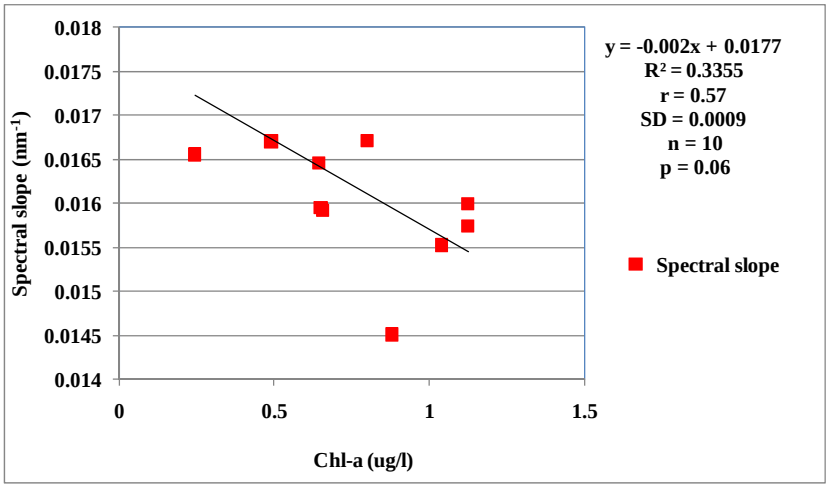

Figure 16. Correlation analysis between Chl-*a* (µg/l) vs. TSS (mg/l).

DISCUSSION

Salinity distribution in the Mayagüez Bay

River systems are fundamental to the global carbon cycling because they receive produce, transport, and transform organic material and therefore link the terrestrially produced organic matter with marine environments (Hedges *et al.,* 1997). Previous works in the Mayagüez Bay have shown an inshore to offshore salinity gradient, (Alfaro, 2002; Parilla, 1996; Rosado-Torres, 2000; Gilbes, 1992; Gilbes *et al*., 1996; Tapia-Lario, 2007). Low salinities of 31-33 psu were measured by Gilbes *et al*., (1996; 2002), at inshore stations (closer to shore than during the present study) which they related to high river discharge to the Bay during the rainy season.

Salinity T-test spatial analysis (temporally pooled), (Table 4) demonstrated that significant differences ($p < 0.05$) were observed between inshore 34.78 ($n = 31$) and offshore 35.29 ($n = 37$), within a range of values that spanned from a minimum 33.20 to a maximum of 35.91 psu for the entire study period). Fresh water discharge to the Mayagüez Bay resulted in a maximum proportional dilution of 7 % of the highest observed salinity of the marine receiving waters. Temporal T-test analysis (spatially pooled) also demonstrated significant differences ($p < 0.05$) between dry 35.51 ($n = 23$) and rainy 34.82 ($n = 45$) seasons (Table 5). Even though statistical significant spatial differences were found, the water column was well-mixed at 1 meter, depth at which the samples were taken.

Regression analysis between river discharge and salinity (Figure 3) indicates a moderately significant inverse relation $R^2 = 0.41$; $p < 0.05$ ($n = 11$), indicating that river discharge explains only the 41 % of the variance of salinity. Fresh water discharge by rivers onto the Bay disperses as a this surface layer of low salinity turbid/colored water that is visible

due to the contrast at fronts with the marine end-member. Our sampling missed this thin surface layer as samples and *in situ* instrument measurements were taken at 1m-depth. Our observations on the measured variables are, therefore of a fixed 1m deep subsurface layer that has undergone significant additional mixing as compared to the visible surface slick.

Significant covariation related to CDOM a_{g355} are those between salinity vs. spectral slope (Figure 8) $R^2 = 0.31$ ($p > 0.05$) and Salinity vs. slope ratios (Figure 10) $R^2 = 0.42$ ($p < 0.05$). Borderline covariation where found between Salinity vs. Chl-*a* at inshore and offshore stations. Regression analysis using salinity as the independent variable demonstrated only moderate covariation with the other variables at inshore stations (Table 6).

CDOM a_{g355} Salinity relation

The regression analysis between salinity and CDOM a_{g355} (Figure 6) demonstrated a significant ($p < 0.05$) inverse relation $R^2 = 0.48$ ($n = 11$). Since it was established that river discharge co-varies with salinity, and salinity varies with CDOM $a_{g355,}$ this suggest that, river discharges influence CDOM inputs to the Bay.

In a number of estuarine areas, salinity and CDOM have been showed to covary conservatively in an inverse relation (Blough *et al.,* 1993; Bowers *et al.,* 2000; Del Castillo *et al.,* 1999; 2000a; Hu *et al.,* 2003; Hong *et al.,* 2005; Retamal *et al.,* 2007; Rochelle-Newall and Fisher, 2002b). Photochemical and biological processes cause only small, negligible variations in the relatively high concentrations of CDOM in estuarine systems, which explains the apparently conservative behavior of CDOM (Blough and Del Vecchio, 2002; Rochelle-Newall and Fisher, 2002b; Kowalczuk *et al.,* 2003; Chen *et al.,* 2004). Small variations make difficult the assessment and quantification of changes due to lack of appropriate temporal and spatial resolution of all relevant processes.

But non-conservative CDOM behavior has been reported in other estuaries (Alberts *et al.,* 2004; Chen *et al.,* 2003; Chen *et al.,* 2007; Gallegos, 2005; Zepp *et al.,* 2004).

At the salinities encountered at our stations, CDOM a_{g355} demonstrated conservative mixing behavior. This can be explained , by the relatively minor proportion of fresh river water, compared to the dominant proportion of the receiving sea water, in which the riverine end-member becomes highly diluted. It would require the addition of a mass of CDOM, far greater than that supplied by local sources, in order to significantly alter the marine end-member CDOM values. Influence of terrestrial CDOM flux from rivers is restricted to a small region near the river mouth.

Flocculation and adsorption processes only take place significantly at low salinity (< 8). At the higher salinities predominant in Mayagüez Bay (33.20 to 35.91 psu), the occurrence of these processes is limited or negligible and of difficult quantification Changes in ionic strength and the presence of particulates were proposed to be important in driving the removal of CDOM (Shank *et al.,* 2005). The high molecular weight (HMW) fraction of CDOM appears to preferentially participate in sorption/desorption reactions with suspended particulates leading to selective modification of CDOM spectral composition during its transited from river to ocean as well as within bottom sediments in the pore water (Mannino and Harvey, 1999; 2000; Shank *et al.,* 2005). As a result, CDOM spectra may become relatively enriched or devoid of absorption signal (a slope and slope-ratios) at corresponding spectral regions. More studies in turbid environments are needed to understand the processes that affect the distribution of organic compounds among particulate and dissolved phases.

River plumes have two characteristic regions based on optical properties. The first is a region where CDOM absorption changes due to dilution but where optical properties (spectral slope and fluorescence) do not change due to dominance of the freshwater end-member at salinities < 30 psu; and the other is where both absorption and the other optical properties change with increasing salinity found above > 30 psu (Del Castillo, 2005). In our study salinities were > 30. Significant terrestrial CDOM optical signature contribution is observed.

CDOM (a_{g355}) absorption coefficient distribution

CDOM has a well established inshore-offshore gradient with higher absorption coefficients found near its terrestrial origin and a decrease occurs towards offshore waters (Vodacek *et al.,* 1997; Boss *et al.,* 2001; Rochell-Newall and Fisher, 2002b). These relation of higher concentration near the coast and lower at offshore waters was noticed in the Mayagüez Bay. A marked statistical significant difference ($p < 0.05$) was observed between inshore 0.55 m^{-1} ($n = 35$) and offshore 0.22 m^{-1} ($n = 23$) stations, with inshore stations having 2.5 times more CDOM a_{g355} than offshore stations.

Significant differences in CDOM a_{g355} were observed between seasons ($p < 0.05$). The mean absorption coefficient for the dry season was 0.23 m^{-1} ($n = 23$) and for the rainy season is 0.51 m^{-1} ($n = 35$). The lowest absorption coefficients (almost half) recorded for the dry season can be related to minimal terrestrial allochtonous CDOM sources; evidence of lack of riverine inputs, with the dilution effect with offshore waters. In Tampa Bay, seasonality was clearly linked to variations in river discharge rates, suggesting that CDOM was primarily derived from river inputs (Chen *et al.,* 2007). Other removal processes that can be working in the Mayagüez Bay are Photo-degradation (Blough and Del Vecchio, 2002) and microbial degradation (Amon and Benner, 1996a; Blough and Del Vecchio, 2002; Hermes and Benner, 2003), CDOM

concentrations were two fold higher during the rainy period than during the dry season in Lower St. Johns River (Gallegos, 2005), similar to what has been observed in the present study. Elsewhere, higher CDOM a_{g355} absorption coefficients were recorded during spring than during summer due to higher river discharges in the spring (Chen and Gardner, 2004; Chen *et al.,* 2004; Nelson and Guarda, 1995; DeGrandpre *et al.,* 1996; Vodacek *et al.,* 1997; Boss *et al.,* 2001).

After evaluating Salinity vs. CDOM a_{g355} spatial and temporal distribution the next step was to answer the next questions

a-Are the local rivers really an important CDOM source to the Mayagüez Bay?

To answer these question we proceeded to compare our measured CDOM a_{g355} values with CDOM values from the Caribbean Sea, Western Tropical North Atlantic (WTNA), Atlantic Ocean, and Gulf of Mexico (Figure 17). It becomes evident that the absorption coefficients measured at the Mayagüez Bay are higher than those reported from the selected end-members Caribbean Time Series (CaTS), Bermuda Atlantic Time Series (BATS), and WTNA.

Mean CDOM a_{g355} surface values reported for CaTS, 0.100 m^{-1} (Méndez-Silvagnoli, 2008), are half those found in the present study for offshore stations, but are of similar magnitude as those reported for the Gulf of Mexico (Green and Blough, 1994). Inshore stations had CDOM a_{g355} mean values almost six times higher than those reported for CaTS surface waters (Méndez-Silvagnoli, 2008). Only during high Amazon River plume discharges, are CDOM a_{g355} slightly higher than those found at our inshore stations(Del Vecchio and Subramaniam, 2004).

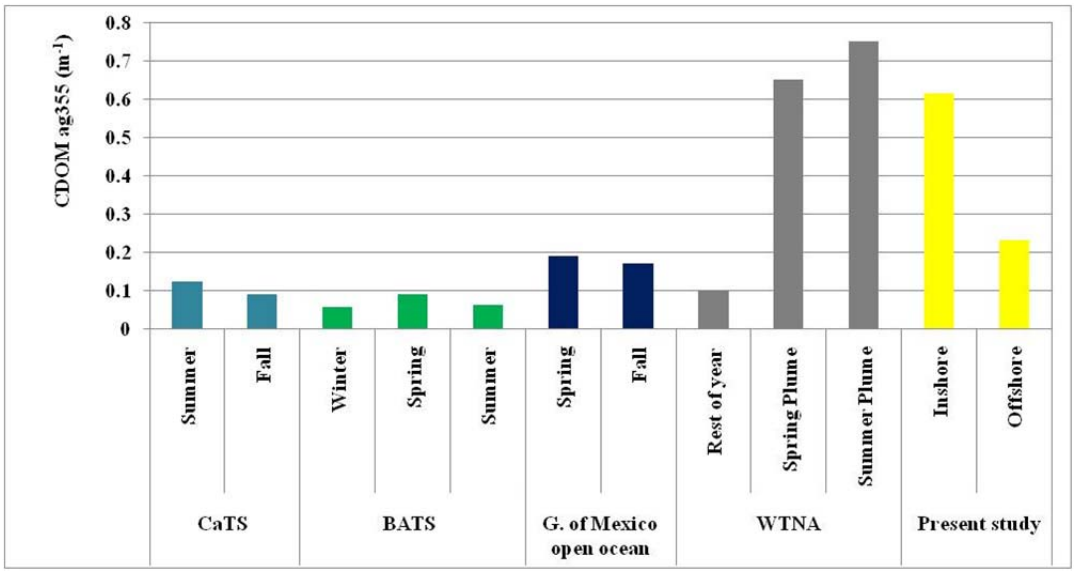

CaTS (Méndez-Silvagnoli, 2008)
BATS (Nelson *et al.*, 1998)
Gulf of Mexico (Green and Blough, 1994)
Western Tropical North Atlantic (Del Vecchio and Subramaniam, 2004)

Figure 17. CDOM a_{g355} comparison between CaTS, Atlantic Ocean, Gulf of Mexico and Western Tropical North Atlantic and Mayagüez Bay.

To further corroborate the importance of CDOM in the Mayagüez Bay, two previously published empirical correlation models between salinity and CDOM a_{g355} were evaluated (Méndez-Silvagnoli, 2008 and Del Vecchio and Subramaniam, 2004);. *In situ* measured salinity was used to calculate the modeled CDOM $a_{g355,}$ (Figure 18).

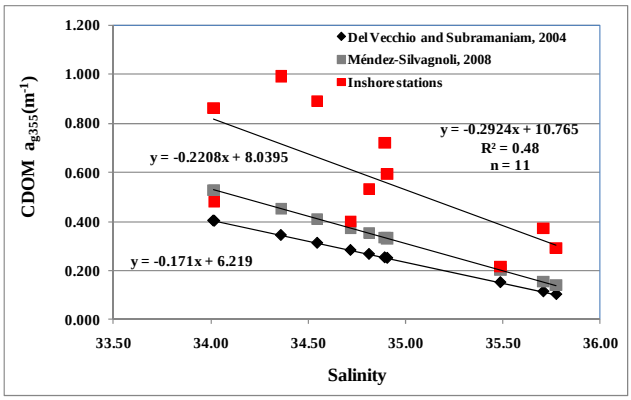

Figure 18. CDOM a_{g355} dependency on Salinity measured for the Mayagüez Bay inshore station compared to other previously published works.

After including our data set on the generated plot it results obvious that in most of the cases our CDOM a_{g355} values are found above those modeled for CaTS and WTNA (Figure 18). On three occasions measured values were found on the dilution line modeled for CaTS (Méndez-Silvagnoli, 2008). This suggests that most of the time CDOM a_{g355} measured at our salinities, are found above those of CaTS and of the WTNA, evidencing significant allochtonous CDOM sources, such as local river discharge or bottom sediments

Our measured CDOM a_{g355} values located within the dilution line of CaTS are more difficult to explain, since low CDOM values are found with low salinity suggesting that CDOM a_{g355} occurrences was diluted possibly by and extreme river discharge. The high salinity low CDOM a_{g355} situation can be explained by mixing, advected offshore waters of low CDOM a_{g355} and high in salinity, photodegradation and biological degradation. could explain this observation. It is important to mention that all our mean inshore CDOM a_{g355} values were above those measured in Caribbean surface waters (0.100 m^{-1}) by Méndez-Silvagnoli (2008). Offshore Mayagüez Bay stations had mean CDOM a_{g355} double of those reported for Caribbean surface waters, it is possible that minor contribution of terrestrial CDOM can still be important at our inshore stations with other processes like mixing being the most relevant.

b-Are the spectral slopes of CDOM measured in Mayagüez Bay different from those of surrounding oceanic end-members (Caribbean Sea or Atlantic Ocean)?

The second question that we wanted to answer was if the spectral slopes from the Mayagüez Bay mean 0.017 nm^{-1} (n = 58) were different from those of our marine end-member.

Firstly Spectral slopes from the Mayagüez Bay (Figure 19) were of similar magnitude between seasons (winter-spring; summer-fall) and from inshore-offshore.

Secondly These spectral slopes were of similar magnitude as those of CaTS; WTNA and the Gulf of Mexico during spring.

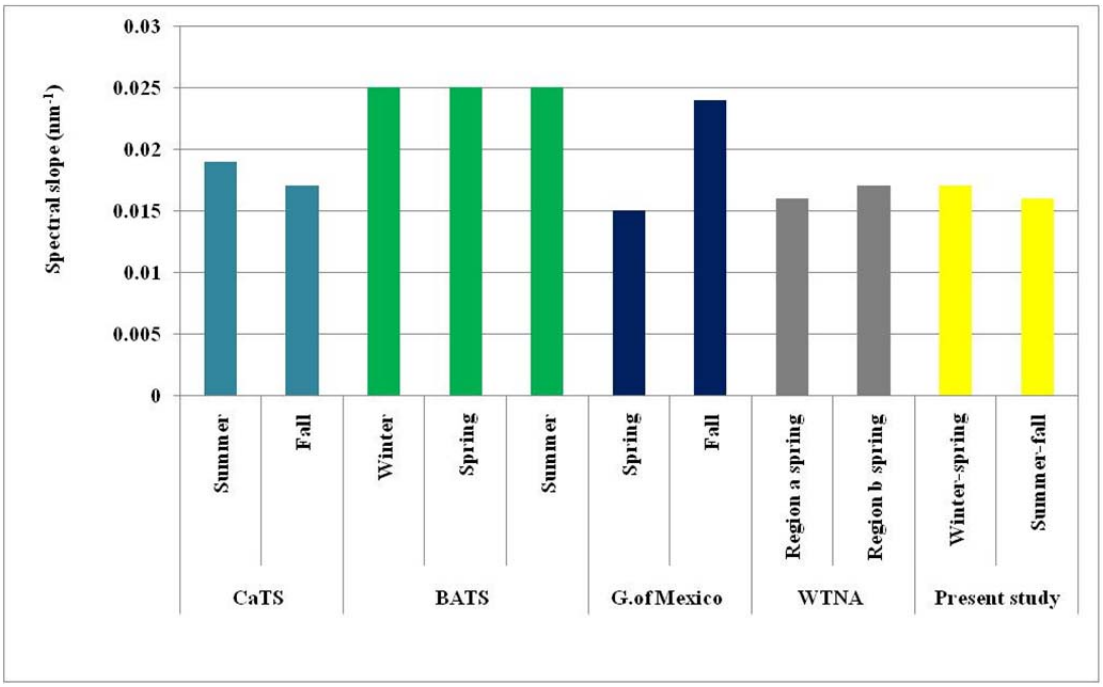

CaTS (Méndez-Silvagnoli, 2008)
BATS (Nelson *et al*., 1998)
Gulf of Mexico (Green and Blough, 1994)
Western Tropical North Atlantic (Del Vecchio and Subramaniam, 2004)

Figure 19. Spectral slope comparison between Caribbean, Atlantic Ocean, Gulf of Mexico and Western Tropical North Atlantic and Mayagüez Bay.

Thirdly BATS had higher spectral slopes, than our offshore stations.

Fourthly Inshore waters have a marked terrestrial CDOM input (very high CDOM a_{g355}), of similar spectral slope as that found in CaTS. But at our inshore and offshore stations spectral slope cannot be differentiated from those of Caribbean surface waters. Where the mean spectral slope values for inshore and offshore stations (0.017 m^{-1}) at Mayagüez Bay are similar to those found in other coastal areas (0.013-0.018 m^{-1}) that are influenced by river inputs (Blough and Del Vecchio, 2002).

TSS in Mayagüez Bay

TSS inshore-offshore gradient has been previously reported in other studies from the Mayagüez Bay (Gilbes, 1994; Gilbes *et al*., 1996, Otero *et al*., 1992; Parilla, 1996; Rodríguez-Guzmán, 2008; Rosado-Torres, 2000). Statistically significant differences ($p < 0.05$) were found between inshore 7.93 mg/l; ($n = 35$) and offshore stations 2.76 mg/l; ($n = 23$). Similar TSS concentrations for inshore, and offshore stations 7.5 and 2.7 mg/l respectively were reported for the Mayagüez Bay (Rodríguez-Guzmán, 2008).

In some studies larger concentrations than those reported here where found by other researchers in the Mayagüez Bay. Concentrations between 0.1- 40.0 mg/l were obtained during a two-day study in the Mayagüez Bay (Otero *et al.,* 1992). TSS concentrations 80-100 mg/l were recorded near the Añasco River (Gilbes, 1992). Large river discharge at the Guanajibo River resulted in mean concentration of 0.4 g/l (400 mg/l) (Cruise and Miller, 1994).

TSS concentrations during the present study were similar to those reported for other estuarine systems. Mean concentrations of 12.55 mg/l were reported for the Conway Estuary in North Wales (Bowers *et al*. 2004). Between 15 and 22 mg/l were reported in the Zuari Estuary India during non-monsoon (Menon *et al*., 2006). During a cold front TSS varied between 0.50-5.67 mg/l in the Mississippi River (D'Sa *et al*., 2006).

Maximum concentrations were recorded near Guanajibo River, 27.6 mg/l and for the Yagüez 18.5 mg/l station (Rosado-Torres, 2000). These concentrations were similar to those, found during the present study 24.15 mg/l for Añasco and 28.45 mg/l for Guanajibo River respectively. During a six-month study period TSS concentrations ranged between 0.02-14.6 mg/l in the Mayagüez Bay (Parilla, 1996).

TSS used as re-suspension evidence

No significant difference ($p > 0.05$) was noticed between the dry and rainy season means TSS concentration. The mean values for the dry season were 5.76 mg/l; ($n = 24$) and for the rainy season 6.03 mg/l; ($n = 35$). Non significant differences were obtained using our data set and additional observations by Rodríguez-Guzmán (2008). Lower river discharge and similar TSS concentrations during the dry season can be related to bottom resuspension and thus affect the correlation since this is a source of material not related to riverine sources and thus to salinity. Higher TSS concentrations were associated with shoreline proximity and not only attributed to river discharge, but also, was related to re-suspension events (Rodríguez-Guzmán, 2008). This could only mean that seasonal re-suspension and minor river discharge during the dry season can maintain TSS concentrations at similar levels during both the dry rainy seasons.

Re-suspension events in the Mayagüez Bay are mostly observed during the dry season (Alfonso, 1995; Cruise and Miller, 1994; Gilbes *et al*., 1996; Miller *et al*., 1994; Otero, *et al*., 1992; Rodríguez-Guzmán, 2008; Rosado-Torres, 2008). Wave action can cause continued suspension of the mud in the Mayagüez Bay (Morelock *et al*., 1983). Bottom sediments re-suspension can liberate CDOM pumped from the sediments, contributing significant sources of CDOM in coastal areas (Del Castillo *et al.,* 2000; Del Castillo, 2005; Boss *et al.,* 2001). Mayagüez shelf sediment samples contained up to 2.5% organic carbon derived from vascular plant detritus plants indicating a land source (Morelock *et al*., 1983). It is possible that significant CDOM inputs can be liberated from bottom sediments through resuspension processes in the Mayagüez Bay, The same physical processes that causes resuspension causes the mixing and further dilution of materials in the water column. This might explain the similar

spectral slopes observed between seasons and the lower absorption coefficients found during the dry season.

Regression analysis between TSS and the other measured variables

The lack of covariance between salinity and TSS can be related to physical processes independent of river discharges that influence the TSS distribution Table 6). The lack of relation with other variables suggests that complex factors can influence the concentration of TSS. The only significant co-variation found between TSS as independent variable was with $aCDM_{412}$ (Figure 13) in a positive relation $R^2 = 0.77$ ($p < 0.05$) (Table 7 and 8). This covariance can be related to a common factor acting simultaneously on both variables. Detritus and CDOM was found to dominate absorption at the inshore stations (Rosado, 2000). Salinity correlation between both of these variables did not demonstrate any relation suggesting that other processes (other than river discharge), can be controlling these variables. $aCDM_{412}$ has a strong detrital matter particle and CDOM signal component that is subject to same physical processes as those acting on TSS. River discharges and bottom resuspension could be acting as a source TSS and $aCDM_{412}$ explaining the tight relation between these two variables. The poor relation between TSS and CDOM a_{g355} ($R^2 = 0.23$) can be related to complex processes relation controlling both variables. CDOM absorption had no significant correlation with TSS during the dry season (Chen *et al.,* 2007). Coastal estuarine areas are areas of high productivity, intense physical process (like mixing due to currents, tides) and seasonal variability of material and multiple sources of freshwater, this makes them a complex region for the study of biogeochemical processes (Chen and Gardner, 2004).

Another problem related to Chl-*a* and TSS relationship was documented indirectly with the possible underestimation of Chl-*a* concentrations due to adsorption of Chl-*a* to clay-mineral

particles, increasing sediment concentration enhanced the problem (Rosado-Torres, 2008). The adsorption of Chl-*a* pigment to clay mineral particles is one important possibility that has to be further investigated and taken into account in all further studies.

Spectral slope

Temporal T-test analysis demonstrated non-significant differences ($p > 0.05$) in spectral slope means between the dry 0.017 nm^{-1} ($n = 23$) and rainy season 0.016 nm^{-1}($n = 35$). The spatial distribution T-test analysis (Table 4) also demonstrated non-significant differences ($p > 0.05$) between inshore 0.016 nm^{-1} ($n = 35$) and offshore stations 0.017 nm^{-1} ($n = 23$). This indicates that, CDOM of very similar spectral slopes are found during both seasons and between inshore and offshore stations. This lack of variability in CDOM spectral slope can in the future be an advantage in the development of remote sensing algorithm that used fixed CDOM spectral slopes. Dry season CDOM a_{g355} is half that of the rainy season, yet the spectral slopes are of similar magnitudes. Our measured spectral slopes are within those found for the coastal areas 0.013-0.018 nm^{-1} (Blough and Del Vecchio, 2002).

CDOM distribution is mainly determined by coastal riverine and shelf bottom inputs as sources, and photodegradation as a sink at the surface, (Boss *et al*., 2001). It is only at salinities > 30 when optical properties (fluorescence and spectral slope) in a river plume start to be diluted by marine waters and marine waters dominate the optical signature (Del Castillo, 2005).

But, in this case since inshore and offshore waters have similar spectral slope, the only clue that the S comes from terrestrial source in the higher absorption coefficients found at inshore. At the measured salinities it should be inferred that spectral slope of marine water CDOM should dominate them to be yet we found to be undistinguishable between inshore and offshore waters.

Other possible factors like photodegradation and microbial alteration of CDOM shifting the spectral slope to higher values cannot be dismissed but similar spectral slopes can confirm that a common factor is controlling CDOM distribution and maintaining its optical properties at inshore and offshore station possibly being dilution by mixing the most likely responsible.. Other processes like *in situ* production of CDOM by decomposing organic matter deposited in bottom sediments or altered by digenetic processes and later liberated from pore water could be a more reasonable explanation for the distribution of CDOM in the Mayagüez Bay. Understanding CDOM distribution can be complicated by physical advection and by local mixing which transport and erase signatures associated with sources and sinks respectively (Boss *et al*., 2001).

Chl-*a* for the Mayagüez Bay

Temporal T-test analysis demonstrated significant differences ($p < 0.05$) in Chl-*a* mean concentration between the dry 0.41 μg/l (n = 23) and rainy season 0.62 μg/l nm^{-1}(n = 35). Inshore and offshore Chl-*a* distribution concentrations were not only related to local river discharges during the rainy season (Gilbes *et al*., 1996). But can also be related to regional events as inputs from the Amazon and Orinoco River (Müller-Karger *et al*., 1989, Morell and Corredor, 2001) , during the rainy season (Gilbes *et al.,* 1996).

The spatial distribution T-test analysis (Table 4) demonstrated significant differences ($p < 0.05$) in Chl-*a* mean concentration between inshore 0.70 μg/l (n = 35) and offshore stations 0.28 μg/l (n = 23). In previous studies, a marked Chl-*a* inshore-offshore spatial distribution was reported for the Mayagüez Bay (Rosado-Torres, 2000; Alfaro, 2002; Parilla, 1996; Gilbes, 1992; Gilbes *et al*., 1996; Ludeña-Hinojosa, 2007; Tapia-Larios, 2007).

Chl-*a* distribution in the Mayagüez Bay

In the Mayagüez Bay had maximum concentrations up to 2.4 µg/l were reported at Añasco River mouth (Gilbes, 1992; Gilbes *et al*., 1996). Chl-*a* concentrations between 0.4-10.75 µg/l where found at inshore stations (Parilla, 1996). During the dry season Chl-*a* ranged from 0.3-0.9 µg/l (Otero *et al.,* 1992). The highest value measured at inshore stations was 11.75 µg/l, and the lowest value 0.097 µg/l was for offshore station (Rosado-Torres, 2000). Chl-*a* concentrations at inshore stations reached maximum values of 1.47-1.21 µg/l, with minimum of 0.08 µg/l for offshore stations station (Ludeña-Hinojosa, 2007). During the present study maximum Chl-*a* concentration found where 2.20 µg/l for inshore and minimum of 0.03 µg/l for offshore stations.

Maximum Chl-*a* concentrations previously reported for the Mayagüez Bay were not observed during the present study it seems that Chl-*a* are actually lower than those previously reported for the Bay, this needs further investigation. Actual lower Chl-*a* concentrations could be related to the fact that during previous studies (Alfaro, 2002; Gilbes, 1992; Gilbes *et al*., 1996; Parilla, 1996; Rosado-Torres, 2000), inputs from a primary treatment plant, tuna canning factory disposal of used water and agricultural practices increased nutrients inputs to the Bay. Other studies in two Indian estuarine zones recorded that the spatial distribution of Chl-*a* was 3.3-5.0 µg/l (Menon *et al*., 2006).

Correlation analysis performed between Chl-*a* as the independent variable demonstrated that the only co-variation that could be identified was between Chl-*a* and spectral slope (Table 9) for inshore stations (Figure 16). The lack of correlation between Chl-*a* and CDOM a_{g355} indicates that phytoplankton do not have a marked role in the production of CDOM in the Mayagüez Bay or at least mixing mask any possible phytoplankton production of CDOM. A

similar result was observed in Tampa Bay were a poor correlation between a_{g400} and Chl-*a* indicates that phytoplankton did not controlled CDOM abundance (Chen *et al.,* 2007). Poor relationship between CDOM and Chl-*a* concentration has been reported in other studies, implying that CDOM is not directly released by phytoplankton (Nelson *et al.,* 1998; Rochelle-Newall *et al.,* 1999; Rochell-Newall and Fisher, 2002a; DeGrandpre *et al.,* 1996).

CDOM is not directly released by phytoplankton through cell lysis or zooplankton grazing, a secondary processes mediated by bacterio-plankton can be responsible for the increase of CDOM in field and laboratory experiments (Rochell-Newall and Fisher, 2002a). The possibility that phytoplankton could be an important source of CDOM by in the Bay has to be further investigate. When salinity was used as the independent variable it Chl-*a* demonstrated a borderline significant co-variation (Table 6) with inshore R^2= 0.32; $p > 0.05$ ($n = 11$) and offshore R^2= 0.35 ($p > 0.05$ $n = 11$). During the present work no evidence of Chl-*a* relation with CDOM a_{g355} could be identified suggesting that phytoplankton was not a direct sour of CDOM to the Mayagüez Bay and that Riverine and other coastal related processes could mask any possible CDOM related production from phytoplankton. High temporal frequency variability suggest that other processes that controlling CDOM distribution have a masking effect in the contribution from other source, but there is no means to resolved these processes (Boss *et al.,* 2001).

Spectral slope ratio S-ratios

Spectral slope Ratio (S-ratios) was calculated to determine the possible modification of CDOM along a small salinity gradient as measured during the present study. We observed S-ratios values of 1-1.45 at salinities between 34-35.8 psu. At salinities between 0-30 psu, higher values of S-ratios of 1.6-1.8, were observed for the Delaware Estuary Helms *et al*., (2008). It should be mentioned that our S-ratios were not calculated in the spectral region suggested by

Helms *et al*., (2008). In our case we used the 250-300 nm and 300-350 nm ranges instead of the suggested 275–295 nm and 350–400 nm region. Differences in the S-ratios can be related to photobleaching, mixing; flocculation or microbial alteration or production of CDOM and inputs from marshes and sediments. At the high salinities recorded in our study it is difficult to determine the relative importance of each of the above mention factors in regulating CDOM S-ratios can give information on the transformations and CDOM history in natural waters A comparison between salinity and spectral slope and salinity and S-ratios correlation analysis indicates that the salinity vs. S-ratios relation demonstrated a better fit with a significant positive relation. CDOM.

Photodegradation

The main problem here is how to differentiate between the effects of photodegradation and the effects caused by turbulent mixing on dilution on CDOM distribution. Significant transformation of CDOM in surface waters by the action of photodegradation occurs over temporal scales days/weeks and spatial scales of tens of kilometers (Morell and Corredor, 2001). Our study covers spatial scales of only 2.5 km from shore and temporal observations spaced more than one month apart. Within the available resolution of this study changes due to photodegradation would be undetectable Similar spectral slope values between Mayagüez Bay stations and Caribbean waters might suggest that relatively rapid mixing processes are occurring in short time and spatial scales. This causes that changes that take longer time periods cannot be resolved and that mixing between end-members with similar spectral slopes can mask any phtodegradation processes. Due to our stations proximity to shore, mixing should be considered as the most important factor controlling CDOM distribution (Del Castillo, personal communication).

CONCLUSION

1-An inshore-offshore gradient prevails for the variables TSS, Chl-*a*, CDOM a_{g355}, $aCDM_{412}$ with higher values inshore to lower values offshore in Mayagüez Bay.

2-A salinity gradient going from lower values inshore to higher offshore occurs as expected from river discharge plume dilution of marine receiving waters.

3-Spectral slope of CDOM remained relatively constant value of 0.017 nm^{-1} undistinguishable from the values for surrounding ocean waters. No significant variation was detectable, temporally nor spatially in Mayagüez Bay, suggesting the prevalence of a stable background oceanic CDOM.

4-CDOM absorption coefficient variability at inshore stations is significantly influenced by local river discharge and can be traced to local river inputs. CDOM a_{g355} inshore values were 2 times the offshore values and 6 time the values reported for CaTS.

5-Mayagüez Bay seems is influenced by seasonal processes that can control the distribution of CDOM and TSS on a seasonal basis. During the rainy season higher CDOM a_{g355} absorption coefficients are related to higher river discharges. Similar TSS concentrations during the rainy season and dry seasons (and a reduction by almost half CDOM absorption coefficients during the latter) might suggest that the CDOM has a common terrestrial origin but, when not directly

delivered by the riverine source (dry season) it may come from sediments of terrestrial origin deposited on near shore bottom and resuspended by wave energy and tidal energy

6-The lack of significant correlation between Chl-*a* and CDOM a_{g355} suggests that liberation of CDOM precursors by phytoplankton seems to be of minor importance.

RECOMMENDATIONS

1-Design extensive CDOM quantification and characterization studies to monitor the seasonal export of soil-leached CDOM from the Añasco River basin, to marine environment..

2-Developed integrated runoff, nutrient, sediment erosion, precipitation and bacterial transport models for the Añasco, and Guanajibo Rivers as part of to the land-sea interface approach to study the biogeochemistry of CDOM.

3-Establishe a continuous automated water flow and relevant constituent's quality monitoring station at the Añasco River mouth.

4-Sampling trips have to be designed, taking in account seasonal terrestrial CDOM inputs as production, transport and alteration processes. These trips will require carefully planning so that the established seasonal and fate-and transport questions can be effectively answered with a minimum of waste time and resources.

5-Field sampling needs to track abrupt changes in physico-chemical condition during especially at low salinities estuarine conditions where important processes between CDOM and clay-mineral particles undergo partitioning change between dissolved and particulate phases .

6-Determine and quantify the possible adsorption of Chl-*a* to clay-mineral particles and its impact in pigment quantification since this can help in a multitude of areas related in bio-optics

and further ecological and biogeochemical studies in which precise concentrations of Chl-*a* are needed.

CHAPTER II

SIMULATED ESTUARINE DILUTION EXPERIMENT FOR THE DETERMINATION OF CDOM BEHAVIOUR WITH AND WITHOUT PARTICLES

INTRODUCTION

Estuaries are among the most challenging environments on earth in which to study the origins, pathways and fates of dissolved and particulate materials, since these are highly dynamic transitional zones between terrestrially derived material and the marine environment (Hedges and Keil, 1999). Colored dissolved organic matter (CDOM), an important component of estuarine systems, can be defined optically as dissolved organic matter capable of absorbing UV and visible light (Blough and Del Vecchio, 2002). Chemically, CDOM is a highly heterogeneous and incompletely defined mixture of organic compounds. Overall, humic and fulvic acids are consistently important components of CDOM (Del Castillo, 2005; Kirk, 1976; 1994).

The main biogeochemical processes responsible for changes of CDOM in coastal and oceanic environments are flocculation, particle adsorption, biological activity, dilution and photodegradation (Blough and Del Vecchio, 2002; Del Castillo, 2005, Nelson and Siegel, 2002b). Some studies have examined how the flocculation, adsorbtion, precipitation of dissolved organic matter (DOM) as it transits through estuarine systems into coastal waters (Ding and Henrichs, 2002; Del Castillo *et al.,*1999; Eckert and Sholkovitz, 1976; Sholkovitz, 1976; Sholkovitz *et al.,* 1978; Shank *et al.,* 2005). Alternatively, other research consider the role of suspended particles and estuarine chemical changes leading to alternating states of dissolved and particulate organic matter (Chen *et al.,* 2004; Shank *et al.,* 2005). Overall, the biogeochemistry of CDOM-clay complexes, specifically the alternation between dissolved and

particulate state of CDOM at the land-sea interface in tropical and subtropical environments have been understudied. Although the association of humic substances and clays-minerals (Ghabbour, *et al.,* 2004; Gosh and Schnitzer, 1980; Heil and Sposito, 1993a, b; Krestzschmar *et al.,* 1997; Swift, 1989; Tarchitzky *et al.,* 1993) and their effect on mobility of colloids (Heil and Sposito, 1993b), nutrients (Ghabbour *et al.,* 2004), and contaminants migration (Ghabbour *et al.,* 2004; Heil and Sposito, 1993b), and water retention (Ghabbour *et al.,* 2004) in soil has been extensively addressed, only recently, has its partition (and that of the overall CDOM) into dissolved and particulate fractions driven by clay-minerals interactions has been studied given its important role in DOM dynamics (Shank *et al.,* 2005; Spencer *et al*., 2007; Uher *et al.,* 2001), global carbon budget and its implications in global warming (Hedges, 1992)

This chapter presents results of adsorption desorption experiments under different river/marine water mixtures under the influence of clay amendments simulation conditions extant in Mayaguez Bay proximate to the Añasco river mouth. Changes in absorption coefficient (a_{g375}) and spectral slope (S) are presented and evaluated against a conservative mixing curve in order to assess effects unexplained by simple dilution as suggested by Liss (1976).

OBJECTIVES

The objective of this work is to assess the possible role of flocculation and adsorption of CDOM to clay-mineral particles during simulated estuarine dilution between riverine and marine water end-members. The working hypothesis can be stated as: Simple dilution of river derived CDOM can explain its distribution and quality in Mayagüez Bay.

The specific objectives are the following

1. Determine a theoretical conservative dilution model between Salinity and CDOM a_{g375} from an Añasco River and offshore marine water end-member.

2. Compare actual CDOM a_{g375} measurements taken from a series of dilutions with the theoretical dilution model.

3. Perform a similar dilution experiment amended with particles that will be used to evaluate their role in defining the quantity and quality of CDOM during estuarine transport.

4. Qualitatively identify the suspended clay-mineral particles from the Añasco and Guanajibo River.

5. Determine the CDOM a_{g375} loss by flocculation and by adsorption to particles.

MATERIALS AND METHODS

Suspended sediments sample collection

River water were collected during the rainy season (November, 2007) at the Añasco and Guanajibo Rivers. The Añasco River water sample was collected under the two bridges located on road PR-2. Guanajibo River water was collected at the bridge that runs over Road PR-102 located at the river mouth. All containers and tubing were acid washed (with what acid, concentration). In addition containers were treated with bleach (what type, hopefully no added fragrances). Water was collected by means of 5 gallon plastic buckets attached to a new clean plastic rope. The water was transferred to a 208-liter food grade, plastic drum that was filled to capacity. Water was transferred to another plastic drum by siphoning while being simultaneously prefiltered through a mosquito mm mesh in order to remove large detritus.

The prefiltered water was left undisturbed for a week to allow for the settlement of smaller particulates. ,The supernatant was siphoned using a Teflon hose without disturbing the particles at the bottom. As the drum was drained it was tilted carefully (not to disturb the sludge) so that the majority of the water could be siphoned out with a minimum of particle loss. The remaining particles where resuspended using the final volume of water (ca. 1L) using a swirling motion.

The resulting "sludge" was collected in a gallon-sized ziplock® plastic bag and placed in a large beaker so that the particles could settled in one of the corners for 24 hours. The corner of the bag with the settled particles was cut and the sludge was transferred to a clean beaker. The excesses water with some material was also collected in another beaker and left to settle. The sample was left in the beaker for three days to facilitate the recovery of suspended material by centrifugation.

Four, 15 ml Falcon® plastic centrifuge tubes, were prepared and filled to capacity with sludge; capped and were centrifuged at maximum power (3,500 rpm) for 10 minutes and the remaining water was decanted and more sludge material was added. The samples were refrigerated at -4^{o}C until further use for dilution experiment and XRD clay-mineral identification.

Treatment of Sediment Samples for XRD Analysis

A tube of the collected material (6.0 ml of settled sediment) was defrosted and transferred to a 250mLbeaker.where a 1 mL aliquot of 30% H_2O_2 was added to oxidize its organic matter. Peroxide addition was repeated 4 additional times every hour. The sample was left undisturbed under a fume hood for 24 hours. Five ml of distilled water was added and the total volume was transferred to two clean 15 ml plastic tubes and centrifuged at full speed for 10 minutes. The resulting pellet was resuspended in 10mL distilled water and centrifuged twice. The H_2O_2 free particles were pooled and transferred to an aluminum dish and dried overnight at 60 ^{o}C, to avoid clays agglutination, and later transferred to a desiccator.

One gram dry clay-like material from both rivers was pulverized using an agate mortar and pestle and the resulting powder was transferred to the XRD sample holder. A Siemens Model D5000 X-Ray Diffractometer was used for analysis. Qualitative identification of clay minerals was conducted by scanning samples for 8 hours and comparing difractograms against the internal mineral library database of the analyzer.

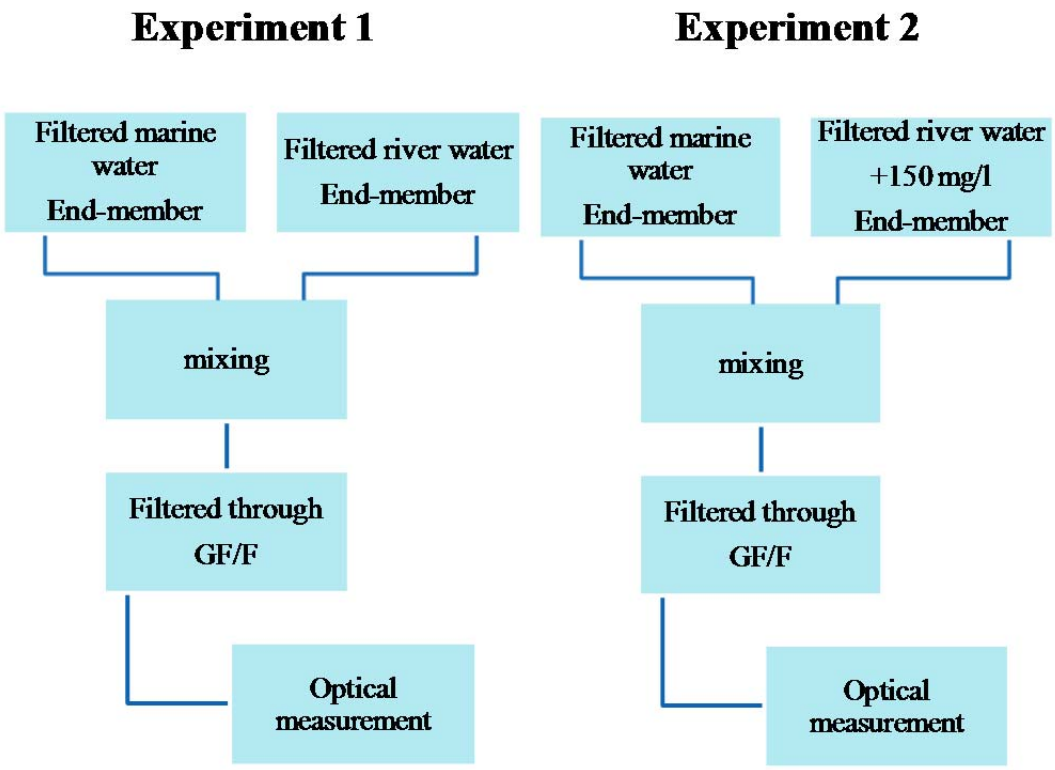

Figure 20. Experimental layout for the dilution experiment with and without added particles.

Dilution and clay adsorption experiments of CDOM end-members

Four liter water samples were collected using ashed glass bottles from station Y2 (offshore end member, Figure 1, Chapter 1) and from the Añasco River. The samples were kept in an ice box until arrival to the laboratory. Both samples were filtered the day after collection using an all glass unit, which have been previously soaked overnight in 1M NaOH washed with 20% HCl; rinsed with MiliQ water and finally rinsed 3X with HPLC grade methanol; and oven dried (60^0C) covered with methanol rinsed aluminum foil.

Sample were filtered using low vacuum (<7in Hg) through ashed (500^oC for 6 hours) 25 mm o.d. Whatman® GF/F filters thus minimizing the addition of ruptured cells material to the

sample. The filters were changed as needed when clogged. The filtered water samples were collected in an ashed amber 4 L bottle and immediately refrigerated.

Prior to initiating mixing experiments all glassware was cleaned as the filtration unit mentioned above. The filtered water samples were brought to room temperature and duplicate 1/10 stepwise serial dilutions (100% marine to 100% river water) were made using the marine and river end-member samples . The samples were capped, agitated by hand for five minutes, left at room temperature in a reciprocal shaker to equilibrate for 24 hours.

After equilibration, all samples were re-filtered as described above since some samples, especially those of lower salinity developed turbidity. After filtration of each sample the glass filtration unit was rinsed, with HPLC certified ultrapure water (Burdick and Jackson), and HPLC grade methanol, and completely air dried. The samples were later transferred to clean ashed 125 ml amber glass bottles.

A second dilution series was conducted using 1 L of the Añasco river water end-member amended with 0.150 g of the previously isolated water particles untreated with H2O2 (see above XRD analysis)a final concentration similar to those of reported earlier in nearby waters and in the Añasco river proper (Gilbes, 1992;Rodriguez-Guzman, 2008). Equilibration, filtration in preparation for absorbance measurements were conducted as above.

Spectrophotometry and Salinity

Absorption measurements were conducted as in Chapter 1. CDOM absorption (a_{g375}) was estimated from the calculated absorption coefficient curves and used as a proxy of CDOM concentration for each sample. Salinity was measured after absorbance readings using an YSI portable salinometer Model 30 with a precision of ± 0.05.

Spectral slope calculation

The spectral slope (S parameter) was calculated using only the UV region of the spectrum (250-300 nm) and a liner least square fit as there should be very little difference between lineal vs. nonlinear estimates (Stedmon and Markarger, 2003). The UV region used offered adequate sensitivity (considering that CDOM levels were low) and the effects on S due to flocculation, absorption modification due to pH, adsorption onto clay minerals of humic and fulvic fractions are maximized.

CDOM dilution diagrams for conservative or non-conservative behavior

Since, a Salinity vs. a_{g375} theoretical dilution diagram must first be generated to check if CDOM absorption coefficient behaves conservatively or non-conservatively during the dilution experiment, it was decided to use the approach of (Morell and Corredor, 2001) where a series of expected values were calculated for fluorescence, in our case absorption coefficients were calculated but this approach using another optical property as a proxy of concentration is a valid one. In our case, since we knew the proportions of waters used during the dilution experiment and had the absorption coefficient values of the end-members the resulting a_{g375} values were easily calculated with a similar equation as that used by Morell and Corredor (2001), where CDOM fluorescence was used instead of a_{g375}.

$$a_{g375}\,(\mathrm{m}^{-1}) = (Ma_{g375}\,M_{iff}) + (Ra_{g375}\,R_{uff}) \qquad (1)$$

Where
a_{g375} = Calculated total absorption coefficient of CDOM a_{g375} (m^{-1})
Ma_{g375} = Marine water end-member measured a_{g375}
M_{iff} = Marine water fraction
Ra_{g375} = River water end-member measured a_{g375}
R_{uff} = River water fraction

A theoretical a_{g375} value was determined for each of mixed proportions and the generated values were used with the measured salinities to create the dilution diagram. The dilution diagram was created between Salinity and the absorption coefficient a_{g375}. Theoretical spectral slopes similar to those of Helms et al (2008) were calculated (per Otero, personal communication). using the riverine and marine water end-member CDOM a_{g375} (*in lieu* of CDOM concentration) and the spectral slope.

$$S(\mathrm{nm}^{-1}) = \frac{(\underline{Sw(a_{g375})} * (SwS)) * ((Rwa_{g375}) * (RwS))}{Sw(a_{g375}) + Rw(\underline{a_{g375}})} \qquad (2)$$

Where:

$S(\mathrm{nm}^{-1})$ = Resulting spectral slope of the mix
$\underline{Sw(a_{g375})}$ = Sea water end-member a_{g375}
$\underline{SwS}$ = Sea water end-member Spectral slope
$\underline{Rw(a_{g375})}$ = River water end-member a_{g375}
$\underline{RwS}$ = River water ends member Spectral slope

The resulting theoretical spectral slopes (per dilution) were used to plot a conservative dilution diagram and the resulting spectral slope for experiment 1 and 2 were plotted against it to examine the conservative behavior S during dilution experiments.

RESULTS

It was observed that during the dilution experiments (without particles) after 24 hour equilibration period (shaking at room temperature) all solution of salinities (< 20 salinities) were hazy; confirms that an alteration occurred at lower salinities that could be identified visually. It was decided to filter the samples again (ashed GF/F filters) since they were not suitable for absorbance optical measurements. This filtration was not intended in the first place, since particles were removed and the resulting dilutions were going to be measured directly. These Since the filtration of sample with particles was necessary in for optical measurements this gave both experiment the same treatment..

To further study the effects of simulated estuarine dilution on the optical properties of CDOM a dilution diagrams was developed. Salinity and conservative constituent and a_{g375} was used as proxy of CDOM concentration and spectral slope (S) as an index of possible CDOM modification. During estuarine dilution two possible outcomes can be possible; linear behavior (conservative) and a non-linear behavior (non-conservative). In the case of non-conservative dilution if the dependent variable goes below the theoretical dilution line a "sink" effect is observed, on the other hand if the dependent variable goes over the theoretical dilution line there is a "source" of the material during mixing. CDOM a_{g375} theoretical absorption coefficients values were calculated from the end-members a_{g375} (Table 10). The theoretical absorption coefficients a_{g375} values were plotted against the resulting Salinity to creating a theoretical dilution diagram (Figure 21).

Table 10. Theoretical CDOM a_{g375} absorption coefficient a_{g375} (m^{-1}).

Proportion	Salinity	Calculated CDOMa_{g375} (m^{-1})	Measured CDOM a_{g375} (m^{-1}) no particles
100	0.00	2.440	2.440
90	3.80	2.213	2.020
80	7.15	1.985	1.616
70	10.80	1.758	1.306
60	14.25	1.531	1.140
50	18.00	1.304	0.904
40	21.45	1.077	0.753
30	24.95	0.849	0.643
20	28.35	0.622	0.351
10	31.80	0.395	0.271
0	35.00	0.168	0.168

The dilution diagram between Salinity and CDOM a_{g375} (Figure 21) indicates a non-conservative dilution processes for both experiment in the absence and presence of particles. The lack of particles during dilution suggest that some component of the CDOM alternated between dissolved t and particulate form was retained during filtration. In the second experiment the presence of particle , caused decrease a_{g375} at salinities >10. The presence of particles during dilution caused contrasting effects were at low salinities a reduction in a_{g375} is apparent and at intermediate salinities a very small increases is observed.

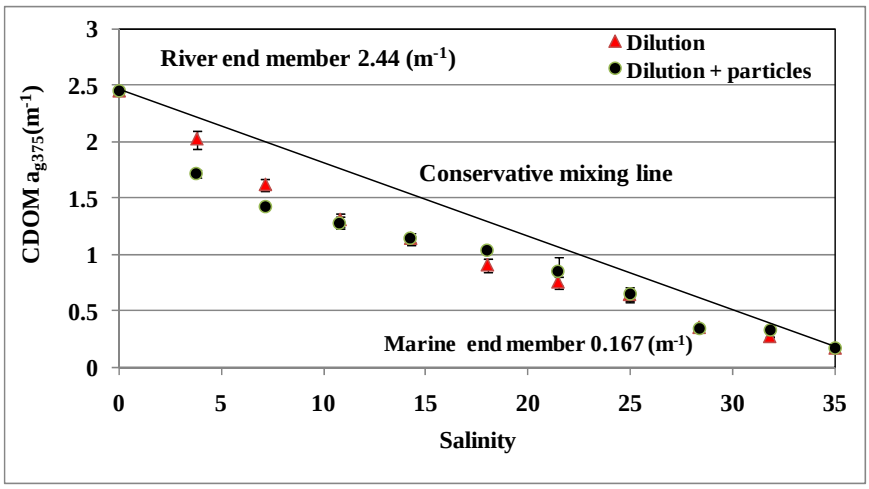

Figure 21. Dilution diagram between theoretical and measured CDOM (a_{g375}) with and without particles vs. Salinity.

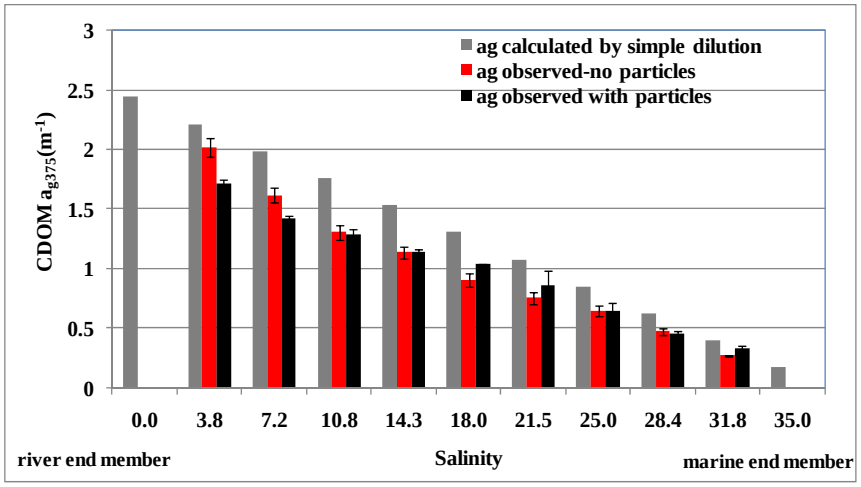

Figure 22. Absorption coefficients between the two experimental treatments and simple dilution at 95% confidence intervals.

When the spectral slope is used in a dilution diagram (Figure 23) the generated graph indicates an inverse relation to the one generated with a_{g375} this would be expected since the lower spectral slope values will be found associated to the riverine waters end-member and the highest values will be found with the marine water end-members. The same tendency was observed at the lower salinities (< 10) were a higher spectral slopes values were recorded when particles were added. This indicates that changes in the optical properties were due to the

removal of some dissolved component when particle are present in the medium, this material changed from the dissolved phase to the particulate phase and was removed during the filtration processes.

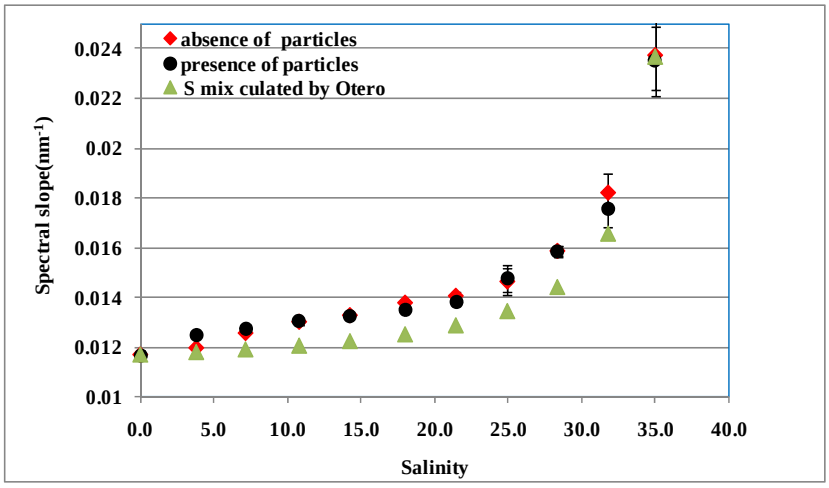

Figure 23. Dilution diagram between theoretical and measured CDOM Spectral slope (nm^{-1}) with and without particles vs. Salinity .

When spectral slope and a_{g375} was plotted (Figure 23) as suggested by (Stedmon and Markarger, 2003) due to the non-linear behavior of CDOM during dilution , it was noticed that the presence of particles caused a minimal reduction in the spectral slope at the lower salinities (<10) of 0.005 nm^{-1} suggesting the possibility that a minor fraction of CDOM could removed from the dissolved phase during filtration possesses associated to particles. But a better means are need to clear demonstrate that changes in the quality of CDOM can be induced by particles.

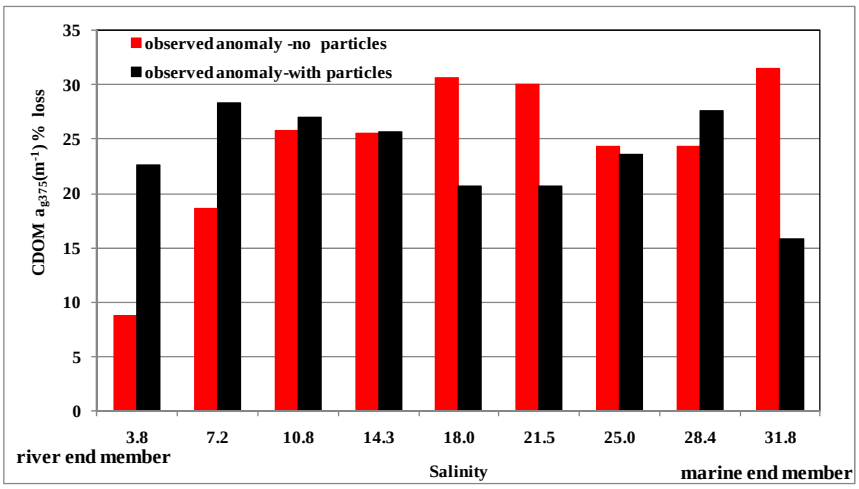

Figure 24. CDOM ag375 (m-1) percent loss Theoretical – Observed for dilution with no particles and with particles.

XRD clay-mineral transported in the Añasco and Guanajibo waters

The particle matter samples from the Añasco and Guanajibo Rivers were examined by the X-Ray diffraction techniques (XRD). The difractograms indicated the presence of gadolinite, halloysite, montmorillonite, vermiculite, hematite and quartz for the Añasco River. In the case of the Guanajibo River the same clay-mineral were identified with the addition of bementite (Table 11). The clays-minerals identified in the river waters were similar to those found in the Mayagüez Bay bottom sediments (Ramirez unpublished data) and from other studies (Table 12).

Table 11. Clay-minerals identified in collected particles from the Añasco and Guanajibo Rivers.

Añasco River	Guanajibo River
kaolinite	kaolinite
montmorillonite	montmorillonite
hematite	hematite
halloysite	halloysite
quartz	quartz
Not identified	bementite

Table 12 . Clay-mineral identified by XRD from sediment samples from the Añasco River and Mayagüez Bay sediments.

Clay minerals	Pirie, 1967	Morelock and Grove, 1976	Rivera-Rivera unpublished	Cameron-González unpublished	Present Work*
Illite	yes	no	yes	no	yes
Chlorite	yes	no	no	no	yes
Kaolinite	yes	yes	yes	yes	yes
Montmorillonite	yes	yes	yes	no	yes

***Añasco and Guanajibo river water samples important in CDOM–clay-mineral interactions**

DISCUSSION

Simulated Estuarine Dilution Processes

For a full comprehension of estuarine dilution we suggest the study of (Liss, 1976) "During conservative dilution the distribution of a substance is controlled by the physical mixing of two end-members causing the concentration to vary linearly with the resultant Salinity, the points lie on a theoretical dilution line that joins the two end-members of the series (Liss, 1976). CDOM optical measurements of the absorption coefficient (a_{g375}) and spectral slope, were used to evaluate their variation during simulated estuarine dilution in the absence and in the presence of particles based on theoretical dilution diagram. Dilution diagrams between Salinity vs. CDOM a_{g375} (with and without particles) (Figure 21 and 22), indicate the loss of CDOM at all salinities. The "sink effect" was greater at salinities below < 10 than at salinities >10 (with and without particles). The observed reductions in the absorption coefficient (a_{g375}) in our dilution experiments suggest that flocculation, might be responsible for lowering the absorption coefficient of CDOM and the material during filtration. At salinities > 32 the flocculation effects are negligible as in De Souza-Sierra *et al.* (1997).

In an unpublished study Rosado-Torres (personal communication), suggested that a fraction of the humic material was lost when different concentrations of clay material collected from the Añasco River was added to Sewanee River humic acid standard in Mayaguez Bay, marine end- member. No humic acid was loss prior to addition of the clay material. Adsorption of humic material to-clay-minerals particles was suggested as the most likely processes causing the reduction of humic acid absorption coefficient.

Salinity changes effects on humic substances

At high electrolyte concentration, intra and intermolecular charge repulsion decreases, causing the humic molecules that are in a low solvated state to start to precipitate and/or to aggregate causing optical changes (Ghabbour *et al*., 2004; Swift, 1989). The addition of NaCl to filtered waters (river) samples showed little variations to CDOM absorption and spectral slope (Guo *et al*., 2007). Similar observations were reported during simple dilution experiments between marine and river water end-members (Del Castillo *et al*., 2000a; Presto and Riley, 1982; Stedmon and Markarger, 2003). Humic acids-clay-mineral interactions are known to be co-affected by pH and ionic strength in soils (Ghabbour *et al*., 2004; Heil and Sposito, 1993b; Krestzschmar *et al*., 1993).

In some estuaries, non-conservative dilution behavior at low salinities has been attributed to removal of specific DOM components (Benner and Opsahl, 2001; Hermes and Benner, 2003), by flocculation or adsorption to particles of humic-rich high molecular weight (HMW) fraction of DOM (De Souza-Sierra *et al*., 1997; Fox, 1983; Sholkovitz, 1976; Sholkovitz *et al*., 1978; Uher *et al*., 2001). Our observed reduction in the absorption coefficients can be the result of different variables (pH, ionic strength and presence or absence of cations), but probably the most important factor could be pH changes at low salinities (<10).

Changes in the spectral slope can give more useful information than adsorption values on the characteristics (chemical, sources and diagenesis) of CDOM that are independent of CDOM concentrations (Helms *et al*., 2008). Changes in the proportion of humic and fulvic acids of the CDOM pool results in spectral slope variations (Carder *et al.,* 1989). Variations in CDOM optical properties (S) become evident only when riverine CDOM has been diluted sufficiently by marine water to allow detection of marine water end-member optical characteristics (Del

Castillo, 2005; Stedmon and Markager, 2003) and it is well-established that this occurs at or close to salinities over 30 (Del Castillo, 2005). Our observation indicates that this deviations can be observed at salinities lower than 30 but higher than 12. (Figure 23). Beyond salinities of 12 a marked increase of the spectral slope is observed relative to the conservative dilution line. The same tendency as above was recorded in the second experiment where almost no differences in the spectral slope between treatments suggest the lack of alteration or selective adsorption of CDOM material to particles.

The behavior of the estimated S values does not produce a straight line between end-member values during dilution , but varies non-linearly with mixing. Overall, these results reveal that it is not only the initial S values of each pool, but also the relative contribution of each pool of CDOM that determine how S will behave. The marine end-member only becomes influential when the CDOM in the freshwater end-member is diluted to a concentration comparable with the CDOM concentration in the marine end-member (Stedmon and Markager, 2003). Alterations in S can be related to alteration and distribution of humic and fulvic acids (Carder *et al.,* 1989). A shift is observed in the spectral slope to higher values at almost all salinities. If humic acids are eliminated from the dissolved pool this has the effect of shifting the absorption spectra to shorter wavelengths, decreasing the absorption coefficient and increasing the spectral slope (Del Castillo *et al.,* 2005). This behavior is observed in both experiments in the presence and absence of particles. But, the presence of particles did not further enhance the removal of humic material. Increases in the spectral slope values are consistent with the removal of high molecular weight (HMW) fraction (humic acids) from the dissolved pool by freshwater particles (Blough and Green, 1995; Uher *et al*., 2001). A 10% increase in spectral slope was sufficient to use as likely explanation for the removal of HMW fraction. This was not our case.

This lack of a significant difference between both experiments can be explained due to the dominant proportion in the marine end-member CDOM spectral signature at salinities > 12 prevalent in Mayaguez Bay. A marked difference in spectral slope would have been evidence of the preference for the humic acid fraction over the fulvic fraction to be adsorbed in the presence of clay-mineral particles. At highly dominant river water end-member conditions, it is possible that changes in the spectral slope are occurring but are difficult to observe due to the riverine end-member spectral signature dominance.

pH effects on humic substances

Variation in pH value of the medium also causes changes in the optical properties of CDOM in marine environments (Carder *et al*., 1989; Del Castillo, 1999; 2005; Ferrari and Tassen., 1991). pH values determines the protonation state of the humic acids (Krestzschmar *et al.,* 1993) is different between humic and fulvic acids. Changes in pH and ionic strength are known to cause conformational changes in humic acids Chen and Schnitzer, 1976; Gosh and Schnitzer, 1980; Krestzschmar, 1997; Tarchitzky *et al*., 1993). As pH increases, the humic acid molecules' carboxyl functional groups de-protonate (Chen and Schnitzer, 1976; Tarchitzky *et al*., 1993) as also phenolic hydroxyl groups (Chen and Schnitzer, 1976; Miano and Senesi, 1992). Also, it causes the disruption of inter-and intra-molecular hydrogen bonds, and de-coiling of macromolecular structures (Krestzschmar *et al*., 1997; Tarchitzky *et al*., 1993). In solution, humic acids changing from a compact coil or spherical molecule (at low pH) to a extended chain at higher pH due to the intra and intermolecular charge–charge repulsion in the same molecule (Gosh and Schnitzel, 1980). At low salinities in estuarine zones is where most drastic changes in pH are observed. All the above factors could be important in the explanation for the observed

reduction in CDOM absorption coefficient in the experiment in the absence of particles, where changes in pH causing changes in CDOM optical properties cannot be ruled out entirely.

Effects of multivalent cations

Our second experimental design was used to quantify the effects of particles during simulated estuarine dilution. The presence of particles may in some environments, alter the optical properties of CDOM lowering the absorption coefficient. Availability of metallic bivalent cations (Heil and Sposito, 1993a) are important in the complexation between clay-minerals and humic matter (Heil and Sposito, 1993a; Varadachari *et al.,* 1994). Clay-minerals and dissolved ions (preferentially multivalent cations Ca^{+2} and Mg^{+2}) usually control the organic matter distributions in the estuaries where these particles and their entrained organic molecules meet the sea (Hedges and Keil, 1999). Ca^{+2} and Mg^{+2} ions decrease the solubility of CDOM thereby increasing its ability to adsorb to sediments (Shank *et al*., 2005). It is difficult to say which of the above factors or combination are causing the reduction in CDOM absorption coefficient.

Clay-minerals identified in the Guanajibo and Añasco Rivers waters

No previous study on the complete characterization and quantification for the clay-minerals in the suspended solids in river waters has been found for the West Coast Rivers of Puerto Rico. One unpublished study made by Ramirez *et al*., (2002) identifies the qualitative composition of the clay-minerals in the Mayagüez Bay sediments (Ramirez, personal communication). Other research address minor studies that identify some components of the Bay sediments like sand on the beach of the Bay area's (Cameron-González unpublished).

Clay-minerals were identified in the Añasco River and estuarine area (Morelock and Grove, 1976) and sediments collected in the Bay (Morelock *et al*., 1983; Pirie, 1967) (Table 12).

In this respect, this is the first effort to identify clay-mineral found in suspension in the Añasco and Guanajibo Rivers from a qualitative perspective (Table11). Difractograms indicated the presence of kaolinite, halloysite, vermiculite, montmorillonite, halloysite, hematite and quartz in the Añasco River. Guanajibo River had a similar clay-mineral composition.

Clay-minerals were identified from the Mayagüez Bay samples (Ramirez unpublished data) with mineral composition similar to the minerals found in the present study. Difractograms did not indicate the presence of montmorillonite in the samples, but this mineral should be present in all samples and in abundance in the bottom sediments of the Mayagüez Bay (Ramirez, personal communication). The relative proportions of clay-minerals found were illite (average of 4/10) chlorite (average 2.5/10) kaolinite (average 1.9/10) and montmorillonite the least abundant (average 0.5/10) in Añasco Bay (Pirie, 1967).

Clay-minerals and humic acids interaction under different conditions

Adsorption of organic matter onto clay-minerals surface is variable, and dependent upon both clay-minerals and source of Dissolved Organic Carbon (DOC) (Tietjen, *et al*., 2005). Clay-minerals are an important component of the particulate suspended material that is involved in the adsorption of organic matter such as humic substances (Arnarson and Keil, 2000; Clapp and Hayes, 1999; Lawless, 1986; Lunsdorf *et al*., 2000; Preston and Riley, 1982; Namjesnik-Dejanovic *et al*., 2000; Shank *et al*., 2005; Tietjen *et al*., 2005). Recently, the importance of particles (in this case clays-minerals) as aggregation nuclei for DOM and CDOM have been considered of significance (Spencer *et al*., 2007).

All this changes affect humic materials and the clay-mineral by enhancing or decreasing their affinity between them under the same conditions. During estuarine mixing chemical changes affect both components (CDOM and clay-minerals) simultaneously that may encourage

the interaction between CDOM-clays causing the selective partitioning of organic components between dissolved and particulate phases. Significant amounts of DOM can be desorbed from the clay-organic aggregates into water of low ionic strength and of low DOM concentrations (Tietjen *et al*., 2005). In our experiment a slight increase in the absorption coefficient at intermediate salinities suggest the release of some desorbed material.

Humic acids adsorption to clay-minerals, has a combination of factors that facilitate their interactions such as, specific adsorption to edge surfaces of clay-minerals (Krestzschmar *et al*., 1997;) cations bridging, water bridging in the presence of hydrated cations on the surface, and hydrophobic adsorption of uncharged parts of humic acids macromolecules (Murphy and Zachara, 1995). Fulvic acids fixation to clay-minerals is related to their negative charge and their hydrophilic nature (Varadachari *et al*., 1994). This explains why fulvic acids molecules are less readily fixed than humic acids in spite of the fact they have more interactive groups (Varadachari *et al*., 1995).

Kaolinite, montmorillonite and illite were identified in the particulate fraction from the Añasco and Guanajibo Rivers waters samples. Montmorillonite was found to be more effective than kaolinite in removing DOC from solution by adsorption (Tietjen, *et al*., 2005). In the case of Na-montmorillonite-humic substances the stability of this is explained by the interactions between the negatively charged humic acid molecules and its conformation with the edge charge sites of the clay (edge-edge and edge-face associations) (Tarchitzky *et al.*, 1993). The positive charges at pH close to the point of zero charge for montmorillonite, values are proposed as the main dominant flocculation mechanism (Tarchitzky *et al*., 1993). This pH values are close to pH 8.0, where the edge charge sites of the clay edge-edge and edge-face associations, may be significant (Tarchitzky *et al*., 1993). Hetereoflocculation is the dominant flocculation

mechanism for Na-montmorillonite-humic acids (Tarchitzky *et al*., 1993). It should be mentioned that this pH values where montmorillonite has its maximum flocculation values are very close to those found in marine waters between 8.0-8.3. pH fluctuations in estuarine zones range between 7 and 8 (Shank *et al.,* 2005). This fact can help explain the reduction in the absorption coefficient related to adsorption of humic material from CDOM to possibly montmorillonite.

Since montmorillonite has been identified as one of the clay-minerals found on our samples and was previously identified in other samples of the Mayagüez Bay (Pirie, 1967) and in the Añasco River bottom sediments (Morelock and Grove, 1976), this clay could be in part responsible for the adsorption of humic substances during the simulated dilution experiments. The change in the ionic strength and pH during mixing and montmorillonite maximum positive charge is achieved and that of humic acids have a negative charge and are unfolded would be a logical mechanism for the partition between particulate and dissolved fraction of CDOM. The implication of this clay-mineral and other clay mineral humic substance relation under natural condition has to be further investigated in the Mayagüez Bay.

Percent removal of material by flocculation and adsorption

Approximately 56% of DOM can be removed of due to flocculation (Amon and Menon, 2004; Uher *et al.,* 2001). CDOM was not conservatively mixed in Tampa Bay and 15% CDOM was lost at Salinity ~ 13.0 (Chen *et al.,* 2007). Flocculation processes were suggested as the cause of a 20% reduction in the turbid Mississippi water plume (Chen and Gardner, 2004). This field observation contrasts with our dilution experiment observation of flocculation and adsorption percent loss during the present study (Figure 24). In our experiment, a_{g375} had a total reduction of 8.7 and 18.6% at salinities of 3.8 and 7.15 respectively.

Sediment concentration was established as the primary variable controlling the fractioning of CDOM adsorbed in estuarine waters. The partitioning coefficient is inversely related to particle concentration (Shank *et al.,* 2005). Sorption to particles is the most important CDOM removal mechanism accounting for an average of 21% (Uher *et al.,* 2001). Particles sorption has the potential to remove as much as 40% of the light absorbing material in turbid estuarine waters where sediment loads may exceed 1.0 g/l and a 10% increases in spectral slope was the likely explanation for the removal of HMW functionalities (Uher *et al.,* 2001). These concentrations are an order of magnitude higher than those recorded in the Bay at least during the present study and in other previous studies. In the Añasco River, suspended sediment concentrations between 80-100 mg/l have been measured at the river mouth (Gilbes, 1992), and in another study concentrations of 150 mg/l were recorded by (Rodríguez-Gúzman, 2008).

At concentrations of 100 mg/l appropriate turbid conditions in coastal river systems indicate ~ 2.5% of the total CDOM can be adsorbed to particles in the estuarine waters (Shank *et al.,* 2005). Initial concentrations of 150 mg/l and the resulting concentrations of 135 and 120 mg/l of TSS had a loss of CDOM a_{g375} of 13.9 and 9.7% in addition to flocculation.

CONCLUSION

In this study, CDOM non-conservative behavior was observed during simulated estuarine mixing in the presence and absence of particles causing significant losses of a_{g375} . These results suggest that, during estuarine mixing, CDOM can be lost by the proposed mechanism of flocculation from the dissolved fraction especially at low salinities. The presence of particles, further enhanced the loss of a_{g375} in addition to flocculation, at low salinities. Adsorption to clay-mineral particles seems to be an important factor in the reduction of a_{g375} at low salinities in addition to minor adsorption-desorption process occurring at intermediate salinities. At low salinities both humic acids and clay-minerals suffer alterations that can enhance the interaction of both components during estuarine dilution. The presence of particles did not cause spectral slope shifts that could be related to changes in humic acid composition. If changes in the spectral slope occur the dominance of the marine water end-member in the optical properties can make very difficult the detection of these changes.

In our dilution experiment a_{g375} had a total reduction of 8.7 and 18.6% at salinities of 3.8 and 7.15, respectively. Initial concentrations of 150 mg/l of TSS at the initial dilutions resulted in concentrations of 135 and 120 mg/l of TSS and had losses of a_{g375} of 13.9 and 9.7% in addition to flocculation. Even thought loss by flocculation and adsorption were observed at all salinities. It was also noticed that at intermediate salinities between 18 and 21.5 higher a_{g375} could be related to the desorption of CDOM from particles. This results clearly indicate the complexity of the partitioning between dissolved and particulate fractions of CDOM during simulated estuarine dilution and suggest other possible biogeochemical processes that can alter terrestrially derived CDOM during non-conservative estuarine dilution.

RECOMMENDATIONS

1- Fully identify qualitatively and quantitatively the clay-minerals composition of the suspended sediments found in the three main rivers of the area by XRD techniques. This will bring a better view of the bio-geochemical processes related to nutrient dynamics, remote sensing, microbial ecology, and dissolved DOM organic matter and its CDOM components.

2- Evaluate the importance of colloidal stability studies of clay-humic substances material in the estuarine zone and the possible consequence of distribution of river born clay particles suspension.

3- Design experiment where the natural photodegradation of CDOM-clay- minerals interactions of the surface layer materials; can be accounted and its importance evaluated in terms of how this mechanisms can influence the bio-optical properties.

4-Evaluate the importance of re-suspension mechanisms in the liberation of CDOM produced from bottom sediments during the dry season to the water column.

5- The flocculation and adsorption CDOM to clay material in settled particles should be further addressed and its roles in microbiological ecology and other diagenetic processes evaluated, after this material has been deposited

CHAPTER III

REGIONAL EMPIRICAL ALGORITHM DEVELOPMENTFOR CDOM ESTIMATES IN THE MAYAGÜEZ BAY

INTRODUCTION

Ocean color is usually understood in terms of Remote Sensing Reflectance (R_{rs}). An apparent optical property (AOP) defined as the ratio of the upwelling radiance to downwelling irradiance (Kirk, 1994). Ocean color measurements by remote sensing can collect data in spatial and temporal resolution that will be impossible to cover by traditional methods (Del Castillo *et al*., 2001). This technique permits to estimate various components in the water column, like photosynthetic pigments (Chl-*a*, among others) Total Suspended Solids (TSS) and CDOM.

Different approaches (i.e., empirical and semi-analytical) have been used to retrieve estimates of the water constituents from AOPs and IOPs by remote sensing. The most often used IOPs like absorption and scattering have information of the constituents found in the aquatic environment (Gordon *et al*., 1988).

Empirical algorithms are based on statistical relationships between measured reflectance ratios and different constituents like TSS, Chl-*a* (D'Sa *et al*., 2006; O'Reilly *et al*., 1998), $aCDM_{412}$, and CDOM (D'Sa *et al*., 2006; Johannessen *et al*., 2003; Kahru and Mitchell, 2001; Menon *et al*., 2005; 2006). Semi-analytical algorithms used a series of equations derived from radiative transfer theory and empirical relationships related to AOPs such as reflectance and other Inherent Optical Properties (IOPs). Analytical models perform by solving radiative transfer theory. Moreover, all these algorithms have their virtue and their pitfalls.

Remote sensing can be used to effective monitor and evaluate CDOM dynamics in coastal and offshore processes (Blough *et al*., 1993; Del Castillo; 2005; Del Castillo and Miller,

2007; D' Sa and Miller., 2003; Hu *et al*., 2003; 2004; Hoge *et al*., 1995; 2001; Menon *et al*., 2006; Miller, and D'Sa, 2002; Müller-Karger *et al*., 1988; 1989; 1990; 1995; Siegel *et al*., 2002, 2005). Various sensors have channels devoted exclusively for CDOM measurements (centered at 412 nm). But satellites-derived measurements, in particular at 412 nm, are taken near the instrument noise due to atmospheric related issues. Therefore, precise atmospheric corrections are vital to avoid errors in estimates of satellite generated data.

Previous studies like Bricaud, *et al*., (1981) and Carder *et al*., (1989) addressed the importance of CDOM in estimating photosynthetic pigments with remote sensing. A maximum absorption peak of Chl-*a* is located at 443 nm, which is a wavelength where CDOM has a significant contribution in absorption. This fact complicates the use of remote sensing algorithms based on ocean color (Carder *et al*., 1991; O'Reilly *et al*., 1998) especially in coastal environments where CDOM concentrations are higher than in offshore waters (Carder *et al*., 1989; Müller-Karger *et al*., 1989). This causes problems in the development of productivity models based on pigment estimates (Arrigo and Brown, 1996).

Empirical models from *in situ* measurements and developed using band ratios of Rrs with similar channels found in sensors like SeaWiFS or MODIS have had good results estimating CDOM absorption coefficient (D'Sa and Miller, 2003; Del Castillo, 2007). CDOM estimates by remote sensing avoid complicated field and laboratory procedures that are expensive, labor intensive, and time consuming. Since CDOM have been found to co-vary with Salinity and with DOC the use of remote sensing to track Salinity and DOC using inversion models is an active field of study. Surface CDOM variability observed from satellite data can be related to "sources" and "sinks" or seasonal response in offshore waters (Siegel *et al*., 2002; 2005),

estuarine and coastal waters (Del Vecchio and Subramaniam, 2004; Del Castillo, *et al*., 1999; Hu *et al*., 2004; Müller-Karger, *et al*., 1989).

Actually only a limited number of remote sensors (on planes or satellites) have the spatial resolution necessary (tens of meters or less) to measure CDOM in the Mayagüez Bay (95 km^2) and its complicated optical provinces (Rosado-Torres, 2000). The future development of sensors with a smaller spatial resolution (meters) and hyper-spectral characteristics will be of greater help to assess the complicated dynamics found in the Mayagüez Bay. Another limitation in this Bay is related to data acquisition since a large percentage of the image area is found under cloud coverage in satellite images (Rodríguez-Guzmán, 2009), an acute situation during the rainy season afternoons. The use of portable spectroradiometer can circumvent part of this weather difficulty. Another advantages is that the no atmospheric correction is needed, the instrument is easy to use and transport, and the gathered data can be processed in a relative short time. Samples can be taken simultaneously facilitating the ground-truthing. One disadvantage arises due to given the limited in spatial and temporal coverage of data acquisition (even in our small Bay).

OBJECTIVES

1-Develop and validate an empirical algorithm to estimate CDOM absorption coefficients [$a_{g(412)}$] in the Mayagüez Bay with the best general fit of ≤ 35 mean Absolute Percent Difference (APD %).

2-Establish an empirical relationship between $a_{g(412)}$ (CDOM) and $aCDM_{412}$ that can be used in future studies to estimate one variable from the other.

MATERIALS AND METHODS

In situ Remote Sensing Reflectance Measurements (R_{rs})

In situ measurements of above water R_{rs} were taken at each sampled station between 2004 and 2007 (Figure 1). Water leaving radiance [$L_0(\lambda)$], sky radiance [$L_s(\lambda)$], and downwelling irradiance [$E_d(0^+,\lambda)$] were measured between 380-1050 nm with a GER-1500 portable spectroradiometer (from Geophysical and Environmental Research, Inc.). Measurements were performed following the SeaWiFS protocols (Fargion and Mueller, 2000; Mueller and Austin, 1995; Toole *et al*., 2000).

$L_0(\lambda)$ was measured toward the water surface at 45^o from the vertical and at 90^o from the solar plane to eliminate sun glint. $L_s(\lambda)$ was measured by aiming the instrument at 45^o from the vertical to the sky and maintaining the 90^o from the vertical plane. $E_d(0^+,)$ was measured by attaching a cosine collector to the lens and pointing the instrument directly to the sky. Three scans were taken for each parameter.

R_{rs} data editing and processing

Raw $L_0(\lambda)$, $L_s(\lambda)$, and $E_d(0^+, \lambda)$ were plotted for quality control and any curve presenting anomalies due to clouds, sun glint, or boat shadow were eliminated from the data set. Most of the reported mean values were calculated using the three scans. Only few instances were calculated from two scans. $R_{rs}(\lambda)$ was calculated with the mean values using the following equation:

$$R_{rs}(\lambda) = \frac{L_0(\lambda) - f\,(L_s(\lambda))}{E_d(0^+, \lambda)} \qquad (1)$$

Where

$R_{rs}(\lambda)$ = Remote Sensing Reflectance
$L_0(\lambda)$ = Water Leaving Radiance
$L_s(\lambda)$ = Sky Radiance
$E_d(0^+, \lambda)$ = Downwelling Irradiance
f = Fresnell Coefficient, 0.028 at 45^o (Austin, 1974)

The removal of the residual signal at 750 nm (Fargion and Mueller, 2000; Toole *et al*., 2000), based on the assumption that the water-leaving radiance at 750 nm is zero, could not be performed. Hence, the final correction (for sky-light reflection) was applied to the generated R_{rs} curve by subtracting the lowest measured value found between 900-920 nm. In few instances the curves were corrected at even lower wavelengths between 730-900 nm as suggested by Z. Lee, (personal communication). It was noticed that any residual correction at 750 nm removed a component of the water-leaving signal in the near-infrared range. This component can be related to the red clay minerals that resulted in values of R_{rs} that were lower than those derived by other methods (D'Sa *et al*., 2006). In order to make the final correction the R_{rs} data was first sorted and the lowest observed value between 750- and 950 nm was subtracted from the entire curve. The generated R_{rs} values were then plotted against wavelength between 400 and 700 nm and the spectral signature evaluated.

Previously published band ratios (D'Sa and Miller, 2003; 2006; Del Castillo, 2007) were evaluated to develop a site-specific empirical algorithm that can be used for the estimation of $aCDM_{412}$ and CDOM. The data range was extracted from the generated R_{rs} curves.

R_{rs} mean values centered at 412, 443, 510, 555, nm for the band ratios were evaluated as proposed by D'Sa and Miller, (2003); D'Sa *et al*., (2006) ($R_{rs}510$/ $R_{rs}555$). An additional published band ratio was also evaluated ($R_{rs}510/R_{rs}670$) and it was demonstrated as a good

empirical correlation to estimate CDOM a_{g412} (Del Castillo *et al*., 2007). An algorithm based on $R_{rs}510/R_{rs}670$ band ratios was expected to work only under low-Salinity river plume conditions (Del Castillo and Miller; 2007) where most of the light attenuation is due to CDOM (Del Castillo *et al*., 1999; D'Sa and Miller, 2003; D'Sa *et al*., 2006) and where Chl-*a* and accessory pigment absorption are low (Del Castillo, 2005). It should be kept in mind that the remote sensing reflectance signal at 412 nm has the combined contribution of CDOM and NAP (Non-Algal Particles) as suggested by Siegel and Michaels, (1996).

Table 13. Remote sensing specifications.

R_{rs} range used	Center	R_{rs} band ratio	Band used to measure
407-417 nm	412 nm	$R_{rs}412/R_{rs}510$	High CDOM absorption area
438-448 nm	443 nm	$R_{rs}443/R_{rs}510$	High Chl-*a* absorption in blue area
505-515 nm	510 nm	$R_{rs}510/R_{rs}555$	very low Chl-*a* CDOM absorption at high concentrations High absorption by accessory pigments
545-560 nm	555 nm		low Chl-*a*; CDOM; High particles absorption
665-675 nm	670 nm	$R_{rs}510/R_{rs}670$	High Chl-*a* in red area (Q band) very low CDOM absorption*

$aCDM_{412}$ absorption values measured *in situ*

$$aCDM_{412}(\lambda) = a_{CDOM}(\lambda) + a_{NAP}(\lambda) \text{ (Oubelkheir } et\ al\text{., 2007)} \qquad (2a)$$

Where

$aCDM_{412}(\lambda)$ = Colored detrital material (λ)
$a_{CDOM}(\lambda)$ = Colored dissolved organic material (λ)
$a_{NAP}(\lambda)$ = Non-algal particles (λ)

$aCDM_{412}$ measurements were taken *in situ* with an ac-9 absorption and attenuation meter using the absorption channel at 412 nm. All data were edited and pre-processed as previously described (Chapter I). The final profiles were corrected as suggested by Pagau *et al*. (2002). The $aCDM_{412}$ absorption coefficients used for the correlation analysis were taken at 1.0 meter

depth, since at that same depth the CDOM samples were taken. CDOM sample collection, absorption measurements, and absorption coefficient determination were all previously described in Chapter I.

Development of an empirical model

The algorithm can be a simple linear regression or power functions of second- or third-order polynomials (Kowalczuk *et al*., 2005). Correlation analyses were performed between CDOM absorption coefficient (a_{g412}) and each of the calculated R_{rs} band ratios to evaluate which one was the best suited for a possible empirical model. A similar approach was done for $aCDM_{412}$. Finally, another correlation analysis was performed between $aCDM_{412}$ and a_{g412}. The correlation analyses were performed using the complete data set and were separated between seasons to evaluate possible differences (Table 14).

The data set for the G2 station was not included in the regression analysis since this station is a very shallow (< 4 m) with clear offshore waters and it was affected by signal from the bottom. Bottom reflectance can cause bias in upwelling radiance and reflectance signals in optically shallow waters (Maritorena *et al*., 1994) causing problems with the interpretation of water column signals components. The data set for the AAA1 (secondary treatment plant sewage diffuser) station was eliminated from the regression analysis due to the nature of the material found (waste water). This station was found to affect the regression analysis due to the great amount of outliers. It does not represent the general condition of the Bay and can be better described as a highly impacted station.

Validations of the R_{rs} empirical band model for the estimation of CDOM

Empirical algorithms require a sufficient size of highly accurate field measurements, spanning all seasons and adequate spatial coverage for the region of interest (Pan *et al*., 2008). In order to validate the empirical models *in situ* R_{rs} and a_{g412} collected between April, 2001 and October, 2003 cruises were used. These parameters were processed using the same procedure as previously described.

Table 14. Cruises dates were R_{rs} and a_{g412} values were used for the validation of the empirical band ratio model.

Cruise date	Season
April 24-26, 01	dry
October 2-4, 2001	rainy
February 26-28, 2002	rainy
August 20-22, 2002	rainy
February 25-27, 2003	dry
October 7-9, 2003	rainy

The empirical equations obtained for the rainy season were used for the validation purpose because they had the best overall fits ($R^2 > 0.70$). Since the correlation between the evaluated band ratios and a_{g412} were best described by a power law equation this were natural logarithms transformed to become linear (Figure 28 and 29). The band ratios were also natural logarithm transformed so they could fit the linear equation model to estimate the a_{g412}. After each a_{g412} was estimated from its respective band ratio they were regressed against the actual a_{g412} *in situ* measurements. The necessary data for the validation of $aCDM_{412}$ were not available.

The generated algorithms were validated based on statistical parameters by comparing the measured field values with the estimated values calculated with the empirical models. The statistical parameters used were the mean and standard deviation of the Absolute Percent

Difference (APD %) root mean square error (RMSE), R^2, and the slope values from the linear regression analyses.

Equations used for the APD (%) and the RMSE.

$$\text{Mean APD (\%)} = \left[\frac{\sum|(C_{alg} - C_{in-situ})|}{C_{in-situ}}\right]\frac{100}{N} \quad (3)$$

$$\text{RMSE} = \left[\frac{1}{N}\left(\sum\left(C_{alg} - C_{in-situ}\right)^2\right)\right]^{1/2} \quad (4)$$

Where
C_{alg} = Calculated value with the algorithm
$C_{in\ situ}$ = Value measured *in situ*
N = number of sample

This study established a similar threshold for a validated uncertainty of < 35% (Pan *et al*., 2008; Mannino *et al*., 2008) in the performance of our developed empirical algorithm to be successful.

RESULTS

A total of 67 R_{rs} spectra were taken in 14 cruises between 2004 and 2007. Seven cruises were done during the rainy season and seven during the dry season. The collected R_{rs} spectra had variable spectral signature and magnitudes. Also exhibited characteristics associated with oceanic waters (offshore) where Chl-*a* was the main seawater constituent (station A2 and AAA2). Inshore stations had spectral signatures of coastal waters (stations A1, Y1 and G1) where Chl-*a*, $aCDM_{412}$, and TSS have a strong contribution to the reflectance field (Figure 25).

R_{rs} Spectral signature pattern found in the Bay

It was recorded that a series of spectral signature pattern existed in the data set. Specific spectral signatures were also previously noticed for inshore, offshore, and for the AAA1 station in Mayagüez Bay (Rosado-Torres, 2000). It was decided to group the stations by inshore and offshore (Figure 26a).

Spectral signatures shifts can be related to advection of offshore water mass. Another factor can be related to weather events. Under calm conditions, low river discharge, and low CDOM inputs the spectral signature at inshore stations can resemble those of Case 1 waters, more similar to offshore stations.

Maximum R_{rs} was found between 560-580 nm at the inshore station. Offshore stations had maximum reflectance displaced to values between 480-490 nm. Inshore stations (A1, Y1, and G1) can be recognized by its characteristic spectral signature where the main feature is a steady increase from 400 nm to a peak found near 550 nm. After this peak a marked slope continued to near 600 nm and then between 600-700 nm the main feature is a gentle slope curve. R_{rs} values for inshore stations ranged between 0.0090 and 0.0350 Sr^{-1} (at 412-575 nm). Inshore

stations have the strongest phytoplankton and CDOM absorption and backscattering signal due to particles (organic or inorganic) resulting in higher values of R_{rs} in the green region of the electromagnetic spectrum (D'Sa and Miller, 2003). There is a significant influence of dissolved material and detrital particles absorption on the R_{rs} (Rosado-Torres, 2000). While backscattering by phytoplankton and relatively large concentrations of non-algal particles influence ocean color in the green and red parts of the spectrum at other stations (D'Sa *et al*., 2006).

In May 01 of 2007 the spectral signatures were those characteristic of blue waters, suggesting the intrusion of clear water mass and/or very low river discharge. In general, the R_{rs} for the A1 showed a typical inshore signature (Figure 25) with a lowest recorded value at 500 nm of 0.0150 (Sr^{-1}) for April 21, 2006. The highest value was 0.0350 (Sr^{-1}) for September 20, 2005.

Y1 station had the lowest inshore recorded values at 550 nm of 0.0075 (Sr^{-1}) for July 17, 2005 and the highest value of 0.0225 (Sr^{-1}) found during December 06, 2006. A blue water spectral signature was observed for April 21, 2006 during the dry season.

The R_{rs} of G1 station showed an spectral signature characteristic of inshore station except for the August 17, 2005 cruise. The spectral signature was similar to A1 station during the same cruise but of smaller magnitude. It suggests that red clay-minerals were the responsible for that signal. The common process that influenced both stations simultaneously was the recorded heavy river discharge for that date. In one instance (October 19, 2005) the G1 station showed the R_{rs} spectral signature of an inshore station (maximum peak at 550 nm). During October, 1997 a similar situation was observed (Rosado-Torres, 2000). This spectral signature was noticed in other instances at the G1 station for the April 21, 2006; July 17, 2005; and May 01, 2007 cruises.

The lowest R_{rs} value recorded at 550 nm was 0.0050 (Sr^{-1}) for July 17, 2005 and May 01, 2007. Both cruises had similar spectral signatures as those found for the AAA1 station. The highest value was detected in December 06, 2005 with 0.0175 (Sr^{-1}). In general, all cruises had the maximum R_{rs} at inshore station between 550 and 580 nm, in the green region of the spectrum. Also these stations recorded a minimum of 0.0040 (Sr^{-1}) and a maximum 0.0060 (Sr^{-1}) near 480 nm.

Offshore Stations Remote Sensing Reflectance

In most of the cases, the offshore stations A2 and Y2 showed the typical spectral signature of "blue" offshore waters. Higher R_{rs} values between 400 and 500 nm with an unstructured broad peak and then a decreasing R_{rs} beyond 600 nm (Figure 26b) are the main features of this offshore waters. In general, the R_{rs} magnitudes are lower than in inshore stations at all wavelengths. Maximum reflectance is observed between 400 and 500 nm (blue region) where the backscattering and absorption of water molecules and Chl-*a* absorption dominated the R_{rs} signal. The clearest offshore "blue waters" were recorded during March, 2005 and April, 2006; this is considered the peak of the dry season. In some cases lower R_{rs} due to CDOM and detritus absorption were observed at offshore stations during heavy river discharge month with significant effects (August 17, 2005 and October 19, 2005).

A2 station had the typical "blue" offshore water spectral signature during March 10, 2005 when exceptional clear blue water spectral signal was recorded. Y2 station had one instance during April 21, 2006 where the spectral signature was characteristic of inshore stations. This suggests the possibility of inshore processes being exported by a water mass to that station. Meanwhile in a couple of stations the spectral signature was alternated between inshore and offshore.

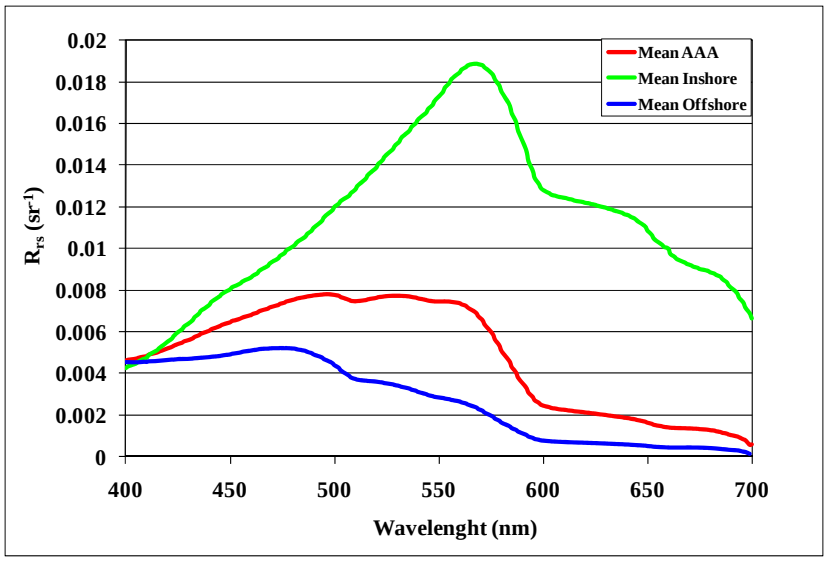

Figure 25 . Mean R_{rs} AAA1, inshore and offshore stations.

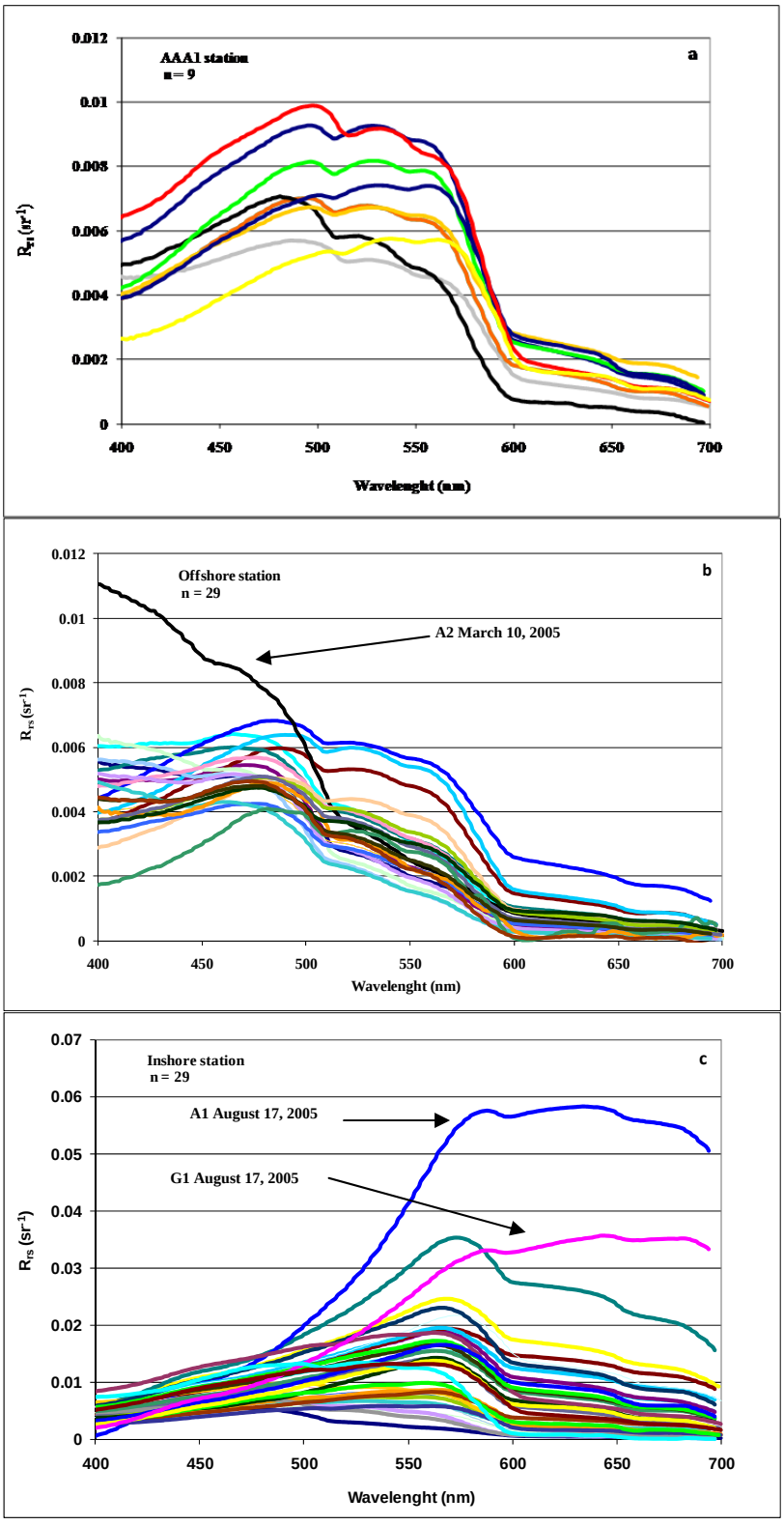

Figure 26. **R_{rs} separated by spectral signature a) AAA1 stations b) offshore and c) inshore stations during the study period (2004-2007).**

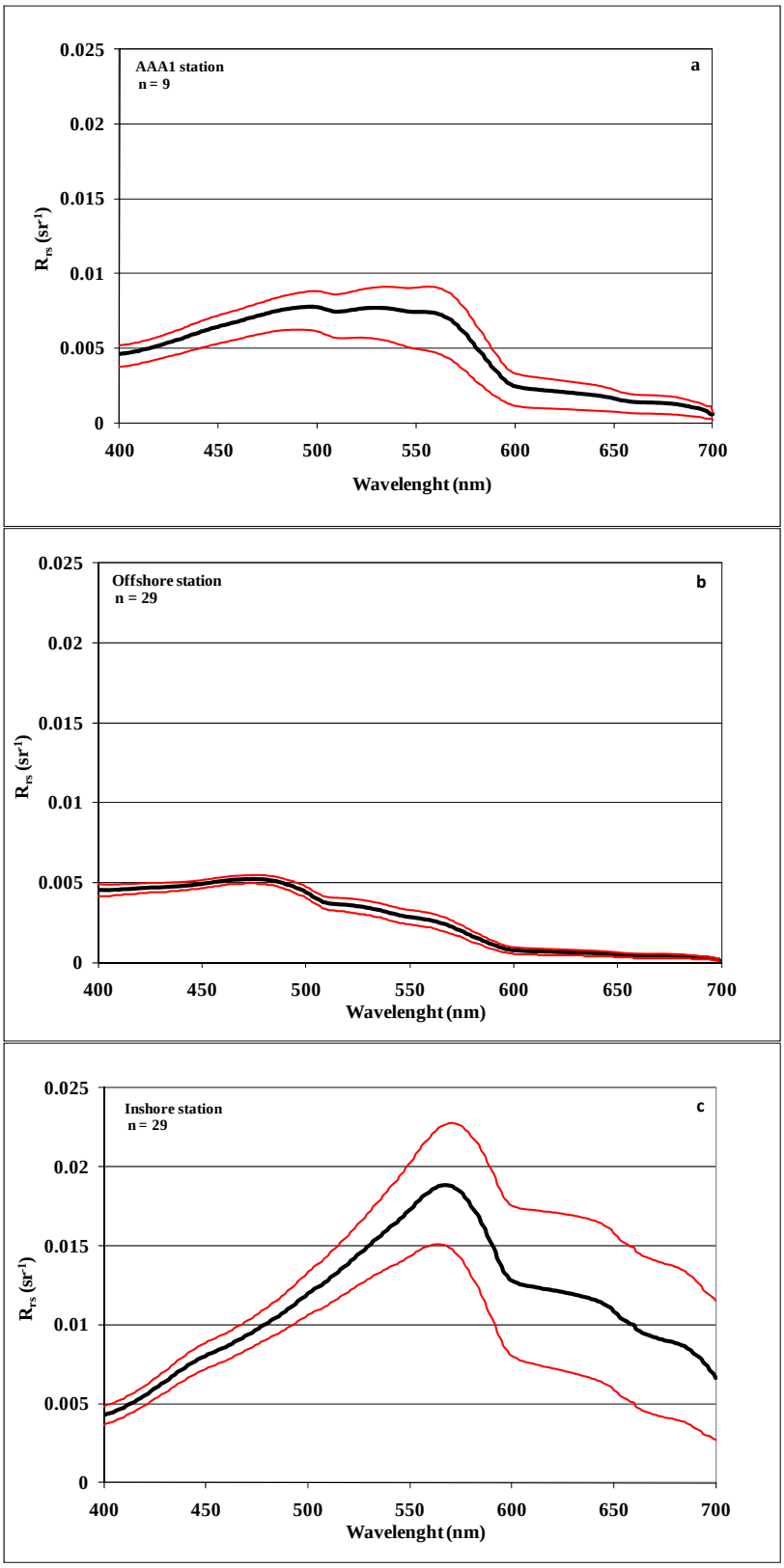

Figure 27. Mean R_{rs} spectral signature for the a) AAA1, inshore b) and offshore c) stations with 95% interval of confidence.

Development of the empirical model using the different band ratios in regression analysis

Previously published studies demonstrated good correlation relating $aCDM_{412}$ and CDOM a_{g412} with R_{rs} (D'Sa and Miller, 2007; D'Sa *et al*., 2006; Del Castillo and Miller, 2007). In two recent studies a similar approach was used, but instead of using CDOM a_{g412} a series of CDOM absorption coefficients were evaluated with band ratios available in SeaWiFS and MODIS sensors (Mannino *et al*., 2008; Pan *et al*., 2008).

The correlation analyses were performed using the complete data set from 2004-2007 and also the data set separated between dry and rainy season to verify any possible differences that could be linked to seasonal CDOM related events (Figure 30).

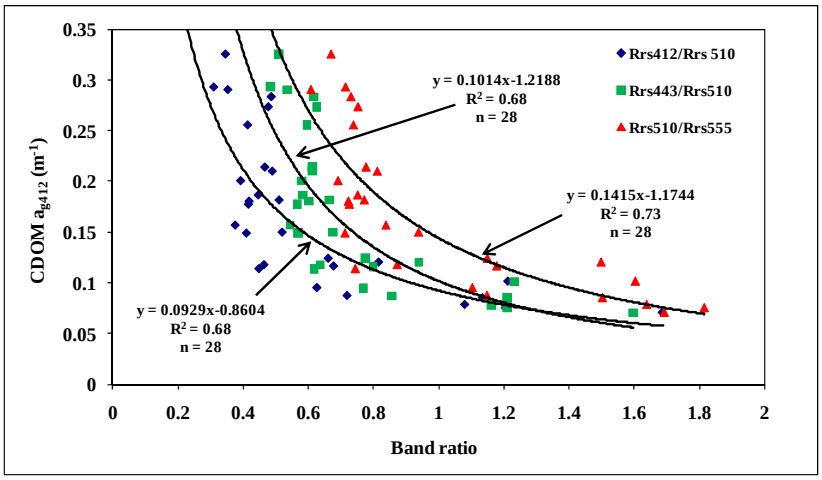

Figure 28. CDOM Power law empirical algorithm equations between three of the four evaluated R_{rs} band ratios vs. a_{g412}.

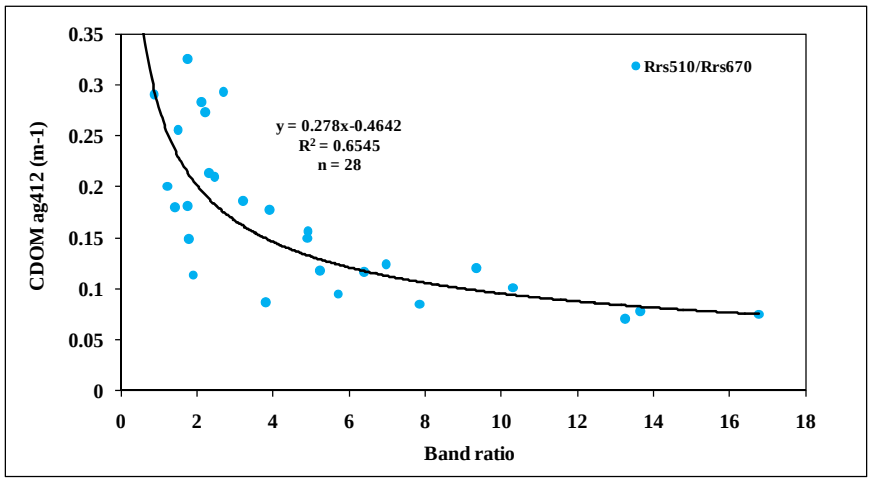

Figure 29. CDOM Power law empirical algorithm equations between $R_{rs}510/R_{rs}670$ band ratios vs. a_{g412}.

Using the complete data set for the correlation analysis (Figure 30 a and Table 15) an acceptable determination coefficient (R^2 = 0.65-0.73 n = 28) was obtained but if the data was separated by seasons the determination coefficient increased slightly. The rainy season data set demonstrated higher determination coefficients (R^2 = 0.70-0.85 n =18) within the band ratios evaluated.

The best band ratios of $R_{rs}510/R_{rs}555$ empirical equations was obtained during the rainy season (R^2 = 0.85), the other two best band ratios were $R_{rs}443/R_{rs}510$ and $R_{rs}412/R_{rs}510$ with R^2 = 0.74 for both (Figure 30 b and Table16). The least effective (but still acceptable) band ratio was of $R_{rs}510/R_{rs}670$ (R^2= 0.70). The analysis for the dry season data set (R^2 = 0.63-0.67 n =10) had lower determination coefficients (Figure 30c and Table 17). It was decided to use the empirical equation data set generated for the rainy season data set for the validation purpose.

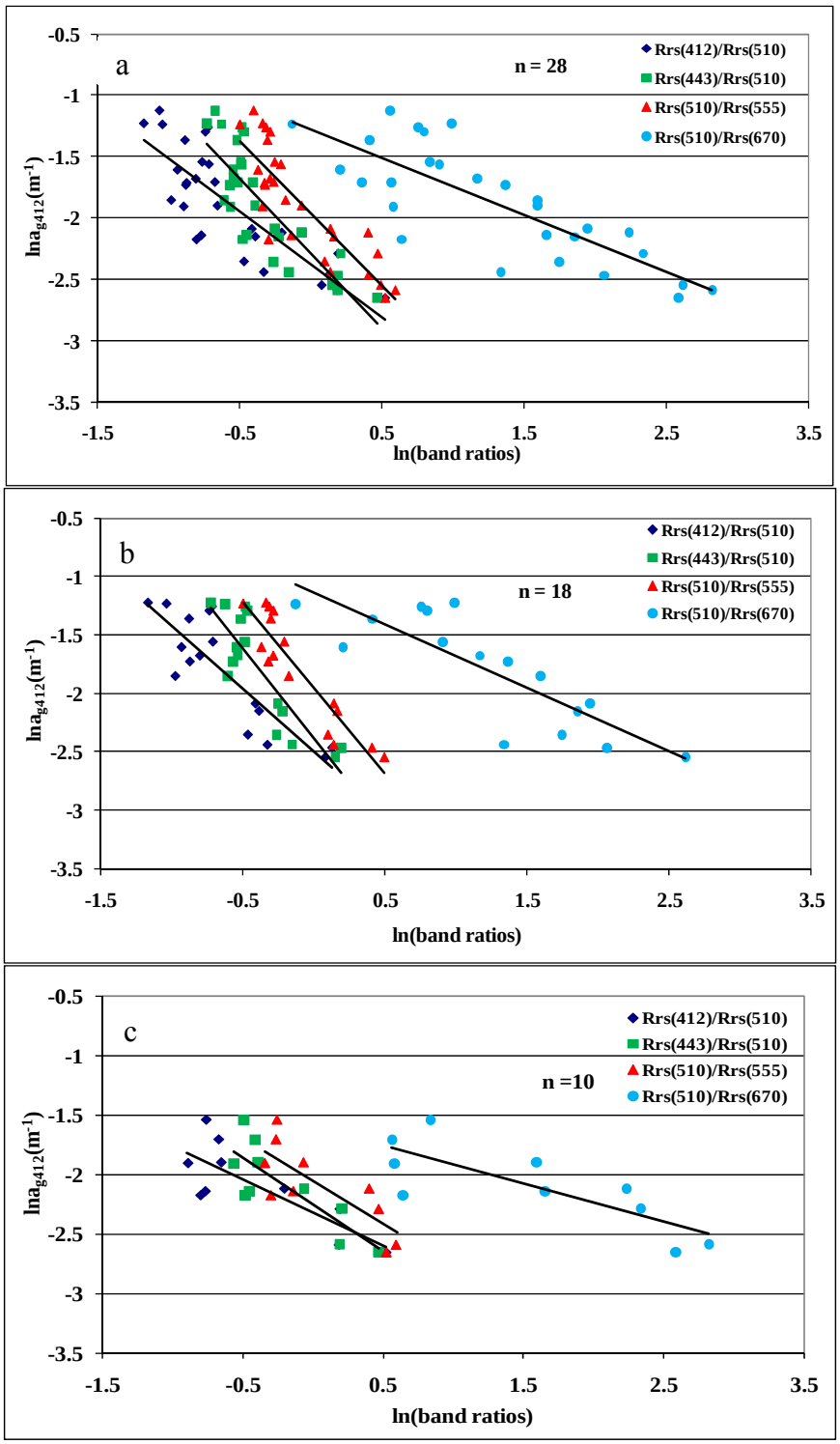

Figure 30. Correlation analysis between the ln(band ratios) vs. ln(a_{g412}) a) complete data set, b) rainy and c) dry season.

Table 15. Band ratios vs. (a_{g412}) resulting power law equation, linearization of power law equation and determination coefficient R^2 (n = 28) for the complete data set (dry and rainy season).

Band Ratios	Lineal model	Determination coefficient
$R_{rs}(412)/R_{rs}(510)$	lny = -0.8604ln(x) - 2.3761	$R^2 = 0.68$
$R_{rs}(443)/R_{rs}(510)$	lny = -1.2188ln(x) - 2.2882	$R^2 = 0.69$
$R_{rs}(510)/R_{rs}(555)$	lny = -1.1744ln(x) - 1.9558	$R^2 = 0.73$
$R_{rs}(510)/R_{rs}(670)$	lny = -0.4642ln(x) - 1.2803	$R^2 = 0.65$

Table 16. Band ratios vs. ln(a_{g412}) correlation equation and the determination coefficient for the rainy season (n =18).

Band ratios	Lineal modeled	Determination coefficient
$R_{rs}(412)/R_{rs}(510)$	lny = -1.0762lnx - 2.4945	$R^2 = 0.74$
$R_{rs}(443)/R_{rs}(510)$	lny = -1.5274lnx - 2.3904	$R^2 = 0.74$
$R_{rs}(510)/R_{rs}(555)$	lny = -1.4709lnx - 1.9568	$R^2 = 0.85$
$R_{rs}(510)/R_{rs}(670)$	lny = -1.2851lnx - 1.0935	$R^2 = 0.70$

Table 17. Band ratios vs. ln(a_{g412}) correlation equation and determination coefficient for the dry season (n =10).

Band ratios	Lineal modeled	Determination coefficient
$R_{rs}(412)/R_{rs}(510)$	lny = -0.5534lnx - 2.3150	$R^2 = 0.65$
$R_{rs}(443)/R_{rs}(510)$	lny = -0.7851lnx - 2.2581	$R^2 = 0.67$
$R_{rs}(510)/R_{rs}(555)$	lny = -0.7297lnx - 2.0546	$R^2 = 0.63$
$R_{rs}(510)/R_{rs}(670)$	lny = -0.3217lnx - 1.5927	$R^2 = 0.64$

$aCDM_{412}$ empirical algorithm development

The best empirical algorithms obtained for $aCDM_{412}$ where for the band ratios $R_{rs}443/R_{rs}510$ and $R_{rs}510/R_{rs}555$ with a $R^2 = 0.84$ and 0.81 respectively. The data set separated for the dry season demonstrated determination coefficient that fluctuated (R^2 = 0.68-0.72) similar to those obtained for CDOM a_{g412} in the previous correlation analysis (Figure 31 and Table 18).

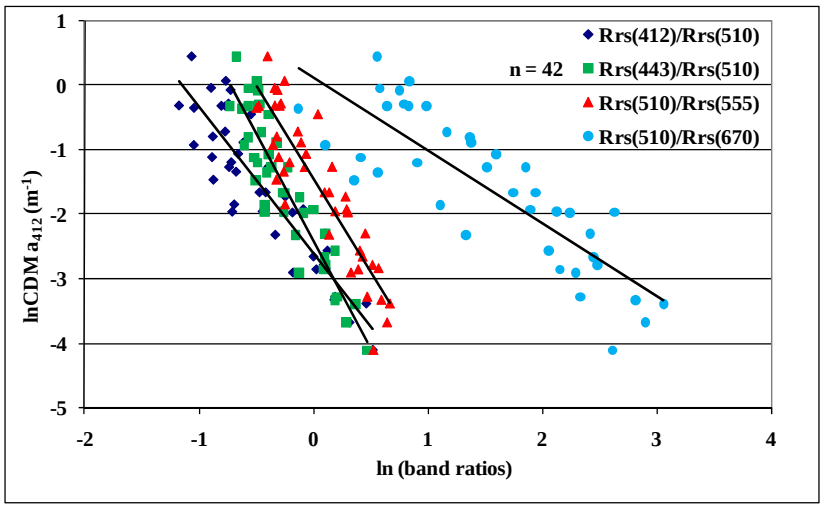

Figure 31. Correlation analysis between the different ln(band ratios) vs. ln($aCDM_{412}$) evaluated for the complete data set (dry and rainy season).

Table 18. Band ratios vs. ln($aCDM_{412}$) correlation for the complete data set (rainy and dry season).

Band ratios	Modeled equation	Determination coefficient
$R_{rs}(412)/R_{rs}(510)$	lny = -2.2681lnx - 2.6000	$R^2 = 0.81$
$R_{rs}(443)/R_{rs}(510)$	lny = -3.3209lnx - 2.4245	$R^2 = 0.84$
$R_{rs}(510)/R_{rs}(555)$	lny = -2.8662lnx - 1.4519	$R^2 = 0.81$
$R_{rs}(510)/R_{rs}(670)$	lny = -1.1271lnx + 0.1172	$R^2 = 0.70$

$aCDM_{412}$ vs. CDOM ag412 correlation analysis

Recorded $aCDM_{412}$ values were 0.0137 (m^{-1}) as minimum and 0.9190 (m^{-1}) as maximum. CDOM a_{g412} were 0.0705 (m^{-1}) as minimum and 0.3254 (m^{-1}) as maximum values. CDOM a_{g412} values should be expected, to be lower than those measured for $aCDM_{412}$ since $aCDM_{412}$ is the sum of CDOM and NAP. $aCDM_{412}$ values are at least, double or triple the values measured for CDOM absorption. For this purpose it was evaluated if a relation could be established between a_{g412} and $aCDM_{412}$ (Figure 32). The resulting correlation analysis empirical equation suggests that it is not suitable since the modeled equation says that when $aCDM_{412}$ values are 0; CDOM values is 0.0816. This is not possible since $aCDM_{412}$ values must always be higher than those

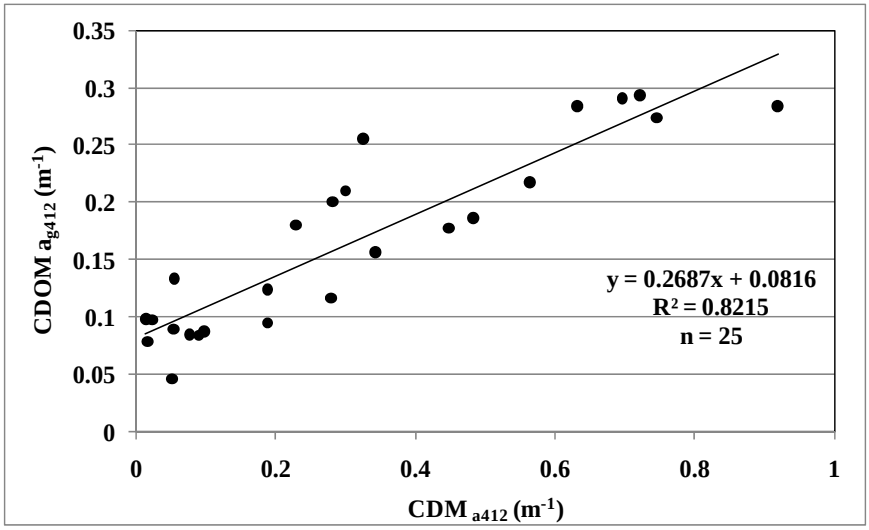

Figure 32. CDM a_{412} vs. CDOM a_{g412} correlation.

Validation of the empirical models

The R_{rs} spectral curves used to validate the empirical models correspond to those of four stations that are complementary to the ones used in this study. Between 2001-2004, 23 scans were used to retrieve the data for the band ratio determination used in the regression analysis. The R_{rs} spectral curves used for the validation were similar in characteristic and magnitude as those used to develop the model. For the rainy season two outlier were identified (A1 and GI) and were eliminated from the data showing the same red clay-mineral spectral signature previously eliminated from the data set.

Table 19. Empirical equation validation for the diferent band ratios between estimated and mesured a_{g412} correlation regression analysis.

Band Ratio	Empirical equation used to estimate a_{g412}	Determination coefficient(n = 23)
ln(x) = ln(R_{rs}412/R_{rs}510)*	lny = -1.0762 **ln(x)** - 2.4945	R^2 = 0.78
ln(x) = ln(R_{rs}443/R_{rs}510)*	lny = -1.5274 **ln(x)** - 2.3904	R^2 = 0.70
ln(x) = ln(R_{rs}510/R_{rs}555)*	lny = -1.4709 **ln(x)** - 1.9568	R^2 = 0.78
ln(x) = ln(R_{rs}510/R_{rs}670)*	lny = -1.2851 **ln(x)** - 1.0935	R^2 = 0.53

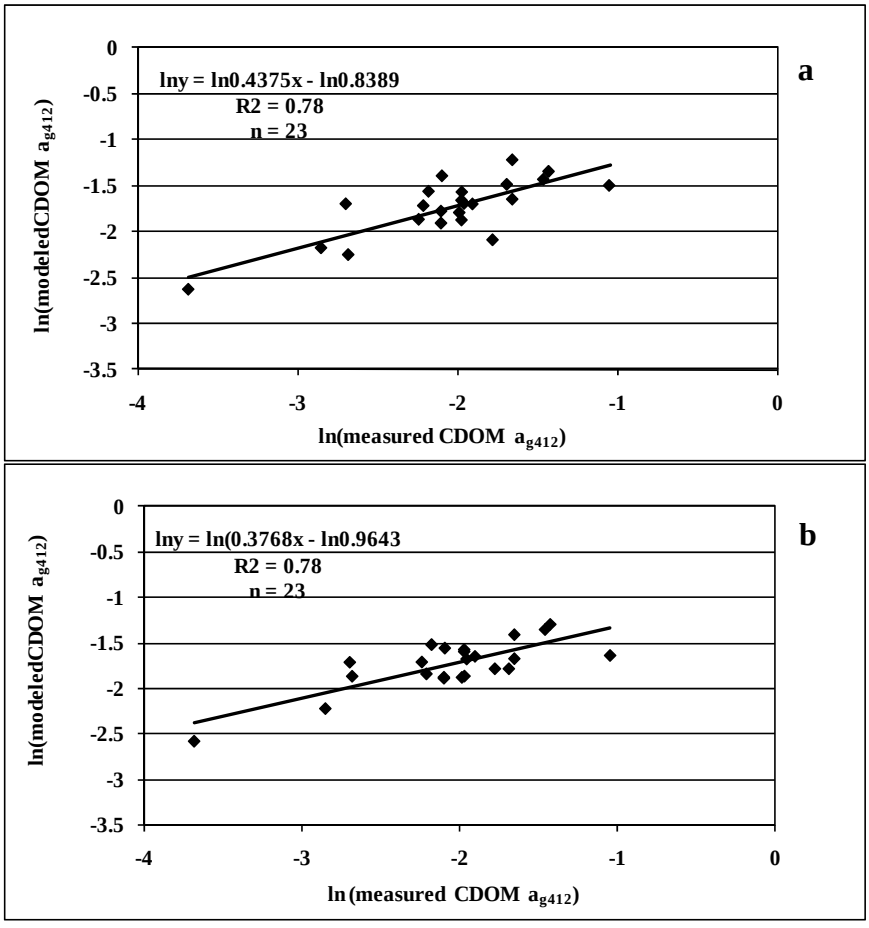

Figure 33. Correlation analysis between measured ln(a_{g412}) vs. modeled ln(a_{g412}) estimated using a) ln(R_{rs}412/R_{rs}510) and b) ln(R_{rs}510/R_{rs}555) band ration.

The regression analysis used to validate the model to estimate a_{g412} from the band ratios extracted from the R_{rs} demonstrated that the best model was with the band ratios of $R_{rs}412/R_{rs}510$ and $R_{rs}510/R_{rs}555$ each with a $R^2 = 0.78$ (Figure 33, 34 and Table 19). CDOM algorithms based on the 412 nm band are known to have atmospheric correction problems (using satellite data) due to the short wavelengths and its related atmospheric correction problems due to signal noise approach (Kahru and Mitchell 1999; Siegel *et al*., 2000). Empirical algorithms using 443 and 510 nm bands are not completely free of Chl-*a* signature but can provide a reasonable index of CDOM estimates (Kahru and Mitchell, 2001). In the case of the $R_{rs}510/R_{rs}670$ band ratio algorithm, were not satisfactory for the estimate of CDOM a_{g412} with a determination coefficient ($R^2 = 0.53$. n = 23), due to problems that will be further discussed.

Statically analysis for the evaluation of algorithm validation

Mean absolute percent difference APD% and root mean square error (RMSE) analyses were performed to the estimated CDOM a_{g412} validation algorithm. The RMSE represents the standard deviation of the residuals for the R_{rs} band ratios from the non-linear regression analysis. The validation match-ups showed that the mean APD% differences were lower (< 35%) for the first three band ratios ($R_{rs}412/R_{rs}510$; $R_{rs}443/R_{rs}510$ and $R_{rs}510/R_{rs}555$) and falling within our established level. In the case of the $R_{rs}510/R_{rs}670$ band ratio it was found to be > 50% higher than our established APD%. The RMSE for the same three band ratios was 0.6391, 0.6041, and 0.6736, respectively. The highest RMSE (0.8670) was observed for the $R_{rs}510/R_{rs}670$ band ratio (Figure 34 and Table 20).

In the slopes of the algorithms, the best relation of 11 was with the $R_{rs}412/R_{rs}510$ ratio was -1.07. For the other two evaluated band ratios ($R_{rs}443/R_{rs}510$; $R_{rs}510/R_{rs}555$) were of -1.52 and -1.47 making this very similar and deviated from the 11 relation. This could suggest that

these empirical algorithms have their merits and they should improve as the data set size increases. By increasing the dynamic range of the algorithms in more waters of the SMAB; a more complete data set will increase the capabilities of the model (Pan *et al*., 2008). This should also be done in our study area but, high TSS can also induce "outliers" (Figure 30 c). Problems related to Inorganic mineral material in the development of algorithms was previously addressed (Rosado-Torres, 2008). This is not an option in this study; by avoiding extreme concentrations of mineral particles it should be possible to develop a more robust empirical algorithm. Concentrations > 5 mg/l of TSS has been indicated to affect the backscattering and thus the R_{rs} and this has limited the development of algorithm for the Chl-*a* retrieval in the Mayagüez Bay (Rosado-Torres, 2008). Due to the nature of the band ratios used in our study, the red clay-mineral particles optical properties reflect most of the light in the red portion of the spectrum. Seems to have a minor effect on scattering on R_{rs} band ratios used between 400-550 nm (Figure 26c), if red clay mineral particles are low, but caution must be taken with water absorption correction when mineral particles are in high concentrations as seen in (Figure;), inducing a greater variability at inshore stations intervals of confidence.

Table 20. Statistical analysis for the evaluated band ratios for the determination of a_{g412}.

Band ratios	Slope	Determination coefficient	Mean APD (%)	RMSE*
lnx = ln(R_{rs}412/R_{rs}510)*	-1.0762	R^2 = 0.78	18.8	0.6391
lnx = ln(R_{rs}443/R_{rs}510)*	-1.5274	R^2 = 0.70	17.2	0.6041
lnx = ln(R_{rs}510/R_{rs}555)*	-1.4709	R^2 = 0.78	18.8	0.6736
lnx = ln(R_{rs}510/R_{rs}670)*	-1.2851	R^2 = 0.53	39.1	0.8670

***N = 23**

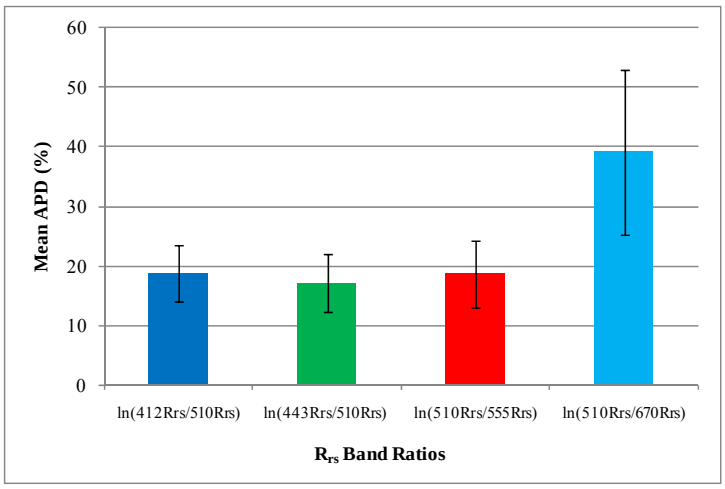

Figure 34. Evaluated band ratios Mean APD % comparison at the 95% confidence level.

DISCUSSION

Characteristic spectral signature, were established by stations (Inshore, offshore and AAA) during the study period (Figure 25). It was decided that the best approach was to separate the R_{rs} spectral data sets in three spectral signatures (Figure 26). This spectral pattern was first noticed in the Mayagüez Bay during a previous study (Rosado-Torres, 2000). The R_{rs} values at inshore stations were slightly higher (Rosado-Torres, 2000) than those recorded in this present study. A possible explanation for the lower R_{rs} during the present study can be related to water absorption correction issues. During this previous study R_{rs} was corrected at a fix wavelength of 720 nm for water absorption (Rosado-Torres, 2000). During the present study the corrections were performed taking the lowest R_{rs} values recorded between $\lambda_{720\text{-}920}$ nm as suggested by Z. Lee, (personal communication). But in general the magnitudes found in the present work (0.001-0.011 Sr^{-1}) are very similar to those reported by Rosado-Torres (2000).

Spectral signatures shifts were recorded in some instances between inshore and offshore stations. Possible causes of these shifts at inshore stations can be related to reduction in river discharge; and the advection of offshore waters causing that the spectral signature of inshore stations resembled those of offshore stations. Heavy river discharge rich in particles and CDOM during the rainy season and/or re-suspension events can directly impact offshore station R_{rs} and other bio-optical components causing that in a few instances offshore stations had similar inshore spectral signatures. Bottom re-suspension, a seasonal event, occurring during the dry season and when the heavy river discharge are almost absent can export from inshore fine particulate (Cruise and Miller, 1994; Miller *et al*., 1994) and dissolved material to offshore waters. The circulation in the Mayagüez Bay is related to oceanic currents that come from the Mona Channel and the

effects of tides, surface winds, waves and river discharges (Alfonso, 1996) are important in the dynamic of the Bay.

After separating the station by spectral signature it becomes evident that mean offshore station present a lack of variability (95% confidence level) maintaining its characteristic oceanic blue water signature (Figure 27). Inshore stations demonstrated the characteristic Chl-*a* peak, with an almost constantan variability between 400-500 nm at inshore stations. After 500 nm a marked increase in variability is observed until reaching 700 nm. The variability between 500-600 nm can be related to Chl-*a* between and that between 600-700 nm to red clay-mineral particles. Rosado-Torres (2008) demonstrated the importance of these inorganic particles dominating R_{rs} the Mayagüez Bay modeled by Hydrolight. The AAA station demonstrated fairly to be constant with low variability through its spectral signature with a slight increase between 500-600 nm related to Chl-*a*. In coastal waters CDOM and sediments often overwhelm phytoplankton in the contribution of bio-optical properties (Gordon and Morel, 1983; Kirk, 1994; Mobley, 1994).

CDOM was an important light absorbing component affecting light penetration in the Mayagüez Bay (Rosado-Torres, 2000; 2008). Inshore stations had characteristics R_{rs} peak broad maximum between 560-590 nm in the green area of the spectrum suggesting that CDOM and Chl-*a* are the main components responsible for this feature (Figure 25). When high concentrations of CDOM and NAP coincides with increased Chl-*a*, the maximum light transmission wavelength and the R_{rs} spectrum are shift towards longer wavelengths (590 nm) (D'Sa *et al*., 2006; Kowalczuk *et al*., 2005).

Empirical algorithm evaluation

The retrieval of Ocean Color Components (OCC) by remote sensing can be a valuable tool to monitor long term ecological consequences in estuarine system (Menon *et al.,* 2006). In order to derive CDOM concentration from ocean color it is necessary to unravel the color signal associated with it from that associated with suspended sediments and phytoplankton pigments (Bowers *et al.,* 2000). This relations has been the most explored and used for CDOM estimate to later retrieve Salinity (Binding and Bowers, 2003; Bower *et al.,* 2000; 2004), or DOM in an inversion mode (Del Castillo and Miller, 2007).

Empirical models can provide a link between satellite-sensed radiance and the relevant bio-optical parameters such as Chl-*a* and K_d on global and regional scales (Johannessen *et al*., 2003; Kowalczuk *et al*., 2005; O'Reilly *et al*., 1998).

When CDOM is the dominating component of color, CDOM absorption can be measured remotely using different band ratio coefficients at two wavelengths (Bowers *et al.,* 2000). A few empirical models for the estimation of CDOM or $aCDM_{412}$ have been published (Bowers *et al.,* 2000; Del Castillo and Miller, 2007; D'Sa *et al*., 2006; Johannessen *et al*., 2003; Kahru and Mitchell, 2001; Kowalczuk *et al*., 2005; Mannino *et al*., 2008; Pan *et al*., 2008; Menon *et al*., 2005; 2006); using different AOPs by various methods like L_w (water leaving radiance); nL_w (normalized water leaving radiance) and R_{rs}. Optimized regional empirical algorithms have been proven effective in CDOM determination (Kahru and Mitchell, 1999). This has the advantage that they do not require an understanding of the fundamental radiative transfer theory (Pan *et al.,* 2008).

In previous studies, regression analysis between CDOM and $aCDM_{412}$, and tested band ratios, was best described by a power-law equations (D'Sa *et al*., 2006; Pan *et al*., 2008 and

Del Castillo and Miller, 2007) and $aCDM_{412}$ (Pan *et al*., 2008 and Mannino *et al*., 2008) (Figure 28 and 29). In the present study, this relation was also described by power-law equations. While in the Baltic Sea it was found that the best-fit was described by a second-order polynomial equation (Kowalczuk *et al*., 2005). For the rainy season, the best band ratio fit was found for $R_{rs}510/R_{rs}555$ (R^2 = 0.85; n = 24). Higher CDOM absorption coefficients during the rainy season (a_{g355} 0.51 m^{-1}) can be an important factor that determines a more robust signal at 510 nm. River discharges play a major role in controlling the distribution of biogeochemical constituents, but it is subjected to seasonal and regional variability (Pan *et al*., 2008). CDOM was found to be the major contributor to the water column light absorption at shorter wavelength < 550 nm during the dry season and on the outer shelf of the SMAB (Pan *et al*., 2008). Seasonal CDOM absorption coefficient might determine the success of the developed algorithms as has been observed during the present study.

During the dry season half CDOM absorption coefficients (a_{g355} 0.29 m^{-1}) can explain the poorer relations encounter during the dry season (Chapter 1). A previous study using SeaWiFS band ratios ($R_{rs}490/R_{rs}555$) and CDOM a_{g380} had a similar determination coefficient (R^2 = 0.83; n = 24) (Pan *et al*., 2008) to the present study. Even though, comparison is difficult, since absorption coefficients and band ratios and a_{g380} used in the correlation analysis were different. It seems that using CDOM a_{g412} is a better approach than using a_{380} since OCS has not a band centered at 380 nm.

Another of the band ratios evaluated in the present study was $R_{rs}412/R_{rs}510$, with a strong determination coefficient R^2 = 0.78 (n = 24) (Figure 30b and Table 16). In a recent study, $R_{rs}490/R_{rs}555$ for SeaWIFS and $R_{rs}490/R_{rs}551$ for MODIS band ratios against CDOM a_{412} showed excellent agreements R^2 of 0.92 n = 25 for the former and R^2 = 0.91 n = 34 for the latter

(Pan *et al*., 2008). A band ratio using R_{rs} at 490 nm band was not evaluated in this study, since Chl-*a* has a great contribution at this wavelength. CDOM's high contribution at 443nm and its low contribution between 510-520 nm was the main point to use this band ratio (Kahru and Mitchell, 2001).

CDOM has been identified as mayor light absorbing component the Mayagüez Bay (Rosado, 2000; 2008). This can explain the success of the empirical model development. Evidence for the important role of CDOM in light absorption in the Mayagüez Bay can be demonstrated with the measured a_{g440} absorption coefficient and with estimated $a\varphi$ absorption coefficient. These absorption coefficients means were separated between the dry and rainy season and it became obvious that a_{g440} was a more important component than $a\varphi$ in light absorption than Chl-*a.* Briefly, between 63-77% of total absorption coefficient of these two parameters at 440 nm, was mainly by CDOM, for both seasons at the surface, indicating that CDOM and NAP (not measured) control the light penetration between 400-500 nm in the Bay. CDOM a_{g412} and a_{g443} in the Mississippi estuary, while variable, formed a significant fraction of the total absorption field at these wavebands (D'Sa *et al*., 2006). CDOM accounted between 50-60% of the total absorption, and after spring bloom CDOM occupied about 80% of the total absorption (Sasaki *et al.,* 2005). CDOM accounted between 35-70% of the total light absorption excluding water absorption as compared to 0-20% for non-pigmented particles and 30-45% for phytoplankton in the SMAB (Pan *et al*., 2008). This previously published percents are in close agreement to those calculated for the Mayagüez Bay. Caribbean a_{g440} in surface water accounted between 60-80% of the total absorption compared to $a\varphi$ on a yearly basis (Méndez-Silvagnoli, 2008). It is interesting that the relative percent recorded for CaTS are very similar to those found in the Mayagüez Bay.

In the Southern Middle Atlantic Bight (SMAB), CDOM and particles accounts between the 35-70% of the absorption at 443 nm (Pan *et al*., 2008). CDOM absorption coefficient at a_{g412}, varied between 0.1030-0.4170 m^{-1} along with phytoplankton absorption coefficient with Chl-*a* varied from 0.68 µg/l to 6.11 µg/l (D'Sa *et al*., 2006). In our study, CDOM accounted for a significant contribution compared to Chl-*a*. In the Mayagüez Bay, phytoplankton absorption was about one order of magnitude less than particulate absorption and was two orders of magnitude less than CDOM absorption (Rosado-Torres, 2000).

Band ratio determination coefficient evaluation

After evaluating the band ratio for the algorithms for the estimation of CDOM, the best model fit was found for the $R_{rs}412/R_{rs}510$ and $R_{rs}510/R_{rs}555$ band ratios (both $R^2 = 0.78$) with both having a APD of 18.8% and RMSE of 0.6391 for the former; and a RMSE of 0.6736 for the later (Figure 33 and 34; Table 19). The $R_{rs}443/R_{rs}510$ band ratio had a reasonable determination coefficient of $R^2 = 0.70$ with an APD = 17.2% and a 0.6041 RMSE. The lower determination coefficient found for the $R_{rs}443/R_{rs}510$ band ratio could be related to the fact that Chl-*a* is an important light absorber at 443 nm. But even though it is found in lower concentrations this can still have a significant Chl-*a* contribution to the R_{rs} signal. The relative high CDOM and low Chl-*a* contribution to absorption and thus its impact on as R_{rs} can explain the fairly good $R^2 = 0.70$ for the $R_{rs}443/ R_{rs}510$ band ratio. The band ratio with the lowest determination coefficient ($R^2 = 0.53$; APD = 39.1% and 0.8670 RMSE) is $R_{rs}510/R_{rs}670$. Samples were taken under highly diluted marine waters end-member salinities ≥ 30. For this band ratio, ($R_{rs}510/R_{rs}670$)_the model works in conditions where CDOM is the main light absorber, which is characteristics of low Salinity conditions in river dominated circumstances and conservative dilution (Del Castillo and Miller, 2007). Riverine CDOM out-weighed marine water CDOM,

with very low Chl-*concentrations* (0.38-4.10 µg/l) recorded in the study by Del Castillo and Miller (2007). Relatively high CDOM absorption coefficient values are necessary at 510 nm to have a robust signal. Beyond 670 nm CDOM absorption is minimal but Chl-*a* has a significant signal if high concentrations are present; low Chl-*a* concentrations are necessary conditions.

In the present study, samples were taken at salinities over 33.5 under highly mixed conditions of low Chl-*a* concentrations (0.026-2.20 µg/l), half the maximum Chl-*a* concentration in the Mississippi and almost half (0.074-0.79 $m^{-1)}$ the recorded values of CDOM a_{g412} 0.50-1.40 m^{-1} (Castillo and Miller, 2007). These lower absorption coefficient values, can explain the poor performance even though Chl-*a* concentrations in the Bay where low in the regression analysis for $R_{rs}510/R_{rs}670$ band ratio (Figure 34 and Table 20) empirical model (R^2 = 0.53 n = 24 and APD = 50%).

The Mayagüez Bay is dominated by high CDOM absorption, "low Chl-concentrations" and abnormally high reflection in the red, caused by the high concentrations of red clays found in the Bay (Rosado-Torres, 2008). Suspended particles are an important factor that complicate the used of remote sensing band ratios (Bowers *et al.,* 2004). High concentrations of particles loads, resulting from re-suspension, beach erosion or riverine input, are known to elevate the remote sensing reflectance values (Kowalczuk *et al*., 2005). It was demonstrated that under high TSS concentrations *in situ* remote sensing can be used to estimate TSS in the Mayagüez Bay (Rodríguez-Guzmán, 2008), and TSS was associated to river discharge and to re-suspension events.

The combined effects of absorption and particle backscattering are known to strongly influenced R_{rs} signal (D'Sa and Miller, 2003). Previous studies found R_{rs} values far from zero at 720 nm at all stations except of offshore; high reflectance in red wavelength ($\lambda > 670$ nm), was

attributed to high concentrations of red clay-minerals that were related to local river sources (Rosado-Torres, 2000). Red-clay-mineral particles of unknown optical properties scatter light at wavelength > 670 nm where water is suppose to be the main absorber at this wavelength. High clay-minerals can be another factor that influences the poor performance of the empirical models by using the 670 nm band where interference of red clay-mineral can have an important effect at 670 nm. It is possible that for this band ratio algorithm the correcting at longer wave length (Lee, personal communication) will be ineffective since a significant signal of red clay-mineral will be found in the R_{rs} signal that wavelength .

In the Mayagüez Bay, inanimate particulate matter can be very important in absorption (Rosado-Torres, 2000), and scattering processes (Rosado-Torres, 2000; 2008). Concentration of clay-minerals (> 5 mg/l) limits the use of remote sensing due to particle backscattering (Rosado-Torres, 2008). Concentrations of TSS > 5 mg/l were all related to outliers in our study were eliminated from the data set, and in only one instance (July 19, 2005), the concentrations were 4.67 mg/l, which are close to the 5 mg/l threshold established by (Rosado-Torres, 2008). At concentration greater than 5 mg/l, both CDOM absorption and Chl-*a* concentration have moderate effect on the spectral shape and the magnitude of the R_{rs} curve (Rosado-Torres, 2008). Hydrolight simulations suggested that red clay-minerals are the single most important optically active seawater constituent in Mayagüez Bay (Rosado-Torres, 2008). We agree with (Rosado-Torres, 2008) that TSS concentrations > 5 mg/l can affect can induce problems in the accurate determination of R_{rs} since TSS can dominate the R_{rs} signal and thus complicate the development of algorithms. In the inner part of the Mayagüez Bay, absorption was found to be dominated by two components; detritus and CDOM, where light is absorbed effectively in the blue end of the spectrum by these components (Rosado-Torres, 2000). Highly stratified river-dominated coastal

waters with its non-uniform vertical bio-optical properties may influenced both the radiometric the IOP-derived estimates of R_{rs} may not always been representative of their effects on the radiance field (D'Sa *et al*., 2006). This condition of non-uniform vertical bio-optical properties can be a persistent situation in the Mayagüez Bay at inshore stations where this can be clearly seen. It is possible that this condition has some influence in the development of the empirical algorithm. Other factors, like short-term variations in CDOM absorption originated by biological, biochemical, microbial and photochemical processes, could be responsible for uncertainty in the empirical relationships between CDOM and R_{rs} (Kowalczuk *et al*., 2005). The possibility of short term variation between CDOM and R_{rs} by a series of physical, chemical and biological and photochemical is a real concern that should be further investigated in the Mayagüez Bay.

The $R_{rs}510/R_{rs}555$ band ratio algorithm for CDOM absorption was demonstrated to perform relatively well for the Mississippi region (D'Sa and Miller, 2003; D'Sa *et al*., 2006). Regression analysis of logarithmic transformed $R_{rs}510/R_{rs}555$ band ratios and CDOM a_{g412} had a satisfactory determination coefficient ($R^2 > 0.70$) adequate to estimate CDOM from R_{rs}. (D'Sa *et al*., 2006).

$aCDM_{412}$ algorithm development

Correlation analysis using the same four R_{rs} band ratios used to develop the empirical relation for CDOM were evaluated for $aCDM_{412}$. The determination coefficients between the four band ratios and $aCDM_{412}$ were higher than those obtained for CDOM a_{g412} (Figure 31 and Table 18). The more robust determination coefficient (R^2) are reasonable since $aCDM_{412}$ is the sum of CDOM and NAP and in coastal water this relation should be expected since the R_{rs} signal has the contribution of both variables.

CDOM and $aCDM_{412}$ empirical relation

A tight correlation between CDOM and $aCDM_{412}$ seems to be established $R^2 = 0.82$, (Figure 32). But the equation $y = 0.2687x + 0.0816$; when $aCDM_{412}$ concentrations are 0 CDOM absorption coefficient is 0.0816 and this is an impossible. $aCDM_{412}$ absorption coefficients should be higher than those of CDOM the feasibility to use *in situ* remote sensing reflectance to derive CDOM or $aCDM_{412}$ absorption coefficients by measuring one of this variables has to be further evaluated. But this relation suggests that similar processes are working simultaneously on both components (river discharge, re-suspension events and dilution and others).

R_{rs} band ratios can be used to develop algorithms in which Salinity could be retrieved from CDOM absorption coefficients (Bower *et al.,* 2000). These algorithms work on the principle of conservative dilution and the low concentration of suspended particles. River and marine waters end-members often mix conservatively (Blough *et al.,* 1993; Bowers *et al.,* 2000; Chen *et al.,* 2007; Del Castillo *et al.,* 1999; 2000a; Hu *et al.,* 2003; Vodacek *et al.,* 1997), but in some estuarine zones this is not always case (Chen *et al.,* 2007; Gallegos, 2005; Sasaki *et al.,* 2005; 2003; Zepp *et al.,* 2004). Preliminary studies must first be done to determine if effectively CDOM and Salinity have a tight relation. In the Mayagüez Bay conservative dilution and low suspended particles concentrations were conditions partially present in the Mayagüez Bay. Another important relation is that between DOM/CDOM that can be used inversion modeling to retrieve DOM concentrations (Del Castillo and Miller, 2007; Kahru and Mitchell, 2001).

CDOM can be estimated synoptically from space (Hu *et al*., 2003 Hong *et al.,* 2005; Müller-Karger, 1989) and is desirable to establish a data base that describes CDOM spatial and spectral distribution and their temporal variations (Hong *et al.,* 2005). The great importance of CDOM biogeochemistry in marine environment and the multiple aspects concerning all the

possible implications for the study of CDOM has been clearly established. Multiple aspects like remote sensing related problems, carbon cycle issues, photo-production of reactive substances, trace metal species control, and light quality and quantity control over primary productivity and the possibility of answering other questions of another complex biochemical processes are also important. Remote sensing techniques give the promise to be a robust tool to monitor complex biogeochemical processes involving the CDOM transit from the terrestrial environment and its fate and transport to marine environments.

CONCLUSION

1-In the Mayagüez Bay three contrasting R_{rs} spectral signature can be found inshore, offshore and one for the sewage discharge outfall station. In some instance, anomalous R_{rs} curves can be related to extreme river discharges and their associated heavy red clay-mineral. These minerals increase backscattering and thus produce water absorption correction issues. Inorganic clay-mineral optical effects should be taken into account at the moment of developing any SA or empirical models for the Mayagüez Bay since their optical properties are unknown.

2- Three of the four empirical algorithms were successful in reaching the threshold for a validated uncertainty of < 35% for the developed algorithm for CDOM. This acceptable APD < 35% validation was found for the first three band ratios evaluated (Figure 34) but this requirement was not achieved for the $R_{rs}510/R_{rs}670$ band ratio (> 50%) for the retrieval of surface CDOM a_{g412} for various factors. Two of the band ratios evaluated $R_{rs}412/R_{rs}510$ and $R_{rs}510/R_{rs}555$ were highly successful for estimating the concentration of CDOM in the Mayagüez Bay ($R^2 > 0.70$). But any of these band ratios can be used to estimate CDOM a_{g412}. We suggest that the $R_{rs}412/R_{rs}510$ should be the one of choice since it will have a maximum CDOM absorption at the lower wavelengths and minimal influence of Chl-*a* at the longer wavelength.

3-To determine $aCDM_{412}$ from R_{rs} , similar R_{rs} band ratios were evaluated with very good determination coefficient ($R^2 > 0.80$) obtained in the regression analysis. This high R^2 was obtained for the first three band ratios evaluated suggests that this have the potential of retrieving $aCDM_{412}$ from R_{rs} measurements. But like for CDOM $R_{rs}510/R_{rs}670$ band ratios, had the lowest $R^2 = 0.70$. The tentative empirical algorithms for $aCDM_{412}$ determination wait further validation.

4- To our knowledge this is the first successfully attempt to develop and validated an empirical algorithm using *in situ* R_{rs} for the estimate of CDOM in coastal marine waters in Puerto Rico.

RECOMMENDATIONS

1-The optical properties of TSS in the Mayagüez Bay must be characterized. High concentration of particulate matter can severely affects the gathering of useful R_{rs} data near the rivers and under Heavy River discharges and a compromise should be met for the usefulness data collected.

2-Humic acids-clay-minerals and flocculation processes occurring during estuarine mixing at low salinities might change the optical properties under. Since partition between dissolved and particulate fraction can cause changes in IOPs.

2-Collect more field data at offshore station since a small number was used in the validation analysis, water samples and R_{rs} data should be increased to further development and validate empirical models. Estuarine condition at salinities (< 30) not observed during the present study should also be monitored to gather data not available at this moment for the development and validation purpose.

3- Studies on bio-optical properties of the surface micro-layer and its relation to remote sensing and other biogeochemical processes related to the water column should be further addressed.

BIBLIOGRAPHY

Alberts, J.J., M. Takacs and J.F. Schalles. 2004. Ultraviolet-visible and fluorescence spectral evidence of natural organic matter (NOM) changes along an estuarine salinity gradient. Estuaries. 27:297-311.

Alfaro, M. 2002. Oceanographic feature and zooplankton community structure Mayagüez Bay, Puerto Rico. Ph.D. Dissertation in Marine Science. University of Puerto Rico, Mayagüez Campus. pp.151.

Alfonso, E. 1996. The costal current regime in Añasco Bay during a one-year period. Master Thesis in Marine Science. University of Puerto Rico, Mayagüez Campus. pp.116.

Alfonso, E. 2001. Variabilidad temporal de la productividad primaria fitoplanctónica en la estación CaTS (Caribbean Time Series Station): con énfasis en el impacto de la marea interna semidiurna sobre la tasa de producción. Disertación Doctoral Universidad de Puerto Rico Mayagüez, Puerto Rico. pp. 486.

Amon, R.M.W., and B. Menon. 2004. The biogeochemistry of dissolved organic matter and nutrients in two large Arctic estuaries and potential implications for our understanding of the Arctic Ocean system. Marine Chemistry. 92:311–330.

Amon, R.M.W., and R. Benner. 1996a. Bacterial utilization of different size classes of dissolved organic matter. Limnology and Oceanography. 41:41-51.

Arnarson, T.S., and R. G. Keil. 2000. Mechanisms of pore water organic matter adsorption to montmorillonite. Marine Chemistry. 71:309-320.

Arrigo, K.R. and C.W. Brown. 1996. Impact of chromophoric dissolved organic matter UV inhibition of primary productivity in the sea. Marine Ecological Progress Series. 140:207-216.

Austin, R., 1974. The remote sensing of spectral radiance from below the ocean surface. In N.G. Jerlov and E. Steemann Nielsen (Eds.) Optical aspects of oceanography. Academic Press. London, New York. pp. 317-344.

Benner, R. and S. Opsahl. 2001. Macromolecular indicator of the source and transformation of dissolved organic matter in the Mississippi plume. Organic Geochemistry. 32:597-611.

Biddanda, B., and R. Benner. 1997. Carbon, nitrogen and carbohydrate fluxes during the production of particulate and dissolved organic matter by marine phytoplankton. Limnology and Oceanography. 42:506-518.

Binding, C.E., and D.G. Bowers. 2003. Measuring the salinity of the Clyde Sea from remote sensed ocean color. Estuarine, Coastal and Shelf Science. 57:605-611.Blough, N.V. and R. Del Vecchio. 2002. Chromophoric DOM in the coastal environment. In D.S. Hansell and C.A.

Carlson, (Eds.). Biogeochemistry of marine dissolved organic matter. Academic Press. Elsevier Science. San Diego, CA. pp. 509-546.

Blough, N.V.; O.C. Zafiriou and J. Bonilla. 1993. Optical absorption spectra of water from the Orinoco River outflow: terrestrial input of colored organic matter to the Caribbean. Journal of Geophysical Research. 98(C):2271-2278.

Blough, N.V. and S.A. Green. 1995. Spectroscopic characterization and Remote Sensing of non-living organic matter. In R. Zepp and C. Sonntag, (Eds.). The role of non living organic matter in the Earth carbon cycle. Wiley. pp. 23-45.

Børsheim, K.Y., S.V. Myklestad and J-A. Sneil. 1999. Monthly profiles of DOC mono and polysaccharides at two locations in the Trondheimsfjord (Norway) during two years. Marine Chemistry. 63:255-272.

Boss, E., W.S. Pegau, J.R.V. Zaneveld, and A.H. Barnard. 2001. Spatial and temporal variability of absorption by dissolved material at a continental shelf. Journal of Geophysical Research. 106(C):9499-9507.

Bowers, D.G., D. Evans, D.N. Thomas, K. Ellis, P.J. Le and B. Williams. 2004. Interpreting the color of an estuary. Estuarine, Coastal and Shelf Science. 59:13-20.

Bowers, D.G., G.E.L. Harker, P.S.D. Smith and P. Tett. 2000. Optical properties of a region of freshwater influence (the Clyde Sea). Estuarine, Coastal and Shelf Science. 50:717–726.

Bricaud, A., A. Morel and L. Prieur. 1981. Absorption by dissolved organic matter of the sea (yellow substance) in the UV and visible domains. Limnology and Oceanography. 26:43-53.

Bricaud, A. and D. Stramski. 1990. Spectral absorption coefficient of living phytoplankton and non-algal biogenous matter: A comparison between the Peru upwelling area and the Sargasso Sea. Limnology and Oceanography. 35:562-582.

Burdige, D.J., S.W. Kline and W.H. Chen. 2004. Fluorescent dissolved organic matter in marine sediment pore waters. Marine Chemistry. 89(1-4):289-311.

Bushaw, K.L. 1996. Photochemical release of biological available nitrogen from dissolved organic matter. Nature. 381:404-407.

Cameron-González, A.E. Spectral analyses and sedimentation of the west coast beaches of Puerto Rico. Undergraduate Research Final Report Geology. Unpublished study.

Capella, J.E. and K.A. Grove. 2002. A review of oceanographic data from the Mayagüez and Añasco Bay system. Final Project Report. University of Puerto Rico, Mayagüez, Puerto Rico. pp.48.

Carder, K.L., F.R., Chen, Z.P. Lee, and S.K. Hawes. 1999. Semianalytic moderate-resolution imaging spectrometer algorithms for chlorophyll-a and absorption with bio-optical domains based on nitrate-depletion temperatures. Journal of Geophysical Research. 104(C):5403–5421.

Carder, K L., R.G. Steward, G.R. Harvey and P.B. Ortner. 1989. Marine humic and fulvic acids: Their effects on remote sensing of ocean chlorophyll. Limnology and Oceanography. 34:68-81.

Carder, K.L., S.K., Hawes, K A., Baker, R C., Smith, R.G. Steward, and B.G. Mitchell, 1991. Reflectance model for quantifying chlorophyll-a in the presence of B.G productivity degradation products. Journal of Geophysical Research. 96(C):20599-20611.

Carlson, D.J. and L.M. Mayer. 1983. Relative influences of riverine and macroalgal phenolic material on UV absorbance in temperate coastal waters. Canadian Journal of Fisheries and Aquatic Science. 40:1258-1263.

Cauwet, G. 2002. DOM in the coastal zone. In D.S. Hansell and C.A. Carlson, (Eds.). Biogeochemistry of Marine Dissolved Organic matter. Academic Press. Elsevier Science. San Diego, CA. pp. 579-609.

Chen, R.F. and J.L. Bada. 1992. The fluorescence of dissolved organic matter in seawater. Marine Chemistry. 37:191–221.

Chen, R.F. and G.B. Gardner. 2004. High–resolution measurements of chromophoric dissolved organic matter in the Mississippi and Atchafalaya Rivers plume regions. Marine Chemistry. 89:103-125.

Chen, Y., and M. Schnitzer., 1976. Scanning electron microscopy of a humic acids and of fulvic acids and its metal and clay complexes. Soil Science Society of America. 40:682-686.

Chen, Z., Hu, Chuamine, R.N. Conmy, F.E. Müller-Karger and P. Swarzensk. 2007. Colored dissolved organic matter in Tampa Bay, Florida. Marine Chemistry. 104:98-109.

Chen, Z., C. Hu, R.N. Conmy, F.E. Müller-Karger and P. Swarzensk. 2007. Colored dissolved organic matter in Tampa Bay, Florida. Marine Chemistry. 104:98-109.

Chen, Z.Q., Y. Li and J.M. Pan. 2004. The distribution of the optical properties of color dissolved organic matter and dissolved organic carbon in the pearl river. Estuarine, Coastal and Shelf Science. 24:1845-1856.

Clapp, C.E. and M.H.B. Hayes. 1999. Characterization of humic substances isolated from clay and silt sized fractions of a corn residue-amended agricultural soil. Soil Science. 164:899-913.

Coble, P.G. 1996. Characterization of marine and terrestrial DOM in seawater using excitation-emission matrix spectroscopy. Marine Chemistry. 51:325-346.

Corredor, J.E. and J.M. Morell. 2001. Seasonal variation of physical and biogeochemical features in eastern Caribbean Surface water. Journal of Geophysical Research. 106(C):4517-4525.

Corvera-Gomringer, R. 2005. Aportación de nitrógeno, fósforo y sedimentos suspendidos durante eventos de tormenta en micro cuencas del Río Grande de Añasco, Puerto Rico. Master Thesis. University of Puerto Rico at Mayagüez, Department of Agronomy. pp.110

Cruise, J.F. and R.L. Miller. 1994. Hydrologic modeling of land processes in Puerto Rico using remotely sensed data. Water Resources Bulletin. 30:419-428.

Del Castillo, C.E. 2005. Remote sensing of organic matter in coastal waters. Chapter 7 In R. Miller, C. Del Castillo and B. Mckee (Eds.). Remote sensing of the aquatic environment. Springer. pp.345.

Del Castillo, C.E., F. Gilbes, P.G. Coble and F.E. Müller-Karger. 1998. Optical characteristics of dissolved organic matter during a bloom on the West Florida Shelf. Ocean Optics XIV Kailua-Kona Hawaii. pp.1-6.

Del Castillo, C.E., F. Gilbes, P.G. Coble, F.E. Müller-Karger. 2000a. On the dispersal of riverine colored dissolved organic matter over the West Florida Shelf. Limnology and Oceanography. 45:1425-1432.

Del Castillo, C.E., P.G. Coble, J.M. Morell, J.M. López and J.E. Corredor.1999. Analysis of the optical properties of the Orinoco River plume by absorption and fluorescence spectroscopy. Marine Chemistry. 66:35-51.

Del Castillo, C.E and P.G. Coble. 2000. Seasonal variability of the colored dissolved organic matter during the 1994-95 NE and SW Monsoon in the Arabian Sea. Deep-Sea Research II. 47:1563-1579.

Del Castillo, C.E. and R.L. Miller. 2007. On the use of ocean color remote sensing to measure the transport of dissolved organic carbon by the Mississippi River Plume. Remote Sensing of Environment. doi:10.1016/j.rse.2007.06.015

Del Castillo, C.E., P.G. Coble, R.N. Conmy, F.E. Müller-Karger, L. Vanderbloemen and G.A. Vargo. 2001. Multispectral *in situ* measurements of organic matter and chlorophyll fluorescence in seawater: Documenting the intrusion of the Mississippi River plume in the West Florida Shelf. Limnology and Oceanography. 46:1836-1843.

DeGrandpre, M.D., A. Vodacek, R.K. Nelson, E.J. Bruce, N.V. Blough. 1996. Seasonal seawater optical properties of the U.S. Middle Atlantic Bight. Journal of Geophysical Research. 101(C): 22727-22736.

Del Vecchio, R. and N.V Blough. 2004. On the origin of the optical properties of humic substances. Environmental Science and Technology. 38:3885-3891.

Del Vecchio, R. and A. Subramaniam. 2004. Influence of the Amazon River on the surface optical properties of the western tropical North Atlantic Ocean. Journal of Geophysical Research. 109(C):C11001.

DeSouza-Sierra, M.M., O.F.X. Donard and M. Lamotte. 1997. Spectral identification and behavior of dissolved organic fluorescent material during estuarine mixing processes. Marine Chemistry. 58:51-58.

Ding, X. and S.M. Henrichs. 2002. Adsorption and desorption of proteins and polyamino acids by clay minerals and marine sediments. Marine Chemistry. 77: 225-237.

D'Sa, E.J., G.R. Steward, A.Vodacek, N.V. Blough and D. Phinney. 1999. Determining optical absorption of colored dissolved organic matter in seawater with a liquid capillary wave-guide. Limnology and Oceanography. 44:1142-1148.

D'Sa, E.J. and R.L. Miller. 2003. Bio-optical properties in waters influenced by the Mississippi River during low flow conditions. Remote Sensing of the Environment. 84:538-549.

D'Sa, E.J., R.L. Miller and C. Del Castillo. 2006. Bio-optical properties and ocean color algorithms for coastal waters influenced by the Mississippi River during a cold front. Applied Optics. 45:7410-7428.

Duce, R.A. and E.K. Duursma. 1977. Inputs of organic matter to the ocean. Marine Chemistry. 5:319-339.

, J. M. and Sholkovitz, E. R. 1976. The flocculation of iron, aluminum and humates from river water by electrolytes. Geochimica et Cosmochimica Acta. 40:847-848.

Ertel, J.R., J.I. Hedges and E.M. Perdue. 1986. Dissolved humic substances of the Amazon River system. Limnology and Oceanography. 31:739-754.

Fargion, G.S. and J.L. Mueller. 2000. Ocean optics protocols for satellite ocean color sensor validation, Revision 2, NASA Technical Memo 2000-209966 (NASA Goddard Space Flight-Center, Greenbelt, Maryland,).

Ferrari, G.M. and S. Tassen. 1991. On the accuracy of determining light absorption of yellow substance through measurement of induce fluorescence. Limnology and Oceanography. 36:777-786.

Ferrari, G.M., and M.D. Dowell. 1998. CDOM absorption characteristics with relation to fluorescence and salinity in coastal areas of the southern Baltic Sea. Estuarine, Costal and Shelf Science. 1:91-105.

Fox, L.E., 1983. The removal of dissolved humic acid during estuarine mixing. Estuarine, Coastal and Shelf Science. 16:431-440.

Gallegos, C.L. 2005. Optical water quality of the blackwater estuary: The Lower St. Johns River, Florida USA. Estuarine, Coastal and Shelf Sciences. 63:57-72.

Ghabbour, E.A., G. Davies, M.E. Goodwillis, K. O'Donaughy and T.L. Smith. 2004. Thermodynamic of peat-plant and soil–derived humic acids sorption on Kaolinite. Environmental Science and Technology. 38:3338-3342.

Gilbes, F., 1992. The relation between phytoplankton chlorophyll-*a* and suspended particulate matter Mayagüez Bay, Puerto Rico. Master Thesis in Marine Science. University of Puerto Rico, Mayagüez Campus. pp.53.

Gilbes, F., J. M. López and P. Yoshioka. 1996. Spatial and temporal variations of phytoplankton chlorophyll-a and suspended particulate matter in Mayagüez Bay, Puerto Rico. Journal of Plankton Research. 18:29-43.

Giovanni-Prieto, M. 2007. Development of a regional integrated hydrological model for a tropical watershed. Master Thesis. University of Puerto Rico at Mayagüez, Department of Civil Engineering. pp.121.

Gjessing, E.T. 1976. Physical and chemical characteristics of aquatic humus. Ann Arbor Science Publisher Inc. Michigan U.S.A. pp.120.

Gordon, H.R. and A. Morel. 1983. Remote assessment of ocean color for interpretation of satellite visible imagery. In R.T. Barber (ed.). A review, lecture notes on coastal and estuarine studies. Springer-Verlag. New York. Vol. 4. pp. 68-114.

Gordon, H.R., O.B. Brown, R.H. Evans, J.W. Brown, R.C. Smith, K.S. Baker and D.K. Clark. 1988. A semianalytic radiance model of ocean color. Journal of Geophysical Research. 93(C):10909–10924.

Gosh, K. and M. Schnitzer. 1980. Macromolecules structure of humic substances. Soil Science. 129:266-276.

Garver, S.A. and D.A. Siegel. 1997. Inherent optical property inversion of ocean color spectra and its biogeochemical interpretation. I Time series from the Sargasso Sea. Journal of Geophysical Research. 102(C):18607-18625.

Green, S. A., and N. V. Blough., 1994. Optical absorption and fluorescence properties of chromophoric dissolved organic matter in natural waters. Limnology and Oceanography. 39:1903-1916.

Grove, K. 1977. Sedimentation in the Añasco Bay and river estuary: Western Puerto Rico. Master Thesis in Marine Science. University of Puerto Rico, Mayagüez Campus. pp.130.

Grove, K. 1998. Nearshore sediment transport and shoreline changes at Añasco Bay, Puerto Rico. Ph.D. Dissertation in Marine Science. University of Puerto Rico, Mayagüez Campus. pp.143.

Guo, W., C.A. Stedmon, Y., Han, F. Wu., X. Yu, and M. Hu. 2007. The conservative and non-conservative behavior of chromophoric dissolved organic matter in Chinese estuarine waters. Marine Chemistry. 107:357-366.

Hair, M.E. and C.R. Bassett. 1973. Dissolved and particulate humic acids in an east coast estuary. Estuarine, Costal Marine Science. 1:107-111.

Harvey, G.R. and D.A. Boran. 1985. Geochemistry of humic substances in seawater. In G.A. Aiken, D. McKnight, R.L. Wershaw and P. MacCarthy, (Eds.). Humic substances in soil, sediment and water: Geochemistry, isolation and characterization. Wiley-Interscience. New York pp. 223-247.

Harvey, G.R., D.A. Boran, L.A. Chesal and J.M. Tokar. 1983. The structure of marine fulvic and humic acids. Marine Chemistry. 12:119-132.

Hedges, J.I. 1992. Global biochemical cycles: progress and problems. Marine Chemistry. 39:67-93.

Hedges, J.I. and R.G. Keil. 1999. Organic geochemical perspectives on estuarine processes: sorption reactions and consequences. Marine Chemistry. 65:55-65.

Heil, D. and G. Sposito. 1993a. Organic matter role in illitic soil colloids flocculation: II Surface charge. Soil Science Society of America Journal. 57:1246-1253.

Heil, D. and G. Sposito. 1993b. Organic matter role in illitic soil colloids flocculation: I Counter ions and pH. Soil Science Society of America Journal. 57:1241-1246.

Helm, J.R., A, Stubbins, J.D. Ritchie, E.C. Minor, D.J. Kieber and K. Mopper. 2008 Absorption spectral slopes and slope ratios as indicators of molecular weight, source, and photobleaching of chromophoric dissolved organic matter.2008. Limnology and Oceanography. 53:955-969.

Hermes, P.J. and R. Benner. 2003. Photochemical and microbial degradation of dissolved lignin phenols: Implication for the fate of terrigenous dissolved organic matter in marine environments. Journal of Geophysical Research. 108(C):3291 doi:10.1029/2002JC001421.

Hoge, F.E., A. Vodacek, R.N. Swift, J.K. Yungel and N.V. Blough. 1995. Inherent optical properties of the ocean: retrieval of the absorption coefficient of chromophoric dissolved organic matter from airborne laser fluorescence measurements. Applied Optics. 34:7032-7038.

Hoge, F.E., C.W. Wright, P.E. Lyon, R.N. Swift and J.K. Yungel. 2001. Inherent optical properties imagery of the western North Atlantic Ocean: Horizontal spatial variability of the upper mixed layer. Journal of Geophysical Research. 106(C):31,129-31,140.

Hoge, F.E., M.E. Williams, R.N. Swift, J.K. Yungel and A. Vodacek. 1995. Satellite retrial of the absorption coefficient of chromophoric dissolved organic matter in continental margins. Journal of Geophysical Research. 100(C):24,847-24,854.

Hong, H., J. Wu, S. Shang and C. Hu. 2005. Absorption and fluorescence of Chromophoric dissolved organic matter in the Pearl River Estuary South China. Marine Chemistry. 97:78-89.

Hu, C., Z. Chen, T.D. Clayton, P. Swarzensk, J.C. Brock and F.E. Müller-Karger. 2004a. Assessment of estuarine water-quality indicators using MODIS medium-resolution bands: Initial results from Tampa Bay. Remote Sensing of Environment. 93:423-441.

Hu, C., E.T. Montgomery, R.W. Schimitt and F.E. Müller-Karger. 2004b. The dispersal of the Amazon and Orinoco Rivers water in the tropical Atlantic and Caribbean Sea: Observation from space and S-PALACE floats. Deep-Sea Research II. 1151-1171.

Hu, C., F.E. Müller-Karger, D.C. Biggs, K.L Carder, B. Nababan, D. Nadeau and J. Vanderbloemen. 2003. Comparison of ship and satellite bio-optical measurements on the continental margin of the NE Gulf of Mexico. International Journal of Remote Sensing. 24:2597-2612.

Johannessen, S.C., W.L. Miller and J.J. Cullen. 2003. Calculation of UV attenuation and colored dissolved organic matter absorption spectra from measurements of ocean color. Journal of Geophysical Research, 108(C):doi:10.1029/2000JC000514

Kalle, K. 1966. The problem of the "*Gelbstoff*" in the sea. Oceanography and Marine Biology Annual Review. 4:91-104.

Kahru, M. and B.G. Mitchell. 1999. Empirical chlorophyll algorithm and preliminary SeaWIFS validation for California current. International Journal of Remote Sensing. 20:3423-3429.

Kahru, M. and B.G. Mitchell. 2001. Seasonal and non-seasonal variability of satellite–derived chlorophyll and dissolved organic matter concentration in the California Current. Journal of Geophysical Research. 106(C):2517-2529.

Kirk, J.T. 1976. Yellow substance (*"Gelbstoff"*) and its contribution to the attenuation of photosynthetically active radiation in some inland and coastal south-eastern Australian waters. Australian Journal of Marine and Freshwater Research. 27:61-71.

Kirk, J.T. 1994. Light and photosynthesis in aquatic ecosystems. Second Edition. Cambridge University Press. Great Britain. pp. 509.

Kishino, M., N. Okami and S. Ichimura. 1985. Estimation of the spectral absorption coefficients of phytoplankton in the sea. Bulletin of Marine Science. 37:634-642.

Kowalczuk, P., J. Olszewski, M. Darecki and S. Kaczmarek 2005. Empirical relationships between coloured dissolved organic matter (CDOM) absorption and apparent optical properties in Baltic Sea waters. International Journal of Remote Sensing. 26: 345-370.

Krestzschmar, R., D. Hesterberg and H. Sticher. 1997. Effects of adsorbed humic acids on surface charge and flocculation of kaolinite. Soil Science Society of America Journal. 61:101-108.

Lawless, J.G. 1986. Clay-organic interactions and the origin of life. In A. G. Cairns-Smith and H. Hartman, (Eds). Clay minerals and the origin of life. Cambridge University Press. New York. pp.135-147.

Lee, Z., K.L. Carder, T.G. Peacock, C.O. Davis and J.L. Mueller. 1996. Methods to derive ocean absorption coefficients from remote-sensing reflectance. Applied Optics. 35:453-462.

Liss, P.S. 1976. Conservative and non-conservative behavior of dissolved constituents during estuarine mixing. In J.D. Burton, and P.S. Liss. (Eds.). Estuarine Chemistry. Academic Press. London. pp.93-130.

Ludeña-Hinojosa, Y. 2007. Cianobacterias en la bahía de Mayagüez: abundancia distribución y su relación con las propiedades Bio-ópticas. Master Thesis. Department of Biology. University of Puerto Rico, Mayagüez Campus. pp. 120.

Lunsdorf, H., R.W. Erb, W.-R. Abrham and K.N. Timmis. 2000. 'Clay hutches': A novel interaction between bacteria and clay minerals. Environmental Microbiology. 2:161-168.

Mannino, A. and H.R. Harvey. 1999. Lipid composition in particulate and dissolved organic matter in the Delaware Estuary: Sources and digenetic pattern. Geochemica and Cosmochimica Acta. 63:2219-2235.

Mannino, A. and H.R. Harvey. 2000. Biochemical composition of particles and dissolved organic matter along an estuarine gradient: sources and implications for DOM reactivity. Limnology and Oceanography. 45:775-788.

Mannino, A., M.E. Russ and S.B. Hooker. 2008. Algorithm development and validation satellite-derived distributions of DOC and CDOM in the U.S. Middle Atlantic Bight. Journal of Geophysical Research. Vol.113:C07051 doi:10.1029/2007JC004493.

Méndez-Silvagnoli, M.M. 2008. Spatial and temporal variation of chromophoric dissolved organic matter absorption in the Caribbean. Master Thesis Department of Marine Science. University of Puerto Rico, Mayagüez Campus. pp.41.

Menon, H.B., A.A. Lotliker and S.R. Nayak. 2005. Pre-monsoon bio-optical properties in estuarine, coastal and Lakshadweep waters. Estuarine, Coastal and Shelf Science.63:211-223.

Menon, H.B., A.A. Lotliker and S.R. Nayak. 2006. Analysis of estuarine components during non-monsoon period through ocean color monitoring. Estuarine, Coastal and Shelf Science. 66:523-531.

Miller, R.L. 2000. Measuring the absorption of CDOM in the field using a multiple pathlenght liquid waveguide system. Ocean Optics XV. Monaco. pp.10.

Miller, R.L. and E.J. D'Sa, 2002. Evaluating the influence of CDOM on the remote sensing signal in the Mississippi River Bight. EOS Transactions AGU, Honolulu, HI. AGU, Washington, DC. pp.171.

Miller, R.L., J.F. Cruise, E. Otero and J.M. López. 1994. Monitoring suspended particulate matter in Puerto Rico: Field measurement and remote sensing. Water Resource Bulletin. 30:271-282.

Miller, L.W. 2000. The optical properties of dissolved organic matter in costal and open ocean waters. Ocean Optics XV Monaco. pp.6.

Miller, W. and M.A. Moran. 1997. Interaction of photochemical and microbial processes in the degradation of refractory dissolved organic matter from a coastal marine environment. Limnology and Oceanography. 42:1317-1324.

Miano T.M. and N. Senesi. 1992. Synchronous excitation fluorescence spectroscopy applied to soil humic substances chemistry. Science of the Total Environments. 11:41-51.

Mitchell, B.G. and D.A. Kiefer. 1984. Determination of absorption and fluorescence excitation spectra of phytoplankton. In Holm-Halsen, O., Bolis L., Giles, R. (Eds.). Marine phytoplankton and productivity. Springer-Verlag. Berlin. pp. 157-169.

Mobley, C.D. 1994. Light and water: Radiative transfer in natural waters. San Diego, CA. Academic Press. pp. 592

Mopper, K. and R.J. Kieber. 2002. The photochemical and cycling of carbon sulfur nitrogen and phosphorus. In D.S. Hansell and C.A. Carlson, (Eds.). Biogeochemistry of marine dissolved organic matter. Academic Press. Elsevier Science. San Diego, CA. pp.455-507.

Mopper, K., X.L. Zhou, R.J. Kieber, D.J. Kieber, R.J. Sikorski and R.D. Jones. 1991. Photochemical degradation of dissolved organic carbon and its impact on the oceanic carbon cycle. Nature. 353:60-62.

Moran, M.A., L.R. Pomeroy, E.S. Sheppard, L.P. Atkinson and R.E. Hodson. 1991. Distribution of terrestrially derived dissolved organic matter on the southeastern U.S. continental shelf. Limnology and Oceanography. 36:1134-1149.

Moran, M.A. and R.G. Zepp. 1997. Role of photoreactions in the formation of biologically labile compounds from dissolved organic matter. Limnology and Oceanography. 42:1307-1316.

Moran, M.A. and R.G. Zepp. 2000. UV Radiation effects on microbes and microbial processes. In D.L. Kirchman (Ed.). Microbial ecology of the oceans. Wiley-Liss. New York. pp.201-228.

Moran, M.A., W.M. Sheldon and R.G. Zepp. 2000. Carbon loss and optical property changes during long term photochemical and biological degradation of estuarine organic matter. Limnology and Oceanography. 45:1254-1264.

Morel, A. and L. Prieur. 1977. Analysis of variations in ocean color. Limnology and Oceanography. 22:709-722.

Morell, J.M. and J.E. Corredor. 2001. Photomineralization of Fluorescent Dissolved organic matter in the Orinoco river plume: Estimation of ammonium release. Journal of Geophysical Research. 106(C):16807-16813.

Morelock, J. and K. Grove. 1976. Particle characteristics and dispersal patterns of sugarcane wastes in selected rivers and estuaries of Puerto Rico. Water Resources Research Institute. Division of Research and Special Programs. College of Engineering Mayagüez Campus. Mayagüez Puerto Rico. pp.53.

Morelock, J., K. Grove and M.L. Hernández. 1983. Oceanography and patterns of shelf sediments, Mayagüez, Puerto Rico. Journal of Sedimentary Petrology. 53:371-381.

Mueller, J.L. and Austin, R.W. 1995. Ocean optics protocols for SeaWiFS validation, revision 1. In S. B. Hooker, and E. R. Firestone (Eds.). NASA Tech. Memo. 104566,Greenbelt, MD: NASA Goddard Space Flight Center. Vol 25. pp. 67.

Müller-Karger, F.E., C.R. McClain and P.L. Richardson. 1988. The dispersal of the Amazon's water. Nature. 333:56-58.

Müller-Karger, F.E., C.R. McClain, T.R. Fisher, W.E. Esaias and R. Varela. 1989. Pigment distribution in the Caribbean Sea: Observations from space. Progress in Oceanography. 23:23-64.

Müller-Karger, F.E., P.L. Richardson and D. McGillicuddy. 1995. On the offshore dispersal of the Amazon's plume in the North Atlantic. Deep-Sea Research I. 42:2127-2137.

Müller-Karger, F. and R.Varela. 1990. Influjo del Río Orinoco en el Mar Caribe; observaciones con el CZCS desde el espacio. Sociedad de ciencias La Salle, tomo L. No 133-134. Contribución No. 186 Estación de Investigaciones Marinas de Margaritas. Fundación La Salle de Ciencias Naturales.

Murphy E.M. and J.M. Zachara. 1995. The role of sorbed humic substances on the distribution of organic and inorganic contaminants in groundwater. Geoderma 67:102-124.

Namjesnik-Dejanovic, K., P.A. Maurice, G. R. Aiken, S. Cabaniss, Y.P. Chin and M.J. Pullin. 2000. Adsorption and fractionation of a muck fulvic acid on kaolinite and goethite at pH 3.7, 6 and 8. Soil Science. 165:545-559.

Nelson, N.B., D.A. Siegel and A.F. Michaels. 1998. Seasonal dynamics of colored dissolved material in the Sargasso Sea. Deep-Sea Research I.45:931-957.

Nelson, N. B., D. A. Seigel., and A. F. Michaels., 1998. Seasonal dynamics of color dissolved organic material in the Sargasso Sea. Deep-Sea Research I. 45:931-957.

Nelson, N.B. and D.A. Seigel. 2002a. Seasonal dynamics of color dissolved organic material in the Sargasso Sea. Deep-Sea Research I. 45:931-957.

Nelson, N.B. and D.A. Siegel. 2002b. Chromophoric DOM in the Open Ocean. In D.A. Hansell and C.A. Carlson, (Eds.). Biogeochemistry of Marine Dissolved Organic Matter. Academic Press. Elsevier Science San Diego, CA. pp.547-578.

Nelson, J. and R.S. Guarda. 1995. Particulated and dissolved spectral absorption on the continental shelf of the Southeastern United Sates. Journal of Geophysical Research. 100(C):8715-8732.

Nissenbaum, A. and I.R. Kaplan. 1972. Chemical and isotopic evidence for the in *situ* origin of marine humic substances. Limnology and Oceanography. 17:570-582.

O'Reilly, J.E., S. Maritorena, G.G. Mitchell, D.A. Siegel, K.L. Carder, S.A. Garver, M. Kahru and C. McClain. 1998. Ocean color algorithms for SeaWiFS. Journal of Geophysical Research. 103(C):24937-24953.

Otero, E., R.L. Miller and J.M. López. 1992. Remote Sensing of Chlorophyll and sediments in coastal water of Puerto Rico. Presented at the First Thematic Conference on Remote Sensing for Marine and Coastal Environment, New Orleans, Louisiana USA 15-17 June 1992. pp. 217-222.

Oubelkheir, K., H. Claustre, A. Bricaud and M. Babin. 2007. Partitioning total spectral absorption in phytoplankton and colored detrital material contributions. Limnology and Oceanography. Methods 5, 2007, 384–395.

Pan, X., A. Mannino, M.E. Russ and S.B. Hooker. 2008. Remote sensing of the absorption coefficients and chlorophyll-a concentration in the United States southern Middle Atlantic Bight from SeaWiFS and MODIS-Aqua. Journal of Geophysical Research. 113(C):C11022 doi:10.1029/2008JC004852.

Parrilla, D. 1996. Distribution of Chlorophyll-a, suspended Particulate matter and Nutrients in the vicinity of the Añasco River outlet. Master Thesis in Marine Science. University of Puerto Rico, Mayagüez Campus. pp. 60.

Pegau, W.S., D. Gray and J.RV. Zaneveld. 1997. Absorption and attenuation of visible and near-infrared light in water: The dependence on temperature and salinity. Applied Optics. 36:6035-6046.

Pegau, W.S., J.R.V. Zenaveld and J.L. Muller. 2003. Volume absorption coefficient: instrument characterization and filed instrument and data analysis protocol. In Muller J.L., G.S. Faringtón and C.R. McClain (Eds.). Ocean optic protocol for satellite ocean sensors validation revision 4. Volume IV, NASA/TM-2003-211261 NASA Goddard Space Flight Center, Greenbelt MD. Chapter 3. pp. 27-38.

Pérez-Alegría, L., D. Sotomayor-Ramírez, G. Suárez and G.A. Martínez. 2005. Hydrologic analysis for nutrient and sediment loading determinations in tropical watersheds. Oral Presentation and Abstract. 41st Annual Meeting. Caribbean Food Crops Society. 10-16 July. Le Gosier, Guadaloupe. F.W.I.

Pettine, M., L. Patrolecco, M. Manganelli, S. Capri and M.G. Farrace. 1999. Seasonal variation of dissolved organic matter in the northern Adriatic Sea. Marine Chemistry. 64:153-169.

Phinney D.A. and C.S. Yentsch, 1985. A novel phytoplankton chlorophyll technique; towards automated analysis. Journal of Plankton Research. 7: 633-642.

Pirie, R.G. 1967. Clay mineralogy of Bahía de Añasco, western Puerto Rico: Puerto Rico Nuclear Center Marine Biology Program, Progress Summary Report No. 5, pp. 148-166.

Preston, M.R. and J.P. Riley. 1982. The interaction of humic compounds with electrolytes and three clay minerals under simulated estuarine condition. Estuarine, Coastal Marine Science. 14:567-576.

Rashid, M.A., D.E. Buckley and K.D. Robertson. 1972. Interaction of natural sediments. Geochemica. 8:11-27.

Retamal, L., W.F. Vincent, C. Martineau and C.L. Osburn. 2007. Comparison of the optical properties of dissolved organic matter in two river-influenced coastal regions of the Canadian Arctic. Estuarine, Coastal and Shelf Science. 72:261-272.

Rivera-Rivera, G. Geographical and temporal variation in sediment influx and composition along the Mayagüez Bay. Undergraduate Research Project for the Geology Department. Unpublished study. Advisor: Wilson Ramirez.

Rochelle-Newall, E.J. and T.R. Fisher. 2002a. Production of chromophoric dissolved organic matter fluorescence in marine and estuarine environment: and investigation into the role of phytoplankton. Marine Chemistry. 77:7-21.

Rochelle-Newall, E.J. and T.R. Fisher. 2002b. Chromophoric dissolved organic matter and dissolved organic carbon in Chesapeake Bay. Marine Chemistry. 77:23-41.

Rochelle-Newall, E.J., T.R. Fisher, C. Fan and P.M. Gilbert. 1999. Dynamics of chromophoric dissolved organic matter and dissolved organic carbon in experimental mesocosmos. International Journal of Remote Sensing. 20:627-641.

Rodríguez-Gúzman, V. 2008. Remote sensing of suspended sediment in Mayagüez Bay associated with inland soil erosion rates. Master Thesis in Geology. University of Puerto Rico, Mayagüez Campus. pp.112.

Rodríguez, I.E. 2004. Characterization of temporal and stratigraphic changes in texture, composition, nutrients, and organic content of bottom sediments in the Mayagüez Bay, Puerto Rico. Master Thesis in Geology. University of Puerto Rico at Mayagüez. pp.82.

Rosado-Torres, M.A. 2000. Variability in the bio-optical properties in the Mayagüez Bay. Master Thesis in Marine Science. University of Puerto Rico, Mayagüez Campus. pp.61.

Rosado-Torres, M.A. 2008. Evaluation and development of bio-optical algorithms for chlorophyll retrieval in western Puerto Rico. Ph.D. Dissertation in Marine Science. University of Puerto Rico, Mayagüez Campus. pp.116.

Sasaki, H., T. Miyamura, S. Saitoh and J. Ishizaka. 2005. Seasonal variation of absorption by particles and color dissolved organic matter (CDOM) in Funka Bay, southwestern Hokkaido Japan. Estuarine, Coastal and Shelf Sciences. 64:447-458.

Schulthess, C.P. and C.P. Huang. 1991. Humic and Fulvic acid adsorption by silicon and aluminum oxide surfaces on clay minerals. Soil Science Society of America Journal. 55:34-42.

Shank, G.C., R.G. Zepp and M.L. Smith. 2004. Variations in the spectral properties of estuaries water caused by CDOM partitioning onto river and estuarine sediments ASLO/TOS. Ocean Research Conference Honolulu Hawaii.

Shank, G.C., R.G. Zepp, R.F. Whitehead and M.A. Moran. 2005. Variations in the spectral properties of freshwater and estuarine CDOM caused by partitioning onto river and estuarine sediments. Estuarine, Coastal and Shelf Sciences. 65:289-301.

Sholkovitz, E.R. 1976. Flocculation of dissolved organic matter and inorganic matter during the mixing of river water and seawater. Geochemica et Cosmochimica Acta. 40:831-845.

Sholkovitz, E.R., E.A. Boyle and N.B. Price. 1978. The removal of dissolved humic acids and iron during estuarine mixing. Earth and Planet Science Letter. 40:130-136.

Siegel, D. A. and A. F. Michaels. 1996. Quantification of non-algal attenuation in the Sargasso Sea: Implication for the biogeochemistry and remote sensing. Deep-Sea Research II. 43:321-345.

Siegel, D.A., S. Maritorena, N.B. Nelson, D.A. Hansell and M. Lorenzi-Kayser. 2002. Global ocean distribution and dynamics of colored dissolved and detrital organic materials. Journal of Geophysical Research. 107(C):c12,3228, doi:10.1029/2001JC000965.

Siegel, D.A., S. Maritorena, N.B. Nelson, M.J. Behrenfeld and C.R. McClain. 2005 Colored dissolved organic matter and the satellite-based characterization of the ocean biosphere. Geophysical Research Letters. 32:L20605.

Siegel, D.A. and A.F. Michaels. 1996. Quantification of non-algal light attenuation in the Sargasso Sea: Implication for biogeochemistry and remote sensing. Deep-Sea Research II. 43:321-345.

Siegel, D.A., M. Wang, S. Maritorena and W. Robinson. 2000. Atmospheric correction of satellite-ocean color imagery: the black pixel assumption. Applied Optics. 39:3582-3591.

Skoog, A., M. Wedborg and E. Fogelqvist. 1996. Photobleaching of fluorescence and the organic carbon concentration in a coastal environment. Marine Chemistry. 55:333-345.

Sotomayor-Ramírez, D., L.R. Pérez-Alegría and G. Martínez. 2004. Nutrient discharges from Mayagüez Bay watershed. Summary Report of Project. PRWRRI - College of Agricultural. Sciences. December, 2004. pp 60.

Specht, C.H., M.U. Kumke and F.H. Frimmel. 2000. Characterization of NOM adsorption to clay minerals by size exclusion chromatography. Water. Research. 34:4063-4069.
Spencer, R.G.M., J.M.E. Ahad, A. Baker, G.L. Cowie, R. Ganeshram, R.C. Upstill-Goddard and G. Uher. 2007. The estuarine mixing behavior of peatland derived dissolved organic carbon and its relationship to chromophoric dissolved organic matter in two North Sea estuaries. Estuarine, Coastal and Shelf Sciences. 74:131-144.

Stedmon, C.A. and S. Markager. 2003. Behavior of the optical properties of coloured dissolved organic matter under conservative mixing. Estuarine, Coastal and Shelf Science. 57:973-978.

Steinberg, D.K., N.B. Nelson, C.A. Carlson and A.C. Prusak. 2004. Production of chromophoric dissolved organic matter (CDOM) in the open ocean by zooplankton and the colonial cyanobacterium *Tricodesmium sp.* Marine Ecology Progressive Series. 267:45-56.

Stuermer, D.H and G.R. Harvey. 1974. Humic substances from seawater. Nature, London. 250:480-481.

Swift, R.S. 1989. Molecular weight, size shape and charge characteristics of humic substances: some basic consideration. In M.H.B. Hayes *et al*., (Eds). Humic substance II In search and structure. John Wiley and Sons. New York. pp.449-465.

Tarchitzky, J., Y. Chen and A. Banin. 1993. Humic substances and pH effects on Sodium and Calcium-Montmorillonite flocculation and dispersion. Soil Science Society of America Journal. 57:367-372.

Tapia-Lario, C.M. 2007. Variación espacial y temporal del fitoplancton en la bahía de Mayagüez, Puerto Rico. Master Thesis. Department of Biology. University of Puerto Rico, Mayagüez Campus. pp.120.

Thurman, E.M. 1985. Organic geochemistry of natural waters. Kluwer Academic Publisher. Nijhoff/Junk, Dordrecht, Netherlands. pp.497.

Thurman, E.M. and R.L. Malcolm. 1981. Preparative isolation of aquatic humic substances. Environmental Science and Technology. 15:463-466.

Tietjen, T., A.V. Vähätalo and R.G. Wetzel. 2005. Effects of clay mineral turbidity on dissolved organic carbon and bacterial production. Aquatic Sciences. 67:51-60.

Toole, D.A., D.A. Siegel, D.W. Menzies, M.J. Neumann and R.C. Smith. 2000. Remote-sensing reflectance determinations in the coastal ocean environment: impact of instrumental characteristics and environmental variability. Applied. Optics. 39:456– 469.

Twardoski, M.S., J.M. Sullivan, P.L. Donaghay and J.R.V. Zaneveld. 1999. Microscale quantification of the absorption by dissolved and particulate material in coastal waters with an AC-9. Journal of Atmospheric and Oceanic Technology. 16:691-707.

Twardowski, M.S., E. Boss, J.M. Sullivan and P.L Donaghay. 2004. Modeling the spectral shape of absorption by Chromophoric Dissolved Organic Matter. Marine Chemistry. 89:69-88.

Uher, G., C. Hughes, G. Henry and R.C. Upstill-Goddard. 2001. Non-conservative mixing behavior of colored dissolved organic matter in a humic-rich, turbid estuary. Geophysical Research Letter. 28:3309-3312.

Varadachari, C., A.H. Mondal, D.C. Nayak and K. Ghosh. 1994. Clay-humus complexation: Effects of pH and the nature of bonding. Soil Biology and Biochemistry. 9:1145-1149.

Villalta, C. 2004. Selección de funciones de transporte de sedimentos para los ríos de la Bahía de Mayagüez usando SAM. Master Thesis. University of Puerto Rico at Mayagüez, Department of Civil Engineering. pp.112

Visser, S.A. 1984. Seasonal changes in the concentration and color of humic substances in some aquatic environments. Freshwater Biology. 14:79-87.

Vodacek, A., F.E. Hoge, R.N. Swift, J.K. Yugel, E.T. Peltzer and N.V. Blough. 1995. The use of *in situ* and airborne fluorescence measurements to determine UV absorption coefficients and DOC concentration in surface waters. Limnology and Oceanography. 40:411-415.

Vodacek, A., N.V. Blough, M.D. De Grandpre, E.T. Peltzer and R.K. Nelson. 1997. Seasonal variation of CDOM and DOC in the middle Atlantic bight: Terrestrial inputs and photo oxidation. Limnology and Oceanography. 42:674-686.

Welschmeyer, N.A. 1994. Fluorometric analysis of chlorophyll-*a* in the presence of chlorophyll-*b* and pheopigments. Limnology and Oceanography. 39:1985-1992.

Zafiriou, O.C. 1977. Marine organic photochemistry previewed. Marine Chemistry. 5:497-522.

Zepp, R.G., T.V. Callaghan and D.J Erickson. 1998. Effects of enhanced ultraviolet radiation on biogeochemical cycles. Journal of Photochemistry and Photobiology. Part B: Biology. 46:69-82.

Zepp, R.G., W.N. Sheldon and M.A. Moran. 2004. Dissolved organic fluorophores in southeastern US coastal waters: Correction method for eliminating Rayleigh and Raman scattering peaks in excitation-emission matrices. Marine Chemistry. 89:15-36.